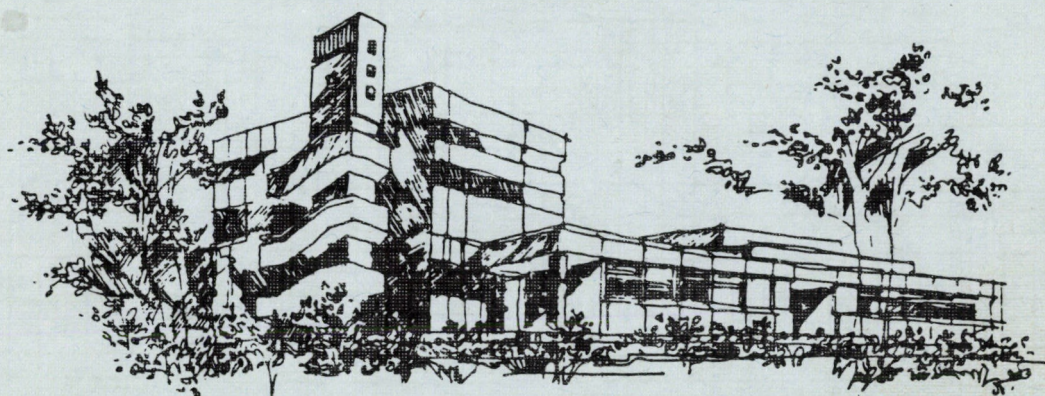


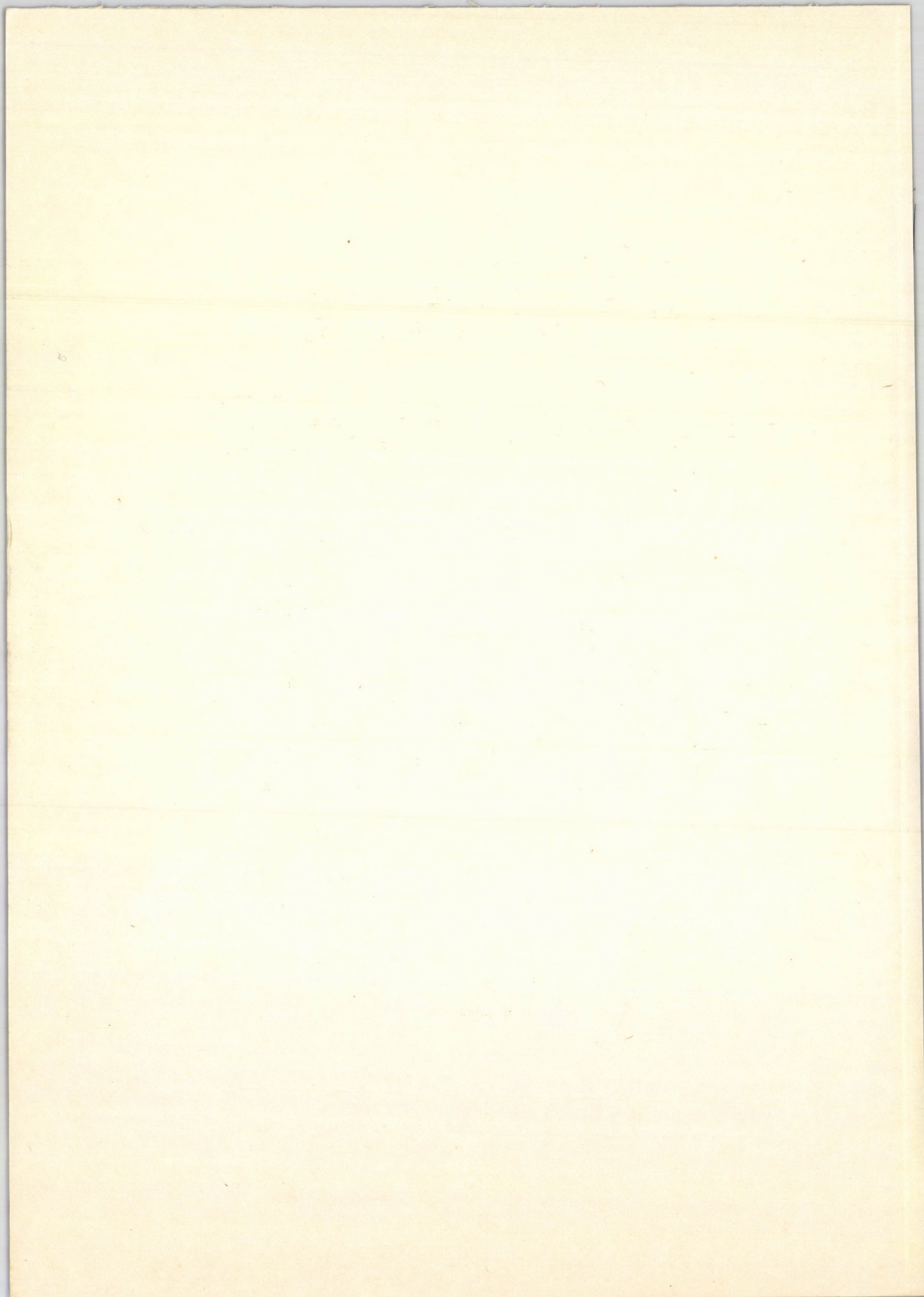
ATOMKI

ANNUAL REPORT

1989



INSTITUTE OF NUCLEAR RESEARCH
OF THE HUNGARIAN ACADEMY OF SCIENCES
DEBRECEN, HUNGARY



INSTITUTE OF NUCLEAR RESEARCH
OF THE HUNGARIAN ACADEMY OF SCIENCES
DEBRECEN, HUNGARY

ANNUAL REPORT 1989

ATOMKI

Postal address:

Debrecen

P. O. Box 51
H-4001

Hungary

Edited by Z. Gácsi
J. Pálincás
J. Tóth

HU ISSN 0231-3596

P R E F A C E

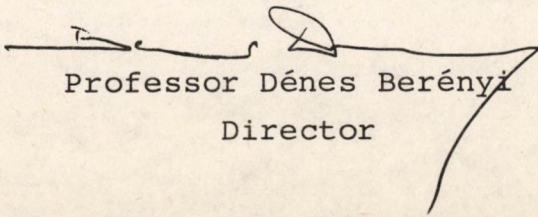
As in the case of the former volumes, the present Annual Report contains short reports on the results /often rather preliminary ones/ obtained in the research works going on in this institute. Results published already have not been included.

As can be seen, nearly half of the reports come from the field of nuclear and atomic /collision/ physics, while the fields of materials science and analysis, earth and cosmic sciences, environmental research, biological and medical sciences, development of methods and instruments make the other half of the reports.

In the last year a discussion was finished in this institute to outline the future of the above six larger research fields in ATOMKI. The work was started on the basis of the written opinion of three-three colleagues in every field concerned, the issue was discussed first in smaller groups, later by the management, and finally by the whole research community of the institute.

One of the main conclusions of the above series of discussions is that the establishment of a modern ion source /probably ECR/ of highly charged ions would be desirable from the point of view of different fields /nuclear and atomic physics, materials science etc./, it is a real step forward in the development of our accelerators too /e.g. the usage of the ECR ion source at the MGC cyclotron/. There is no final decision yet in this issue, but an intensive preparatory work is in progress.

Debrecen, February 9, 1990



Professor Dénes Berényi

Director

C O N T E N T S

PROGRESS REPORTS

Nuclear Physics	1
Atomic Physics	29
Materials Science and Analysis	51
Earth and Cosmic Sciences, Environmental Research	63
Biological and Medical Research	74
Development of Methods and Instruments	86

PUBLICATIONS AND SEMINARS

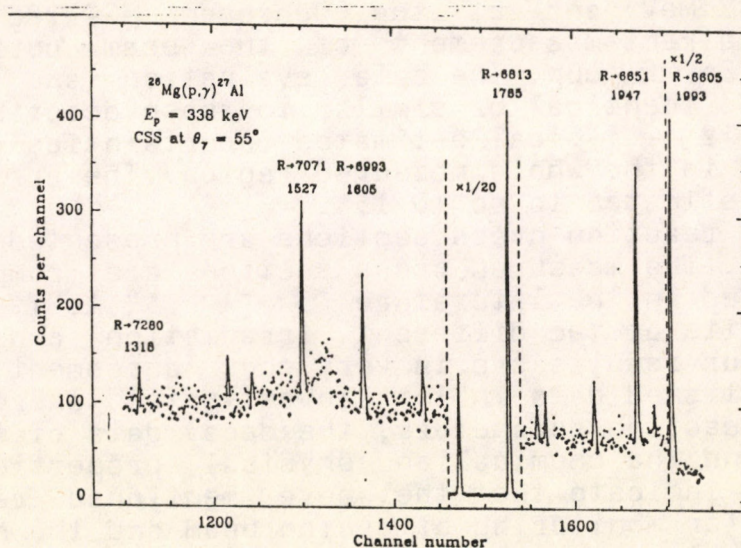
Papers Published in 1989	107
Conference Contributions and Talks	116
Theses Completed	126
Seminars in the ATOMKI	127
Author Index	131

NUCLEAR PHYSICS

LOW-ENERGY RESONANCES IN $^{25}\text{Mg}(p,\gamma)^{26}\text{Al}$, $^{26}\text{Mg}(p,\gamma)^{27}\text{Al}$ AND $^{27}\text{Al}(p,\gamma)^{28}\text{Si}$

Ch. Iliadis*, Th. Schanche*, C. Rolfs*, U. Schröder*, E. Somorjai, H.P. Trautvetter* K. Wolke*, P.M. Endt**, S.W. Kikstra**
A.E. Champagne⁺, M. Arnould⁺⁺, and G. Paulus⁺⁺

Abstract: Gamma-ray decay schemes have been measured with bare and Compton-suppressed Ge detectors at low-energy resonances ($E_p < 340$ keV) in the (p,γ) reactions on ^{25}Mg , ^{26}Mg and ^{27}Al . Altogether 58 new decay branches have been observed and a new $^{26}\text{Mg}(p,\gamma)^{27}\text{Al}$ resonance has been found at $E_p = 154.5 \pm 1.0$ keV. The new branchings lead to J^π determinations (or limitations) for two states in ^{26}Al and four states in ^{28}Si . The absolute strengths of the $^{25}\text{Mg}(p,\gamma)^{26}\text{Al}$ and $^{26}\text{Mg}(p,\gamma)^{27}\text{Al}$ resonances also have been obtained, and the uncertainties of the stellar rates, deduced from the available data for both reactions, are significantly reduced. Some astrophysical consequences are discussed.



Part of a Compton-suppressed γ -ray spectrum showing some of the new primary transitions.

(Submitted for publication in Nucl. Phys.)

- * Institut für Kernphysik, Universität Münster, W. Germany
- ** R.J. Van De Graaff Laboratorium, Rijksuniversiteit Utrecht, The Netherlands
- + Department of Physics, Princeton University, Princeton, USA
- ++ Institut d'Astrophysique, Université Libre, Bruxelles, Belgium

INVESTIGATION OF THE $^{58}\text{Ni}(p,pn)^{57}\text{Ni}$ MONITOR REACTION

F. Tárkányi, F. Szelecsényi, P. Kopecký⁺

The monitor reactions are very useful for beam intensity and effective beam energy measurement in applied field [1]. For low and middle energy protons only very few monitor reactions are used because of the lack of precise cross section data in wide range of energy. Since in our nuclear data program we frequently use chemically resistant nickel backing foils as a continuation of our study of nuclear reactions induced by charged particles we investigate the $^{58}\text{Ni}(p,pn)^{57}\text{Ni}$ reaction as a monitor.

The excitation function of $^{58}\text{Ni}(p,pn)^{57}\text{Ni}$ reaction were measured by usual stacked-foil technique. High purity natural Ni foils of 10 and 25 μm (Goodfellow, Cambridge, England) were used as targets. The Ni stacks were interspersed with 8 and 22 μm thin copper foils (Goodfellow) to degrade the beam energy and to determine in each foil the beam intensity and to control the proton energy. The targets were bombarded in the external beam of Řež U-120M (30 MeV and 22 MeV entrance energies), of the Jülich CV-28 (22 MeV) and of the Debrecen MGC-20E (18 MeV) cyclotron. The direct measurement of the beam currents were performed by a Faraday cup. The data evaluation and the error calculation were identical or similar to those described in our previous study [2]. Typical estimated uncertainties in energy are 0.5-0.8 MeV in the whole measured region. The errors in cross sections were estimated to be 10-15%.

The obtained reaction cross sections are presented in Table 1. In the Fig.1. the measured cross sections are compared with the data obtained in the literature [3] [4] [5]. As it is shown in Fig.1. in spite of the different irradiation and measuring circumstances our results are in very good agreement with all the earlier published data in the investigated energy region. The available reaction parameters, the decay data of the product nuclei [^{57}Ni] and the chemical and physical properties of the target material indicate that the above mentioned reaction is very promising for monitoring of proton beam and the natural Ni could be used complementary to natural copper.

References

- [1] Proceedings of the IAEA Consultants' Meeting on Data Requirements for Medical Radioisotope Production Edited by K. Okamoto, 1988, Vienna. IAEA INDC(NDS)-195/GZ
- [2] F. Tárkányi, F. Szelecsényi, Z. Kovács, S. Sudár, Radiochimica Acta (accepted), ATOMKI Preprint 5-1989P
- [3] S. Kaufman, Phys. Rev. 117(1960)1532
- [4] S. Tanaka, M. Furukawa, M. Chiba, J. Inorg. nucl. Chem. 34(1972)2419
- [5] R. Michel, H. Weigel, W. Herr, Z. Physik A286(1978)393

⁺Dept. of Radiopharmaceuticals, Nucl. Research Institute, 250 68 Řež, Czechoslovakia

Table 1. Formation cross sections of $^{58}\text{Ni}(p,pn)^{57}\text{Ni}$ reaction

Proton energy (MeV)	$\sigma(\text{mb})$ $^{58}\text{Ni}(p,pn)^{57}\text{Ni}$	Proton energy (MeV)	$\sigma(\text{mb})$ $^{58}\text{Ni}(p,pn)^{57}\text{Ni}$
14.4	3.6	20.5	171
14.8	5.6	20.9	198
15.0	7.4	21.0	190
15.7	22.3	21.2	193
16.0	23.1	21.4	191
16.2	29.5	21.5	223
16.8	56.5	22.1	208
17.1	64.7	22.6	225
17.3	67.6	23.4	220
17.7	82.0	24.0	247
17.9	100	24.5	253
18.2	119	25.3	262
18.4	116	25.8	273
18.4	111	26.3	272
19.0	141	27.0	270
19.1	129	27.5	282
19.3	148	27.9	267
19.5	149	28.7	259
20.0	167	29.1	244
20.0	176	29.6	251
20.3	174		

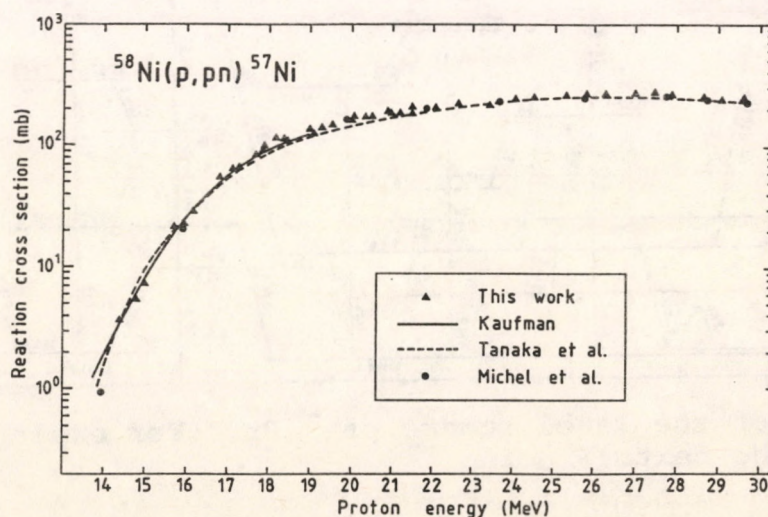


Fig.1. Excitation function for $^{58}\text{Ni}(p,pn)^{57}\text{Ni}$ reaction

LEVEL STRUCTURE OF ^{77}Br FROM THE REACTION $^{78}\text{Se}(p, 2n\gamma)$.

Zs. Fülöp, Á.Z. Kiss, E. Somorjai

In comparison to the neighbouring bromine isotopes relatively little information on the level structure of ^{77}Br was available at the beginning of this study [1].

Thin selenium targets enriched to 90 % in ^{78}Se were bombarded with 12 and 18 MeV protons from the MGC cyclotron of the Institute. The γ -radiation was detected in a Ge(Li) 25 cm³ and in a LEPS γ -detector (for $E_\gamma < 600$ keV). The target material and the whole set-up was tested at $E_p = 12$ MeV, where mostly γ -rays from the ^{78}Br nucleus excited in the well-known $^{78}\text{Se}(p, n)$ reaction [2] were seen. At $E_p = 18$ MeV the measured γ -spectra showed the dominance of γ -rays from ^{77}Br . The ^{77}Br nucleus was excited in the $^{78}\text{Se}(p, 2n)$ reaction ($Q = -12.8$ MeV) for the first time, according to our knowledge.

Preliminary analysis of the experimental results supports the recent ^{77}Br level scheme of Döring et al. [3] deduced mainly from their $^{75}\text{As}(\alpha, 2n)$ studies. Fig. 1. shows the part of the above mentioned level scheme confirmed by our measurement. The dotted lines indicate ambiguous determinations mainly due to the low statistics and the absence of $\gamma\gamma$ coincidence measurements.

Further study of the level structure of ^{77}Br via the $^{78}\text{Se}(p, 2n)$ reaction is under course.

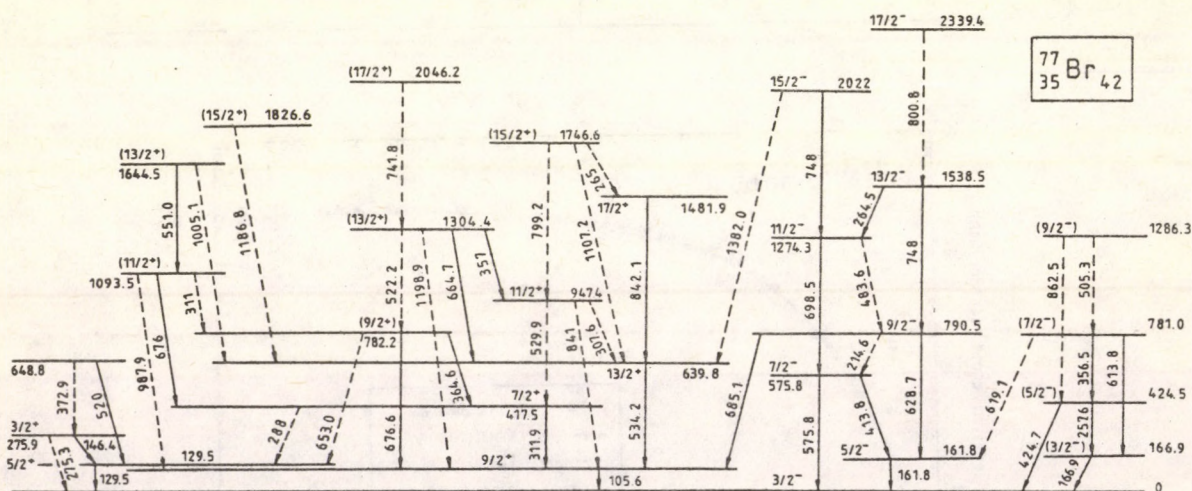


Fig. 1. Part of the level scheme of ^{77}Br . (For explanation see the text.)

REFERENCES

- [1] B. Singh and D.A. Viggars, Nuclear Data Sheets 29(1980)75
- [2] ibid 30(1981)189
- [3] J. Döring, L. Funke, R. Schwenger and G. Winter, Zentralinstitut für Kernforschung, Rossendorf, private communication.

STRUCTURE OF ^{106}In NUCLEUS

J. Gulyás, Zs. Dombrádi, T. Fényes, J. Timár, A. Passoja⁺,
J. Kumpulainen⁺⁺ and R. Julin⁺⁺

The structure of ^{106}In has been studied with in-beam γ - and electron-spectroscopic methods [1, 2]. A more complete level scheme of ^{106}In has been proposed which contains 49 levels below 1650 keV excitation energy. On the basis of the internal conversion coefficients of transitions, Hauser-Feshbach analysis of (p,n) reaction cross sections, γ -ray angular distribution and other arguments spin and parity values have been deduced. The energy splittings of p-n multiplets have been compared with the predictions of the parabolic rule. The energy levels, wave functions, electromagnetic moments, as well as reduced M1 and E2 transition probabilities were calculated in the framework of the interacting boson-fermion-fermion/ odd-odd truncated quadrupole phonon model (IBFFM/OTQM), and reasonably good agreement was obtained with experimental data (Fig.1).

This work was supported partly by the National Scientific Research Foundation /OTKA/.

References:

1. J. Gulyás et al., ATOMKI Ann. Rep. 1988, p. 5.
2. J. Gulyás, Zs. Dombrádi, T. Fényes, J. Timár, A. Passoja, J. Kumpulainen and R. Julin, ATOMKI Preprint 3-1989 P, Debrecen.

⁺ University of Joensuu, Department of Physics, Finland

⁺⁺ University of Jyväskylä, Department of Physics, Finland

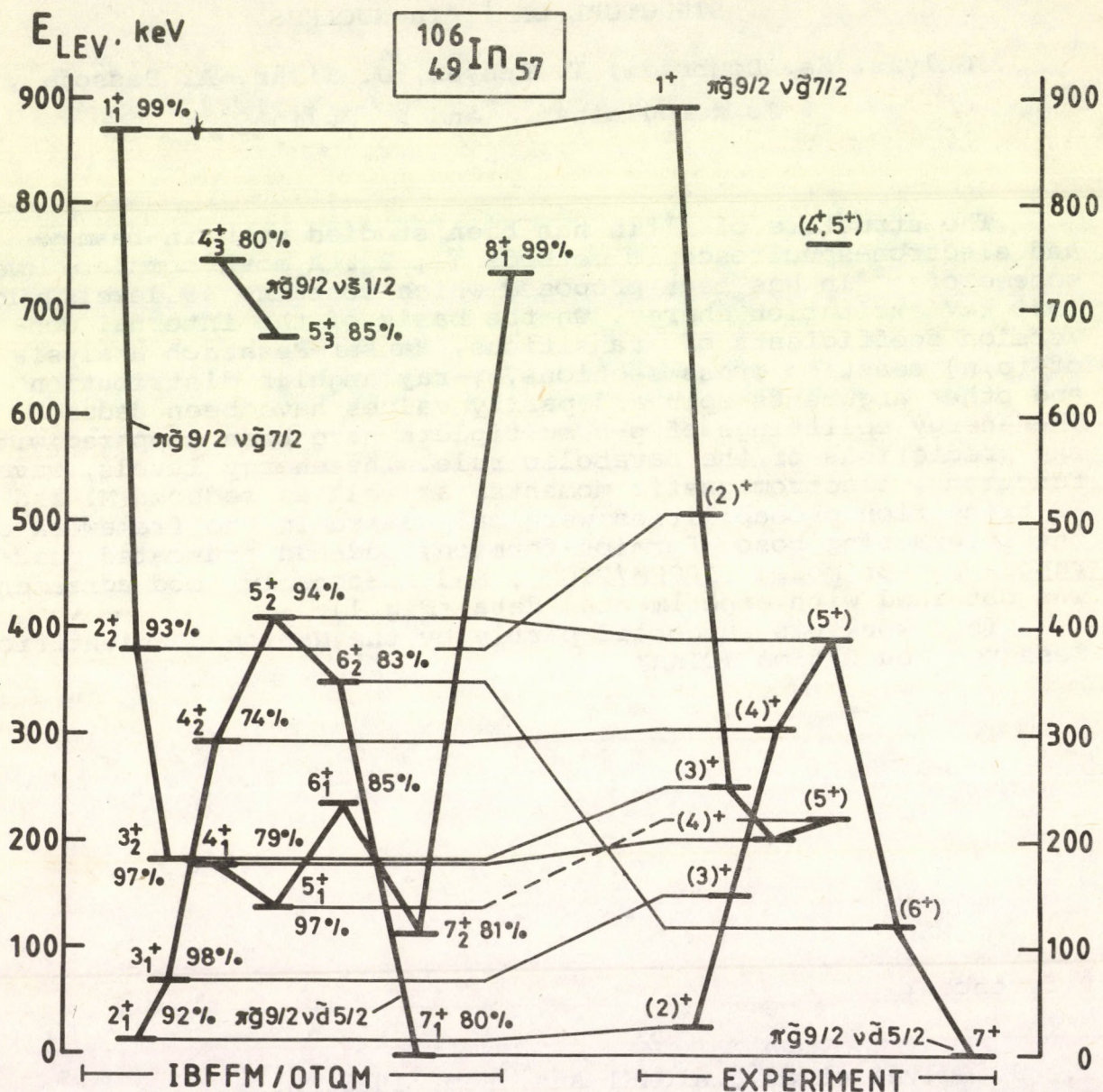


Fig. 1. IBFFM/OTQM energy spectrum of ^{106}In in comparison with experimental data. After the spin and parity of the state "purity" is shown in %, which characterizes the total strength of the indicated configuration in the wave function. States having identical main components are connected with solid lines.

LEVEL SCHEME OF ^{116}Sb FROM $(p, n\gamma)$ REACTION

Z. Gácsi, T. Fényes and F. Horváth

The γ -ray and internal conversion electron spectra of the $^{116}\text{Sn}(p, n\gamma)^{116}\text{Sb}$ reaction were measured at $E_p = 6.3, 6.7,$ and 7.2 MeV bombarding energies with Ge(Li), Ge(HP), Ge(HP, LEPS) γ and superconducting magnetic lens plus Si(Li) electron spectrometers. The energies and relative intensities of 90 ^{116}Sb γ rays (including 25 new ones, compared to the literature [1-3]), as well as internal conversion coefficients of 21 ^{116}Sb transitions were determined. Angular distribution data have been obtained for 56 γ rays. A more complete level scheme of ^{116}Sb has been deduced, which contains 38 (among them 17 new) levels below 1500 keV excitation energy (fig. 1). Multipolarities of transitions and γ -ray branching ratios have been deduced. Calculated Hauser-Feshbach (p, n) cross sections were compared with experimental values. Level spins and parities have been determined on the basis of Hauser-Feshbach analysis, internal conversion coefficients, and γ -ray angular distribution data. The energies of several ^{116}Sb proton-neutron multiplets were calculated using the parabolic rule. Members of different multiplets have been identified.

This work was supported partly by the National Scientific Research Foundation (OTKA).

REFERENCES

- [1] J. Blachot, J.P. Husson, J. Oms, G. Marguire and F. Haas, Nucl. Data Sheets 32 (1981) 287.
- [2] C. B. Morgan, Ph. D. thesis, Michigan State Univ., 1975 (unpublished).
- [3] R. Kamermans, H. W. Jongsma, T. J. Ketel, R. van der Wey, and H. Verheul, Nucl. Phys. A266 (1976) 346.
- [4] Z. Gácsi, T. Fényes and F. Horváth, in this volume.

LEVELS OF ^{116}Sb FROM $(\alpha, n\gamma)$ REACTION

Z. Gácsi, T. Fényes and F. Horváth

The γ -ray and internal conversion electron spectra of the $^{113}\text{In}(\alpha, n\gamma)^{116}\text{Sb}$ reaction were measured at 14.5 and 16.0 MeV bombarding α -particle energies with Ge(Li), Ge(HP), Ge(HP, LEPS) γ and superconducting magnetic lens plus Si(Li) electron spectrometers. The energies and relative intensities of 189 ^{116}Sb γ rays (including 117 new ones, compared to the former results [1-5]), as well as internal conversion coefficients of 59 ^{116}Sb transitions have been determined. $\gamma\gamma$ -coincidences were also measured at $E_\alpha = 16$ MeV. Both low-spin and high-spin level schemes have been deduced, which contain 61 (among them 32 new) levels (figs. 1 and 2). Multipolarities of transitions and γ -ray branching ratios have also been deduced. Level spins and parities have been determined mainly from internal conversion coefficients and the results of our $(p, n\gamma)$ study [6]. Members of different proton-neutron multiplets have been identified on the basis of parabolic rule calculation and other arguments.

This work was supported partly by the National Scientific Research Foundation (OTKA).

REFERENCES

- [1] J. Blachot, J. P. Husson, J. Oms, G. Marguier and F. Haas, Nucl. Data Sheets 32 (1981) 287.
- [2] C. B. Morgan, Ph. D. thesis, Michigan State Univ., 1975 (unpublished).
- [3] R. Kamermans, H. W. Jongsma, T. J. Ketel, R. van der Wey, and H. Verheul, Nucl. Phys. A266 (1976) 346.
- [4] P. van Nes, W. H. A. Hesselink, W. H. Dickhoff, J. J. van Ruyven, M. J. A. de Voigt, and H. Verheul, Nucl. Phys. A379 (1982) 35.
- [5] R. Duffait, J. van Maldeghem, A. Charvet, J. Sau, K. Heyde, A. Emsallem, M. Meyer, R. Béraud, J. Trêherne and J. Genevey, Z. Phys. A307 (1982) 259.
- [6] Z. Gácsi, T. Fényes, F. Horváth, in this volume.

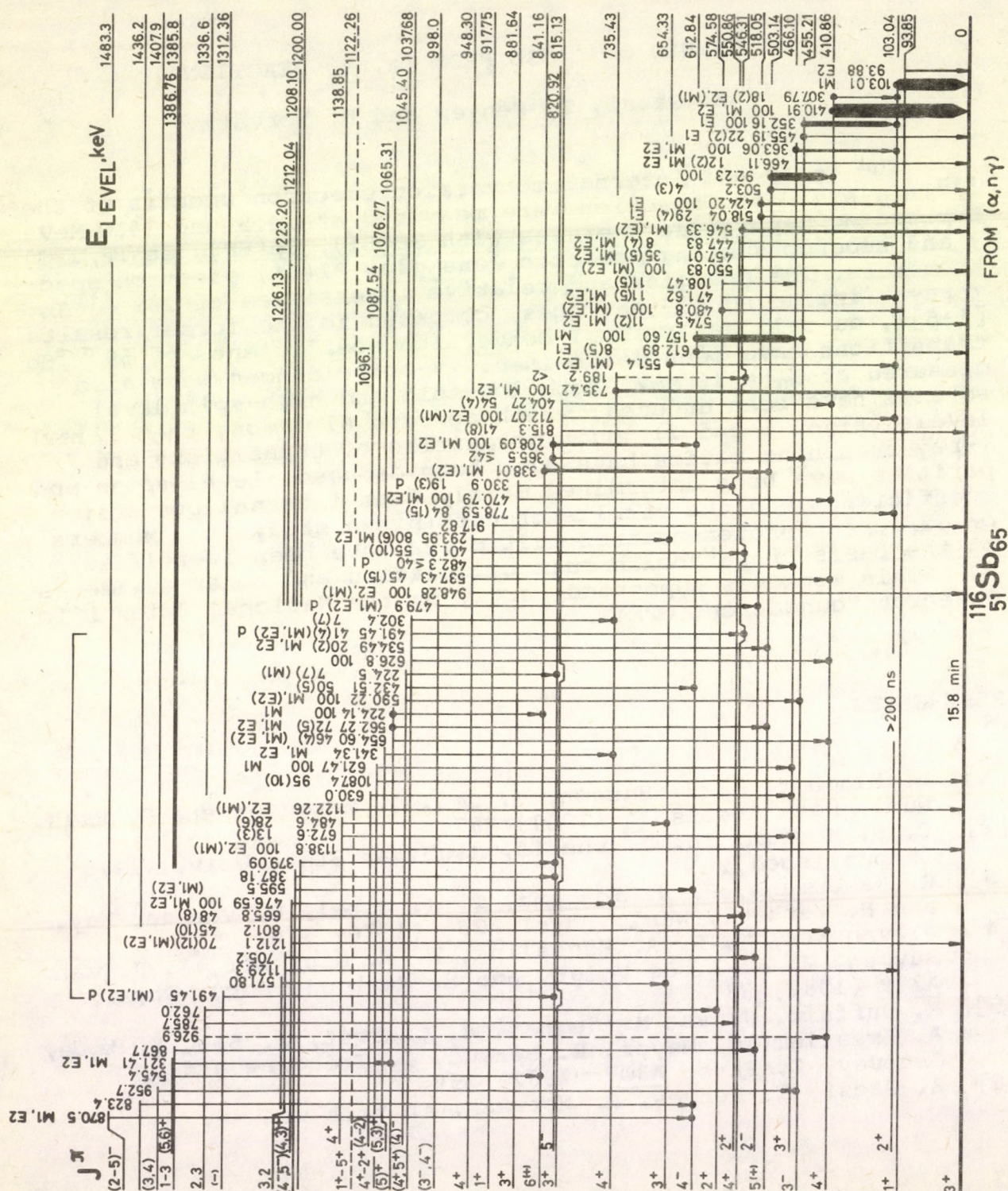


Fig. 1. Proposed low-spin (≤ 6) level scheme of ^{116}Sb (based on the 3^+ ground state) from $^{113}\text{In}(\alpha, n\gamma)^{116}\text{Sb}$ reaction. Solid circles at the ends of arrows indicate $\gamma\gamma$ -coincidence relations. γ -ray branching ratios and multipolarities are also given.

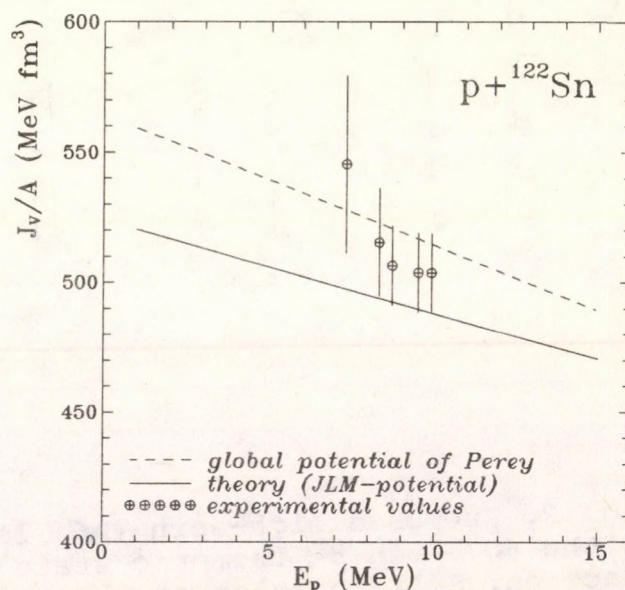
PROTON ELASTIC SCATTERING ON EVEN Sn ISOTOPES NEAR THE COULOMB BARRIER

M. Józsa, Z. Máté, T. Vertse and L. Zolnai

The anomalous behaviour of the optical potential in the neighbourhood of the Coulomb barrier was shown for $p+^{116}\text{Sn}$ and $p+^{120}\text{Sn}$ scattering in the papers [1] and [2]. The real depth of the proton optical potential increased more rapidly than the depth values predicted by the well known global fits (Perey, Becchetti-Greenlees) as the center-of-mass energy came closer to the Coulomb barrier.

Elastically scattered proton angular distribution measurements have been extended for the $^{112,118}\text{Sn}$ nuclei in the same way as it was presented for $^{114,122,124}\text{Sn}$ nuclei in the last Annual Report [3]. From the optical model analysis of the measured angular distributions volume integrals per nucleon of the real potential were derived. The experimental data seems to support the anomalous behaviour of the volume integrals as it is demonstrated for the case of ^{122}Sn in figure 1. The dashed line shows the volume integral calculated from the global potential of Perey [4] and the solid line represents the volume integral based on microscopic optical potential calculus introduced by Jeukenne, Lejeune and Mahaux (JLM-potential) [5].

Fig.1. The energy dependence of the real part of the volume integral of the proton optical potential for ^{122}Sn . The experimental values were obtained from optical model analysis with Perey geometry.



References

- [1] B. Gyarmati, T. Vertse, L. Zolnai, A.I. Baryshnikov, A.F. Gurbich, N.N. Titarenko and E.L. Yadrovsky, J.Phys. G5 (1979) 1225
- [2] A.F. Gurbich, V.P. Lunev and N.N. Titarenko, Yadernaja Fizika 40 (1984) 310
- [3] M. Józsa, Z. Máté, Z. Veress, T. Vertse and L. Zolnai, ATOMKI Annual Report (1988) 18
- [4] F.G. Perey, Phys. Rev. 131 (1963) 745
- [5] J.P. Jeukenne, A. Lejeune and C. Mahaux, Phys. Rev. C16 (1977) 80

STOPPING OF LIGHT IONS IN COMPOSITE AND METALLIC FOILS.

J. Dominguez, Zs. Fülöp, Á.Z. Kiss, M. Bjönberg⁺,
J. Räisänen⁺ and E. Rauhala⁺.

Our programme [1] to measure stopping powers of composite and metallic foils for protons and helium ions has been continued during 1989. This work is motivated by the fact that although accurate stopping power data are needed in many applications they are poorly known yet especially for composite foils and in some cases either for pure elements.

The measurements were performed in the transmission geometry and exploited the wide energy range of protons and alpha particles provided by the Van de Graaff accelerator and the MGC cyclotron of the Institute.

Stopping power values for alpha particles in the Kodak LR 115 nuclear track detector material and in Al and Sn have been measured in the energy range of 1 to 11 MeV. Also stopping power values for protons have been determined in the Kodak LR 115 and Sn nearly in the same energy range. A comparison of the experimentally determined stopping power values with an empirical model based on the Brandt-Kitagawa theory is in progress.

In the frame of a co-operation project with the University of Helsinki the measurements were extended to ions of higher Z number like Li and C.

REFERENCE

Á.Z. Kiss, E. Somorjai, J. Räisänen and E. Rauhala,
Nuclear Instruments and Methods in Physics Research
B39 (1989) 15.

⁺University of Helsinki, Accelerator Laboratory, Helsinki, Finland.

A HALF-LIFE AND ABUNDANCE SYSTEMATICS OF NUCLEI

I. TOROK

About 15 years ago, with the help of the IAEA Nuclear Data Center (Vienna), who provided us with half-life data, we prepared a graphical systematics of the half-lives of radioactive nuclei [1,2]. In the meantime many new nuclides were synthesized. They give a chance to test the predicting power of our old systematics.

Now we are completing the graphs with new half-life and isotope abundance data obtained from IAEA.

Recently it is available a list of solar system abundances of the elements, based on a critical review of all C1 chondrite analyses up to mid-1982 [3]. The authors, Anders and Ebihara, gave also the isotopic abundances of individual nuclides relative to silicon (at./ 10^6 Si). In the new edition of our work, in addition to the two dimensional graphs, we incorporate some three dimensional views of the data. As an example we present the abundances of the even-even stable isotopes (Fig. 1.).

References

- [1] L. Sarkadi, I. Török, ATOMKI Bull. 18(1976)609.
- [2] L. Sarkadi, I. Török, ATOMKI Bull. 19(1977)283.
- [3] E. Anders, M. Ebihara, Geochim. et Cosmochim. Acta 46(1982)2363.

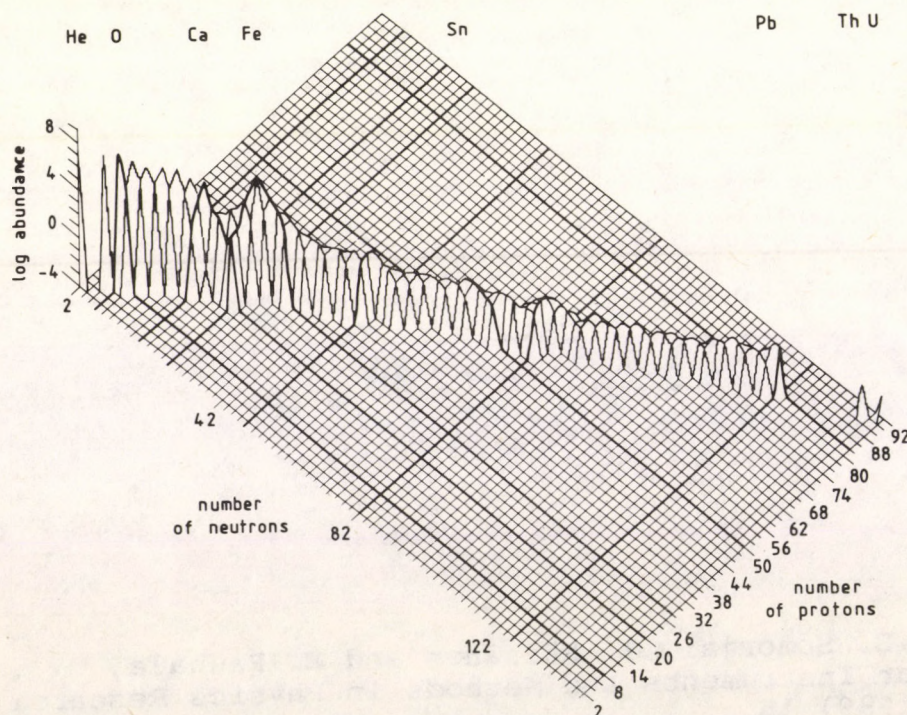


Fig. 1. A logarithmic display of the abundances of the even-even stable isotopes.

Microscopic versus semimicroscopic estimates for the alpha+deuteron spectroscopic factor of ${}^6\text{Li}$

K. Varga and R. G. Lovas

As a continuation of the preliminary work reported on in the Annual Report of 1988 [1], we have studied the $\alpha+d$ clustering in the ground state of ${}^6\text{Li}$ theoretically. We have now characterized the clustering in the most conventional way, viz. via the spectroscopic factor. This is defined as the norm square of the fragmentation amplitude, i.e. the overlap of the ${}^6\text{Li}$ wave function with those of the free fragments. The microscopic models ranging from the harmonic oscillator $\alpha+d$ model [2] to the most realistic dynamical cluster model [3] predict the $\alpha+d$ spectroscopic factor, $S_{\alpha d}$ to be close to unity, while the semimicroscopic $\alpha+p+n$ three-particle models (e.g. [4-6]) give $S_{\alpha d}=0.5-0.75$. Thus far the experiment has been unable to decide unambiguously between these two values [7]. A critical comparison between the microscopic and semimicroscopic models shows that the difference between the dynamics of the two families of models is not enough to account for this discrepancy. It is, however, possible that the difference is due to the treatment of the Pauli principle.

In the three-particle model the α particle is treated as structureless, and the Pauli principle is allowed for through repulsive potential terms or through inclusion of a projection operator to exclude Pauli forbidden states. The model assumes a three-body Schrödinger equation for a wave function $\psi(\mathbf{r}_{pn}, \mathbf{r}_{\alpha d})$. The conventional three-body definition of the fragmentation amplitude is

$$g(\mathbf{r}_{\alpha d}) = \int d\mathbf{r}_{pn} \phi_d^*(\mathbf{r}_{pn}) \psi(\mathbf{r}_{pn}, \mathbf{r}_{\alpha d}), \quad (1)$$

where $\phi_d(\mathbf{r}_{pn})$ is the deuteron wave function. We have pointed out [3], however, that if the nucleon structure of the α particle is taken into account, the Pauli principle implies a different formula:

$$g(\mathbf{r}_{\alpha d}) = \int d\mathbf{r}_{pn} \phi_d^*(\mathbf{r}_{pn}) \hat{A}_{\alpha pn}^{1/2} \psi(\mathbf{r}_{pn}, \mathbf{r}_{\alpha d}), \quad (2)$$

where $\hat{A}_{\alpha pn}$ is the norm operator of the $\alpha+p+n$ resonating-group model. This is an integral operator whose kernel contains the α intrinsic wave function.

We have now calculated the spectroscopic factor with the conventional as well as with the correct definition, eqs. (1) and (2), of the fragmentation amplitude using the three-particle wave functions of Lehman *et al.* [4], Voronchev *et al.* [5] and Kukulin *et al.* [6]. We assumed a 0s harmonic oscillator shell-model state for the α particle. The square-root operator $\hat{A}_{\alpha pn}^{1/2}$ is defined by the spectral decomposition of $\hat{A}_{\alpha pn}$, which can be given in terms of products of harmonic oscillator wave functions $\varphi_{nlm}(\mathbf{r}_{\alpha d})$ and $\varphi_{n'lm}(\mathbf{r}_{pn})$.

Table 1. $\alpha+d$ spectroscopic factors of three-particle models

Definition	Lehman	Voronchev	Kukulin
3-body	0.63	0.76	0.74
Pauli-correct	0.85	0.99	0.96

The results are shown in table 1. The most realistic microscopic estimate is 0.93 [3], while the most reliable experimental value is 0.73 ± 0.09 [7]. We see that the correct definition has brought the value of the spectroscopic factor of the three-particle models close to those of the microscopic models.

We thus conclude that with the microscopically well-founded formula the microscopic and semimicroscopic models produce $\alpha+d$ spectroscopic factors that are reassuringly close to each other. Considering that any refinements on the models are likely to lower the theoretical values, we can say that we are near to understanding the $\alpha+d$ structure of ${}^6\text{Li}$ quantitatively.

- [1] K. Varga and R. G. Lovas, ATOMKI Ann. Report, 1988, p. 27
- [2] I. V. Kurdyumov, V. G. Neudatchin and Yu. F. Smirnov, Phys. Lett. **31B** (1970) 426
- [3] R. G. Lovas, A. T. Kruppa, R. Beck and F. Dickmann, Nucl. Phys. **A474** (1987) 451
- [4] D. R. Lehman and M. Rajan, Phys. Rev. **C25** (1982) 2743
- [5] V. T. Voronchev, V. M. Krasnopol'sky, V. I. Kukulin and P. B. Sazonov, J. Phys. **G8** (1982) 667
- [6] V. I. Kukulin, V. M. Krasnopol'sky, V. T. Voronchev and P. B. Sazonov, Nucl. Phys. **A417** (1984) 128
- [7] R. Ent, H. P. Blok, J. F. A. van Hienen, G. van der Steenhoven, J. F. J. van den Brand, J. W. A. den Herder, E. Jans, P. H. M. Keizer, L. Lapikás, E. N. M. Quint, P. K. A. de Witt Huberts, B. L. Berman, W. J. Briscoe, C. T. Christou, D. R. Lehman, B. E. Norum and A. Saha, Phys. Rev. Lett. **57** (1986) 2367

The reaction ${}^6\text{Li}(e, e'p){}^5\text{He}$ and three-particle clustering in ${}^6\text{Li}$

R. G. Lovas, A. T. Kruppa and J. B. J. M. Lanen[†]

[†] *Fysisch Laboratorium, Rijksuniversiteit Utrecht*

By removing a nucleon from a nucleus, one can study its core plus single-particle structure. When the initial nucleus is ${}^6\text{Li}$, the residual system is likely to be in a two-cluster state. Thus the proton removal is to be described by a cluster model rather than by a shell model.

The ${}^6\text{Li}(e, e'p){}^5\text{He}$ reaction leading to the ${}^5\text{He}$ continuum has been recently studied experimentally at NIKHEF-K, Amsterdam [1]. We used our microscopic cluster model to interpret the inferences drawn from these experiments for nuclear structure [2]. We described the reaction by an unfactorized distorted-wave impulse approximation (DWIA) in comparison with its plane-wave limit (PWIA). The structure amplitudes in these reaction models were supplied by our dynamical microscopic cluster model [3].

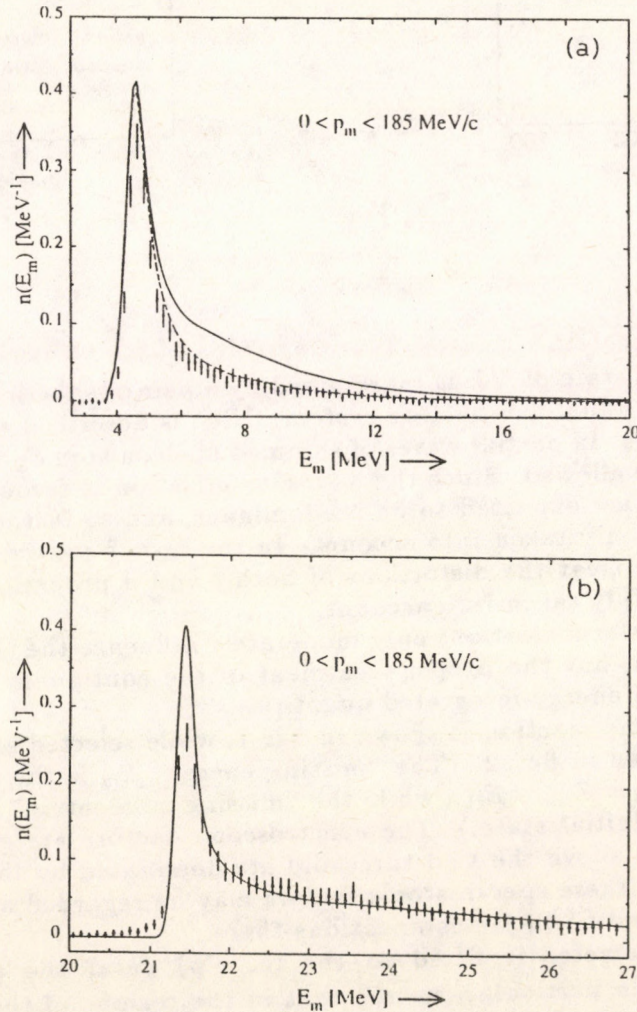


Figure 1

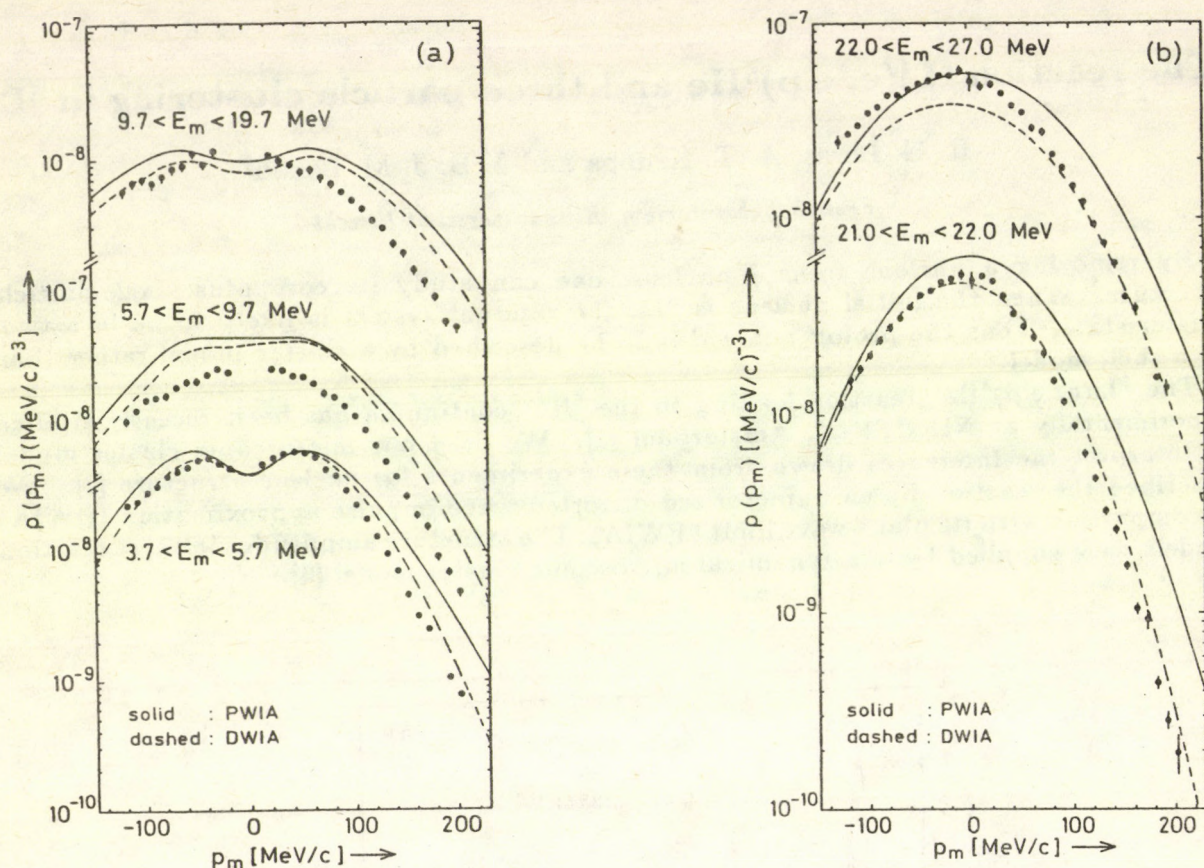


Figure 2

In this model the ground state of ${}^6\text{Li}$ is represented by a pair of spherically distortable α and d clusters, while the residual five-nucleon system, ${}^5\text{He}$, is described as a continuum of $\alpha+n$ and $t+d$ clusterizations. In partial waves of summed nucleon spin $S_5 = \frac{1}{2}$ both the $\alpha+n$ and $t+d$ clusterizations are allowed. Since the $\alpha+n$ clusterization is favoured energetically very much, the $\alpha+n$ terms are expected to be predominant, and so in these partial waves the distortability of α was only taken into account. In the $S_5 = \frac{3}{2}$ partial waves, however, $\alpha+n$ is not allowed, and we treat the distortions of both t and d properly. The scattering boundary conditions were duly taken into account.

It was found that the cluster distortions only moderately influence the ${}^5\text{He}$ - p energy and momentum structure of ${}^6\text{Li}$, but the proper treatment of the continuum is indispensable even for the reproduction of energy-integrated quantities.

The energy spectrum of the reaction is shown in fig. 1, while selected energy-integrated momentum spectra are shown in fig. 2. (The "missing energy" E_m is the difference of the *intrinsic* nuclear energies, $E_m = E_{{}^5\text{He}} - E_{{}^6\text{Li}}$, while the "missing momentum" p_m is the p - ${}^5\text{He}$ relative momentum in the initial state.) The spectroscopic factors are given in table 1. Since the regions below and above the $t+d$ threshold are dominated by the $\alpha+n$ and $t+d$ clusterizations, respectively, these spectroscopic factors may be regarded as characterizing the weights of the $\alpha+p+n$ and $t+d+p$ clusterizations there.

Considering that no parameter is fitted to the $(e, e'p)$ data, the agreement with experiment is satisfactory. In particular, we see that in the regions of the prominent $\frac{3}{2}^-$ and $\frac{3}{2}^+$ peaks the description is excellent. Appreciable discrepancy has only been found in the energy continuum above the $\frac{3}{2}^-$ ground-state resonance of ${}^5\text{He}$, which is the region

Table 1. Spectroscopic factors below and above the t+d threshold ($E_m = 21$ MeV)

	Peak region $E_m=3.7-5.7$ MeV	Off-peak region $E_m=5.7-19.7$ MeV	Peak region $E_m=21-22$ MeV	Off-peak region $E_m=22-27$ MeV
Theory	0.578	0.638	0.357	0.480
Experiment	0.44 ± 0.05	0.32 ± 0.04	0.30 ± 0.04	0.53 ± 0.07

of the broad $\frac{1}{2}^-$ bump. (In the dashed curve in fig. 1a the $\frac{1}{2}^-$ partial wave is omitted.) An improvement here seems to require a component in the ${}^6\text{Li}$ wave function of summed nucleon spin zero and summed orbital momentum unity, which can be generated most naturally as a type of ${}^5\text{He}+p$ structure.

- [1] J. B. J. M. Lanen, A. M. van den Berg, H. P. Blok, J. F. J. van den Brand, C. T. Christou, R. Ent, A. G. M. van Hees, E. Jans, G. J. Kramer, L. Lapikás, D. R. Lehman, W. C. Parke, E. N. M. Quint, G. van der Steenhoven and P. K. A. de Witt Huberts, Phys. Rev. Lett. **62** (1989) 2925
- [2] J. B. J. M. Lanen, R. G. Lovas, A. T. Kruppa, H. P. Blok, J. F. J. van den Brand, R. Ent, E. Jans, G. J. Kramer, L. Lapikás, E. N. M. Quint, G. van der Steenhoven, P. C. Tiemeyer and P. K. A. de Witt Huberts, to appear in Phys. Rev. Lett.;
R. G. Lovas, A. T. Kruppa and J. B. J. M. Lanen, submitted to Nucl. Phys. A
- [3] R. Beck, F. Dickmann and A. T. Kruppa, Phys. Rev. **C30** (1984) 1044;
R. Beck, F. Dickmann and R. G. Lovas, Nucl. Phys. **A446** (1985) 703;
A. T. Kruppa, R. G. Lovas, R. Beck and F. Dickmann, Phys. Lett. **179B** (1986) 317;
R. Beck, F. Dickmann and R. G. Lovas, Ann. Phys. (N.Y.) **173** (1987) 1;
R. G. Lovas, A. T. Kruppa, R. Beck and F. Dickmann, Nucl. Phys. **A474** (1987) 451;
A. T. Kruppa, R. Beck and F. Dickmann, Phys. Rev. **C36** (1987) 327

AN ALGEBRAIC MODEL OF CLUSTER STATES IN ODD MASS NUCLEI

G. Lévai and J. Cseh

The interplay between collective and single particle degrees of freedom is an essential feature of many odd mass nuclei. For the description of nuclear collective motion several phenomenologic algebraic nuclear models have been proposed. The first model of this kind was the Interacting Boson Model giving account of quadrupole collectivity in even-even nuclei. Later the vibron model was introduced as an algebraic approach to dipole type collectivity [1,2]. The $O(4)$ limit of this model has been applied to the description of the rotational-vibrational motion of chemical molecules, while the $U(3)$ limit was used to classify cluster states in even-even light nuclei [3]. In connection with this application the role of the Pauli principle has also been discussed [4].

These phenomenologic models of collective motion have been extended to incorporate single particle degrees of freedom as well. The coupling of collective (bosonic) and fermionic degrees of freedom is formulated in terms of group theory, with a group structure depending on the fermionic states taken into account in these models. While the fermionic extension of the IBM (called IBFM) has been worked out for each dynamical symmetry, the similar treatment of the vibron model has only been carried out for the $O(4)$ limit [5], giving rise to the vibron-electron model of chemical molecules.

We have introduced the missing $U(3)$ limit of the vibron-fermion model [6] as an algebraic approach to the cluster states in light odd-even nuclei. In this model the particle-like or hole-like fermions are allowed to occupy the states of a nuclear shell with n oscillator quanta. An essential point of this model is the decomposition of the fermionic angular momentum into orbital and spin part resulting in the fermionic group structure

$$U^F(m) \supset U_l^F(m/2) \times U_s^F(2) \supset SU_l^F(3) \times U_s^F(2) \supset O_l^F(3) \times SU_s^F(2) \supset Spin^F(3)$$

where l and s refer to the orbital and spin momenta of the fermionic states and

$m = (n + 1)(n + 2)$. This group chain is then coupled to the

$$U^B(4) \supset U^B(3) \supset SU^B(3) \supset O^B(3)$$

group structure of the $U(3)$ limit of the vibron model, leading to the $SU(3) \times U(2)$ dynamical symmetry of the vibron-fermion model. (We chose this name in accordance with the corresponding limit of the IBFM [7].) Besides this strong coupling limit, a weak coupling limit of the model can also be formulated.

Although it is possible to consider several fermions in this model, we took only one as the first step. We calculated the energy eigenvalues of the Hamiltonian associated with this dynamical symmetry and determined the matrix elements of the electromagnetic transition operators $T(E2)$, $T(M1)$ and $T(E1)$. We also studied the one nucleon transfer reactions in terms of this model which enabled us to link the $SU(3) \times U(2)$ states to vibron model states. Among the potential applications here we mention only the cluster states of the nuclei ^{19}F , ^{21}Ne and ^{43}Sc .

Our investigations also clarified somewhat the reason why the field of application of the $O(4)$ and $U(3)$ limits of the vibron model are so different.

The fermionic extension of the vibron model provides a deeper insight into its physical nature and may help us to proceed further towards the microscopic interpretation of this phenomenologic model.

REFERENCES

- 1) F. Iachello, Phys. Rev. **C23**, 2778 (1981).
- 2) F. Iachello and R. D. Levine, J. Chem. Phys. **77**, 3046 (1982).
- 3) J. Cseh and G. Lévai, Phys. Rev. **C38**, 972 (1988).
- 4) J. Cseh, J. Phys. Soc. Jpn. Suppl. **58**, 604 (1989).
- 5) A. Frank, R. Lemus and F. Iachello, J. Chem. Phys. **91**, 29 (1989).
- 6) G. Lévai and J. Cseh, to be published.
- 7) R. Bijker and V. K. B. Kota, Ann. Phys. (N. Y.) **187**, 148 (1988).

STUDY OF THE $^{15}\text{N} + \alpha$ STRUCTURE IN ^{19}F IN TERMS OF THE VIBRON-FERMION MODEL

G. Lévai and J. Cseh

Many low lying ($E_x \leq 10 \text{ MeV}$) states of the ^{19}F nucleus are known to have marked $^{15}\text{N} + \alpha$ or $^{16}\text{O} + t$ cluster character. These states have been studied in terms of various models, such as the local cluster model of Buck *et al.* [1], the coupled-channel orthogonality condition model (OCM) [2] and the generator coordinate method (GCM) [3]. Several cluster bands have been identified, some of which have equivalents in the $^{16}\text{O} + \alpha$ system.

Microscopic studies showed [3] that satisfactory results can be obtained taking only the $^{15}\text{N} + \alpha$ configuration into account and neglecting the $^{16}\text{O} + t$ configuration. At the same time the importance of the excited state of the ^{15}N core with $J^\pi = 3/2^-$ has been emphasized. The coupling of the configurations $^{15}\text{N}(1/2^-) + \alpha$ and $^{15}\text{N}(3/2^-) + \alpha$ has been discussed both in the local cluster model [4] and in the GCM framework [3].

Cluster states of light nuclei have also been interpreted in terms of the vibron model [5], which is an algebraic model of dipole type collectivity. In particular the $U(3)$ limit of the vibron model has been applied to the $^{16}\text{O} + \alpha$ system [6]. The fermionic extension of this model, the vibron-fermion model offers a convenient way to treat the interplay between collective and single particle degrees of freedom, so it seems natural to apply it to the cluster states of the ^{19}F nucleus. In this model [7] the relative motion of the α cluster is coupled to the fermionic structure, which is now a hole on the p shell, accounting for the $J^\pi = 1/2^-$ and $3/2^-$ states of the ^{15}N core. Various limiting cases (dynamical symmetries) of the model correspond to strong and weak coupling of the bosonic (collective) and fermionic (single particle) degrees of freedom.

We fitted a spectrum with $SU(3) \times U(2)$ dynamical symmetry (corresponding to strong coupling) to 25 well known cluster states belonging to 6 cluster bands

[8]. In addition to the usual one- and two-body terms in the Hamiltonian two third order terms were also considered to give a more realistic description of the spin-orbit coupling.

The relatively large amount of experimental information on the $E2$, $M1$ and $E1$ transitions between cluster states of ^{19}F allowed us to test the predictions of the model. Our calculations in the $SU(3) \times U(2)$ limit showed that this simple phenomenologic model is somewhat less successful than other models in reproducing the $E2$ and $M1$ transition rates, nevertheless it gives a better approximation of the $E1$ transition rates. We also studied the one nucleon transfer reaction going from the ground state of the ^{20}Ne nucleus to the cluster states of ^{19}F . These calculations involved both vibron model and vibron-fermion model states. Our results are in good agreement with the available experimental data. The algebraic cluster models are unable at present to describe cluster spectroscopic factors, but work is in progress to overcome this problem [9].

A more refined description of the ^{19}F nucleus could be given in terms of the vibron-fermion model either by maintaining the dynamical symmetry and including higher order terms in the operators, or by breaking the dynamical symmetry with new interaction terms.

REFERENCES

- 1) B. Buck and A. A. Pilt, Nucl. Phys. **A280**, 133 (1977).
- 2) T. Sakuda and F. Nemoto, Prog. Theor. Phys. **62**, 1606 (1979).
- 3) P. Descouvemont and D. Baye, Nucl. Phys. **A463**, 629 (1987).
- 4) A. C. Merchant, Nucl. Phys. **A417**, 109 (1984).
- 5) F. Iachello, Phys. Rev. **C23**, 2778 (1981).
- 6) J. Cseh and G. Lévai, Phys. Rev. **C38**, 972 (1988).
- 7) G. Lévai and J. Cseh, in this volume.
- 8) G. Lévai and J. Cseh, to be published.
- 9) J. Cseh, G. Lévai and K. Kato, in this volume.

CLUSTER SPECTROSCOPIC FACTORS IN THE VIBRON MODEL

J. Cseh, G Lévai, and K. Kato *

The vibron model [1,2] is an algebraic model of the dipole collectivity, so it may be applied both to chemical molecules [2] and to nuclear cluster states [3-6]. However, being a model of bound states, it is unable to describe resonance-widths. It seems to be a serious drawback from the viewpoint of its application to nuclear cluster states [7], which, from other respects, has several advantages [6].

We propose a series expansion, similar to that of the Hamiltonian, to obtain cluster spectroscopic factors in the vibron model. Then resonance-widths can be obtained from them, in the usual way [8], if needed.

The reason for this proposal is given by the link between the vibron model and the microscopic cluster model, in the harmonic oscillator limit [5].

We start with the spectroscopic amplitude, as defined in [9,10]:

$$A_{NL}(A, A') = \langle \Phi_{A'} \Phi_x \Phi_{NLM} | \mathcal{A} | \Phi_A \rangle, \quad (1)$$

where $\Phi_{A'}$, Φ_x , and Φ_A are wave functions of the A' , x , and A nuclei ($A' + x = A$), Φ_{NLM} is a harmonic oscillator wave function, and \mathcal{A} is the antisymmetrizer between the nucleons of A' and x . The cluster model wave function is:

$$\Phi_A = N_{NL}(A, A') \mathcal{A} [\Phi_{A'} \Phi_x \Phi_{NLM}], \quad (2)$$

where N_{NL} is a normalization factor. Consequently, the spectroscopic amplitude of the cluster model (in the harmonic oscillator limit) is:

$$A_{NL}(A, A') = \langle \Phi_{A'} \Phi_x \Phi_{NLM} | \mathcal{A} N_{NL} \mathcal{A} | \Phi_{A'} \Phi_x \Phi_{NLM} \rangle. \quad (3)$$

From the viewpoint of the vibron model the phenomenological treatment of this formula is as follows. The Φ_{NLM} wave function of the relative motion corresponds to the vibron model wave function, while $\Phi_{A'}$ and Φ_x are internal wave functions of

* Hokkaido University, Department of Physics, Sapporo, Japan

the two clusters. In the simple case of the structureless clusters they do not appear, while in case of a deformed core, for instance, $\Phi_{A'}$ can be an IBM wave function. As for the missing operator of

$$\mathbf{A}_{NL} = \mathcal{A} N_{NL} \mathcal{A}, \quad (4)$$

we can apply a series expansion in terms of number conserving bilinear products of boson creation ($\sigma^+, \pi_\mu^+, \mu = -1, 0, 1$) and annihilation ($\tilde{\sigma}, \tilde{\pi}_\mu, \mu = -1, 0, 1$) operators, coupled to $O(3)$ scalars. This is the usual construction method in the interacting boson models for any physical quantity [11]. Because of the relation between the $A_{NL}(A, A')$ amplitudes and the $S_L(A, A')$ spectroscopic factors:

$$S_L(A, A') = \Sigma_N A_{NL}^2(A, A'), \quad (5)$$

it is more useful to apply the expansion to the square of the operator (4). When written explicitly up to two-body terms it reads:

$$\begin{aligned} A_{n_\pi L}^2 = & a_0 + a_1^{(1)} [\sigma^+ \times \tilde{\sigma}]_0^{(0)} + a_2^{(1)} [\pi^+ \times \tilde{\pi}]_0^{(0)} \\ & + a_1^{(2)} [[\pi^+ \times \pi^+]^{(0)} \times [\tilde{\pi} \times \tilde{\pi}]^{(0)}]_0^{(0)} + a_2^{(2)} [[\pi^+ \times \pi^+]^{(2)} \times [\tilde{\pi} \times \tilde{\pi}]^{(2)}]_0^{(0)} \\ & + a_3^{(2)} [[\pi^+ \times \pi^+]^{(0)} \times [\tilde{\sigma} \times \tilde{\sigma}]^{(0)} + [\sigma^+ \times \sigma^+]^{(0)} \times [\tilde{\pi} \times \tilde{\pi}]^{(0)}]_0^{(0)} \\ & + a_4^{(2)} [[\sigma^+ \times \sigma^+]^{(0)} \times [\tilde{\sigma} \times \tilde{\sigma}]^{(0)}]_0^{(0)} + a_5^{(2)} [[\pi^+ \times \sigma^+]^{(1)} \times [\tilde{\pi} \times \tilde{\sigma}]^{(1)}]_0^{(0)} \\ & + \dots \end{aligned} \quad (6)$$

Here we changed to the n_π subscript, which is more appropriate in the vibron model, than N . Their relation is:

$$n_\pi = 2N + L. \quad (7)$$

In the limit of the $U(3)$ dynamic symmetry some of the coefficients vanish, and the matrix elements are diagonal in the $U(3)$ basis:

$$A_{n_\pi L}^2 = \alpha_0 + \alpha_1 n_\pi + \alpha_2 n_\pi^2 + \beta_2 L(L+1) \dots, \quad (8)$$

where the coefficients α_i and β_i are some linear combinations of those in (6).

Hopefully, by calculating spectroscopic factors from the vibron model in the way shown here, it can give a more complete description of the nuclear molecular states.

REFERENCES

- 1) F. Iachello, Phys. Rev. **C23**, 2778 (1981).
- 2) F. Iachello, and R. D. Levine, J. Chem. Phys. **77**, 3046 (1982).
- 3) K. A. Erb, and D. A. Bromley, Phys. Rev. **C23**, 2781 (1981).
- 4) J. Cseh, Phys. Rev. **C31**, 692 (1985).
- 5) J. Cseh and G. Lévai, Phys. Rev. **C38**, 972 (1988).
- 6) J. Cseh, J. Phys. Soc. Jpn. Suppl. **58**, 604 (1989).
- 7) A. Arima, in Proceedings of the International Symposium on Developments in Nuclear Cluster Dynamics, Edited by: Y. Akaishi et. al., World Scientific, Singapore, 1989, p. 338.
- 8) A. M. Lane and R. G. Thomson, Rev. Mod. Phys. **30**, 257 (1958).
- 9) M. Ichimura, A. Arima, E. C. Halbert, and T. Terasawa, Nucl. Phys. **A204**, 225 (1973).
- 10) A. Arima, in Heavy Ion Collisions Vol. 1., Edited by: R. Bock, North-Holland Publ. Co., Amsterdam, 1979, p. 417.
- 11) F. Iachello and A. Arima, The Interacting Boson Model, Cambridge University Press, Cambridge, 1987.

A CRITICAL INVESTIGATION INTO OKHRIMENKO'S APPROXIMATION METHOD

A. Csótó, B. Gyarmati and A. T. Kruppa

Okhrimenko extended [1] a method which had been developed for the bound and scattering solutions of the two-body Schrödinger equation by Okhrimenko and Filippov [2], so as to include resonant (Gamow) solution, as well. The method is based on the expansion of the two-body wave function in terms of harmonic oscillator (HO) functions. This fact not only renders the method very convenient for application in the resonating group method (RGM) but also allows to calculate the coefficients \bar{c}_i of the expansion in the asymptotic region from a three-term recurrence relation. The far-away starting value \bar{c}_M can be calculated from a differential equation. By prescribing the form of its solution the desired asymptotic behaviour can be imposed on the wave function. It has now the form

$$\psi = \sum_{i=0}^n c_i \varphi_i + \sum_{i=n+1}^M \bar{c}_i \varphi_i,$$

where $\{\varphi_i\}$ is the HO basis, n is large enough to assure that φ_n extends to a region where the potential is already negligible. The quantization of the energy comes about by requiring that

$$c_n(E) = \bar{c}_n(E).$$

In Ref. 1 the method was applied for calculating the resonances of the ${}^8\text{Be}$ as an $\alpha - \alpha$ system, in the framework of the RGM. In this calculation n and M were typically 100-200 and 1000-2000, respectively.

When having applied the complex scaling method (CSM) for the same ${}^8\text{Be}$ problem [3] we got suspicious about the results of Ref. 1. In particular we guessed that some of the given energy values are spurious resonances. We decided to scrutinize this problem in a simple model case where the conceptual and practical complications connected to the Coulomb force, and some of the computational difficulties are absent. We used a simple real, local, short-ranged potential: $V(r) = -8.0 \exp(-0.16r^2) + 4.0 \exp(-0.04r^2)$ (atomic units were used). Now the summation can be rigorously extended to $M = \infty$, and all the uncertainties coming about from the approximate treatment of the far-away region are avoided. The results are compiled in Fig. 1. The crosses denote the resonances which can be found also with CSM and the so called Siegert method (see e.g. [4]). Except the crosses belonging to a) and b) the others are stable against the indicated variation of the basis size. The cross a) belongs to $n=110$ and the crosses b) to $n=140$ and 170 , respectively. This is how a resonance reaches its stable n -independent position. The stars lying along the straight lines do not show any tendency to get stabilized.

In Fig.2 the basis size is kept fixed ($n=50$) but we introduced an extra nonlinear parameter in the basis, namely we used $\bar{b} = b \exp(i\theta)$ complex size parameter in the HO functions. Obviously the value of θ must not disturb the position of the physical resonances. Indeed, the crosses are independent of it, but the stars show a strong dependence on the value of θ , they even can be swept out of the physical quarter of the energy sheet. The straight lines belong to the indicated θ values, along the arcs the θ varies by steps 0.02 from 0.48 to 0.70 and from 0.92 to 1.00, respectively. It is to be seen that the use of θ not only provides an efficient tool for distinguishing the true resonances from the false ones, but also speeds up the convergence. (Already at $\theta = 0.2$ with a basis size $n=50$ the third resonance is stable in contrast with the $\theta = 0$ case when it starts getting stable at $n=170$.) The completion of our investigation by extending it to non-local potentials is under-way.

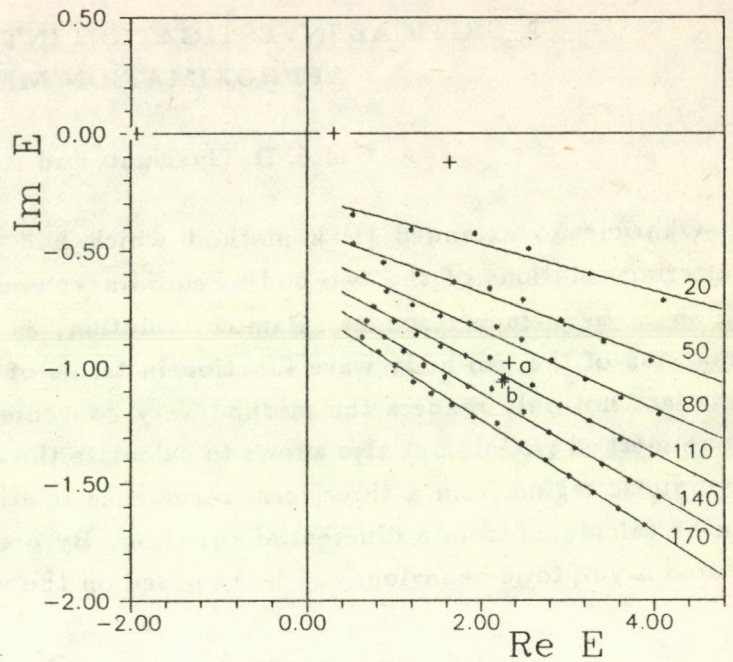


Fig. 1

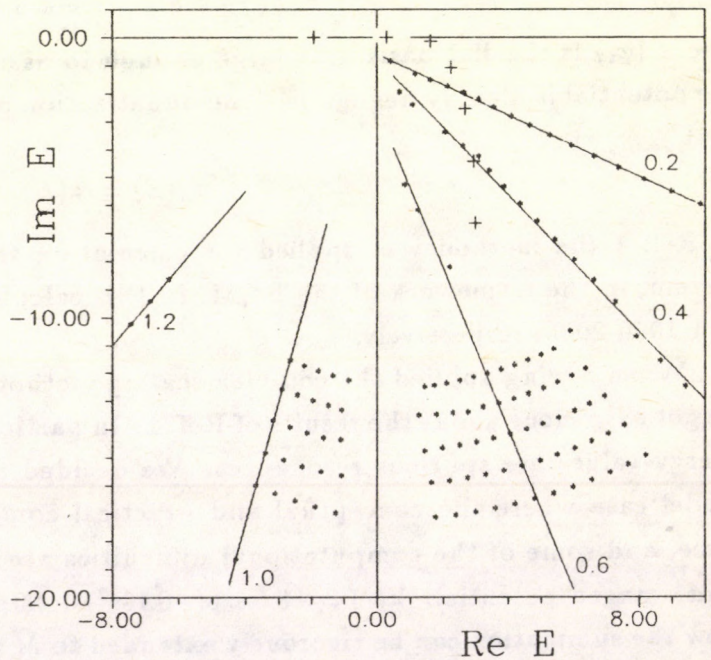


Fig. 2

REFERENCES

- [1] I. P. Okhrimenko, *Few-Body Syst.* **2**, 169 (1987).
- [2] G. F. Filippov and I. P. Okhrimenko, *Sov. J. Nucl. Phys.* **32**, 480 (1980); I. P. Okhrimenko, *Nucl. Phys.* **A424**, 121 (1984).
- [3] A. T. Kruppa, R. G. Lovas and B. Gyarmati, *Phys. Rev. C* **37**, 383 (1988).
- [4] H. R. Fiebig and A. Weiguny, *Z. Phys. A* **279**, 275 (1976).

ATOMIC PHYSICS

**High resolution Ne K-Auger spectra from
 H^+ , Ne^{3+} , Ne^{10+} , Ar^{6+} , Ar^{16+} (5.5 MeV/u) - Ne collisions**

I. Kádár, S. Ricz, J. Vég, B. Sulik, D. Varga and D. Berényi

Energetic heavy ion impact induced Ne Auger KLL spectra has been studied by the high-resolution ESA-21 electron spectrometer. The projectiles were Ne^{3+} , Ne^{10+} , Ar^{6+} , Ar^{16+} (5.5 MeV/u) and also H^+ of the same velocity. To analyse the complex Auger spectra in which many satellite lines are included stemming from multiply ionized neon states, the measured series of interrelated spectra was used by the help of a properly developed computerized procedure [1].

Energy and intensity of the lines in the spectra were determined and an identification procedure was carried out for all the vacancy configurations from Li-like states to the F-like states (diagram lines). In the analysis the fact, that the transitions originating from different vacancy states (or configurations) are represented in different proportion in the spectra at the impact of different ions, has been used to separate the groups of lines belonging to different initial vacancy states (or configurations). The identification of the Auger lines was also helped eventually by the study of their angular distribution from 0° to 180° .

The results were compared with the corresponding theoretical transition energy and intensity values [2]. We found that higher order corrections (configuration mixing, relativistic and QED corrections, etc.) are not negligible in the theoretical calculations even in the case of $Z=10$.

Based on the above results it was possible to obtain information on the multiple ionization process at the impact parameter region of the K-shell ionization. Thus, for the first time we determined the two-dimensional vacancy configuration distribution (2s, 2p vacancies) for all the states which were attainable by Auger transitions (see Fig. 1). The experimentally determined vacancy configuration distributions did not show any significant difference from the predictions of the independent particle model.

We found that the geometrical model of ionization [3] is quite good for strongly ionizing collisions. No definite tendency was found in the ionization probabilities as a function of the degree of ionization.

Finally, there was pointed out, by analysing the Auger line shapes, that the collision and deexcitation processes could not be completely separated from each other even for the high impact velocity region. A definite post collision interaction was found between the ejected electrons and the deexciting ionic core, for the prompt Auger transitions [4]. The above finding may be a warning that separated collisional models and ionic structure calculations should be handled with care for any impact velocities.

The review paper of the present study is in press in Phys. Rev. A.

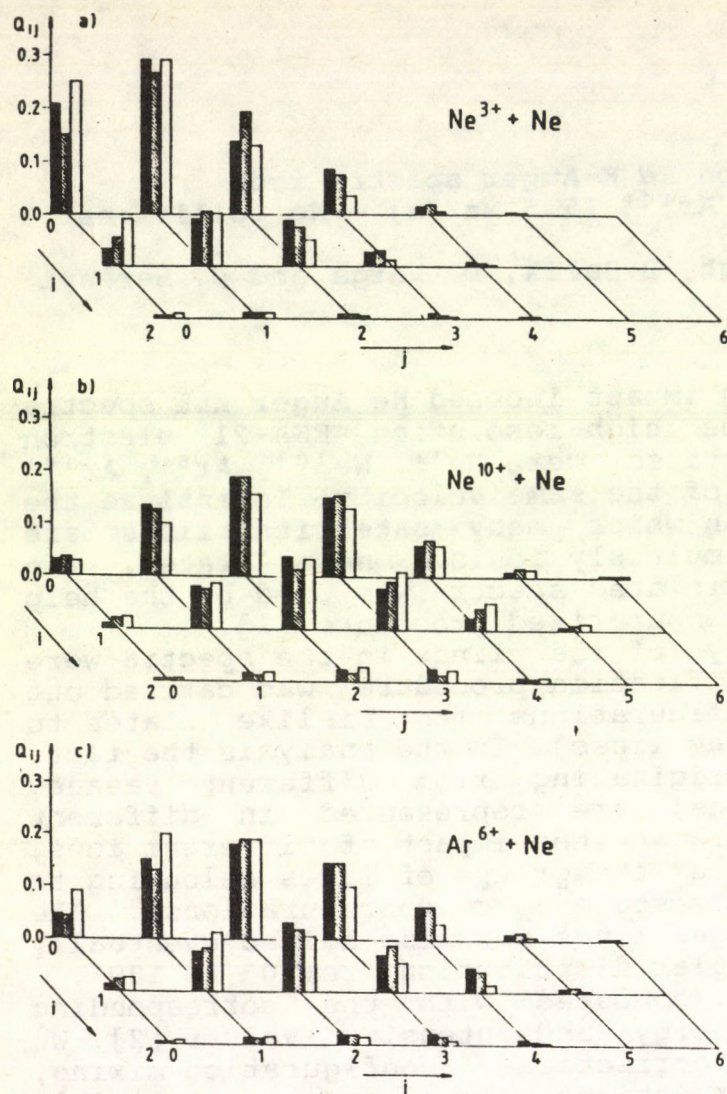


Fig. 1
The experimentally determined vacancy configurations (full bars) compared to the double binomial distributions fitted to the experimental data (shadowed bars) and to the theory [6] (empty bars). i and j are the number of 2s and 2p vacancies.

References:

- [1] J. Vègh, I. Kádár, S. Ricz, B. Sulik, D. Varga and G. Székely, Nucl. Instr. Meth. **A281** 605 (1989)
I. Kádár, S. Ricz, B. Sulik, D. Varga, J. Vègh and D. Berényi, Nucl. Instr. Meth. **B40/41** 60 (1989).
- [2] R. J. Maurer and R. L. Watson, At. Nucl. Data Tables **34** 185 (1986),
M. O. Krause, T. A. Carlson and W. E. Moddeman, J. de Phys. **32** C4-139 (1971),
S. Schumann, K. O. Groeneveld and G. Nolte, Z. Phys. **A289** 245 (1979),
C. E. Moore, Atomic Energy Levels, Vol. I., National Bureau of Standards 467, 1949, Washington,
H. P. Kelly, Phys. Rev. **A11** 556 (1975),
C. P. Bhalla, J. El. Spy. Rel. Phenom. **7** 287 (1975),
M. H. Chen and B. Craseman, At. Nucl. Data Tables, **38** 381 (1988),
M. H. Chen, Phys. Rev. **A31** 1449 (1985),
M. H. Chen and B. Craseman, Phys. Rev. **A12** 959 (1975)
- [3] B. Sulik, I. Kádár, S. Ricz, D. Varga, J. Vègh, G. Hock and D. Berényi, Nucl. Instr. Meth. **B28** 509 (1987).
- [4] S. Ricz, I. Kádár and J. Vègh, Nucl. Instr. Meth. **B40/41** 77 (1989).

HIGHER ORDER MULTIPOLE CONTRIBUTION (A_4) TO THE AUGER ANGULAR DISTRIBUTIONS OBSERVED IN $Ne^{3+} - Ne$ COLLISION

S. Ricz, J. Végh, D. Varga, I. Kádár, B. Sulik, D. Berényi

The angular distribution of $KL_{23}-L_{23}L_{23}L_{23}$ Auger satellites of Ne excited by H^+ , N^{2+} , Ne^{3+} , Ne^{10+} and Ar^{6+} have already been published in refs. 1, 2. We found definite anisotropic angular distributions which were described by using only anisotropy parameter A_2 . There were, however, some indications in ref 2 for the presence of a transition with both A_2 and A_4 if not only the above mentioned satellite group was evaluated.

The measurements were performed using the electrostatic electron spectrometer ESA-21. The spectrometer is the combination of a two-electrode spherical decelerating lens, a spherical mirror, and a double pass, double focussing cylindrical mirror. The experimental details, the evaluation and identification procedure have been published in ref 3.

Recently, the anisotropy parameters of N-like satellite Auger lines of neon target have been determined from Ne^{3+} -Ne collisions. Table 1 shows the measured and calculated energies, intensities and measured anisotropy parameters (see next page). Seven of them shows a definite presence of anisotropy which can be described only by using both anisotropy parameters A_2 and A_4 while several of them by A_2 only. In some cases, the anisotropy values are in contradiction with the identifications in Table 1. For such transition, where the total angular momentum is less than two and the A_4 is not equal to zero, the identification was mistaken in ref 3. In other cases we can say that the simple LS-coupling model is not good for multiply ionized neon.

Although the present results are preliminary ones, the definite presence of a large A_4 value may show the deficiency of the independent particle approximation in describing the collision process causing multiple ionization of neon.

REFERENCES

1. S. Ricz, I. Kádár, V. A. Shchegolev, D. Varga, J. Végh, D. Berényi, G. Hock and B. Sulik, J. Phys. B: 19 (1986) L411.
2. S. Ricz, J. Végh, I. Kádár, B. Sulik, D. Varga and D. Berényi, "High-energy Ion-Atom Collisions" (Proc. 3rd Workshop on High Energy Ion-Atom Collision Processes, August 3-5, 1987, Debrecen, Hungary) Lecture Notes in Physics Vol. 294, Eds. D. Berényi and G. Hock, Springer-Verlag, Heidelberg 1988, p. 197.
3. I. Kádár, S. Ricz, J. Végh, B. Sulik, D. Varga and D. Berényi, in print in Phys. Rev.
4. R. J. Maurer and R. L. Watson, At. Data Nucl. Data Tables, 34 (1986) 185.
5. C. P. Bhalla, J. of Electr. Spectr. Rel. Phenom. 7 (1975) 287.

Table 1

N - like satellite lines

Initial state	Final state	Auger energy		Relative intensity [%]		Anisotropy parameter	
		E_{exp}	E_{th}^*	Exp	Th**	A_2	A_4
124 4P	-204 3P	713.06(12)	714.90	3.69(9)	4.49	0.024(2)	0.012(1)
	-213 3S	730.25(9)	730.70	2.44(7)	1.67	-0.018(6)	
	-213 3P	738.84(3)	740.90	4.40(17)	3.15	0.082(12)	
	-213 3D	742.48(4)	744.80	2.05(5)	5.25	-0.043(4)	
	-222 3P	764.50(3)	766.00	6.26(18)	11.57	-0.082(40)	-0.015(2)
124 2D	-204 1D	717.14(4)	717.30	2.76(10)	3.17	0.016(2)	
	-213 1D	739.76(3)	737.80	1.84(5)	3.78	0.177(21)	
	-222 1S	764.90(5)	762.30	4.65(12)	1.52	-0.108(15)	
	-222 1D	769.29(2)	768.30	5.76(15)	11.20	-0.148(19)	-0.073(11)
124 2P	-204 3P	720.65(1)	721.80	4.12(11)	2.61	0.084(39)	-0.112(65)
	-213 1P	734.42(5)	734.40	2.34(10)	0.34	0.203(55)	
	-213 3S	737.21(1)	737.60	6.02(18)	2.94	-0.197(31)	
	-213 3D	749.95(3)	751.70	3.86(10)	0.21	0.000(0)	
	-222 3P	772.13(2)	772.90	2.28(6)	6.75	-0.203(78)	
124 2S	-213 1P	740.96(3)	739.80	1.67(4)	1.16	0.077(6)	
	-213 3P	752.25(6)	753.20	2.61(7)	0.37	-0.170(23)	
	-222 1D	774.53(4)	774.30	2.68(7)	1.74	-0.100(10)	
115 4P	-204 3P	737.92(4)	738.30	2.91(8)	1.32	0.082(12)	
	-213 3P	762.97(8)	764.30	3.64(9)	5.71	0.116(25)	
	-213 3D	767.03(6)	768.20	11.61(31)	13.18	-0.068(14)	0.067(11)
115 $^2P^+$	-204 3P	747.84(4)	747.50	4.10(13)	2.38	0.051(9)	-0.104(13)
	-213 1P	761.93(2)	760.10	5.57(16)	1.67	0.137(24)	
	-213 1D	765.75(5)	764.10	7.12(18)	3.84	-0.205(29)	-0.017(2)
115 $^2P^-$	-213 1D	773.22(4)	771.70	1.69(4)	0.16	-0.149(16)	
	-213 3P	781.06(3)	781.10	2.01(5)	2.69	-0.122(25)	
	-213 3D	784.44(9)	785.00	0.57(1)	6.17	0.000(0)	

*Maurer&Watson⁴**Bhalla⁵

L₃-SUBSHELL ALIGNMENT INDUCED BY ELECTRON CAPTURE IN H⁺-Ar COLLISION

L. Sarkadi, J. Pálinkás, A. Kövér, T. Vajnai+ and J. Végh

The study of the alignment of inner-shell vacancies is a sensitive tool to test the collision dynamics. Inner-shell vacancies are created two processes: direct Coulomb ionization and electron capture. While the alignment due to ionization has been widely studied, until the present work there has been only indirect information on the degree of the alignment induced by electron capture. For light target atoms and for low collision velocities ($v/v_{n1} < 1$) the role of the electron capture increases. For description of the alignment the simplest capture theory, namely the Oppenheimer-Brinkmann-Kramers approximation (OBK) has been suggested [1]. Most of the measured total (ionization and capture) alignment data [2,3] support the OBK theory.

One can get direct information on the alignment induced by electron capture measuring the angular distribution of the decay products (x-rays, Auger electrons) of the excited state in coincidence with the charge-changed outgoing projectiles. In our experiment we chose the p-Ar collision system and detected the $L_{2,3}-M_{2,3}^2$ Auger electrons. The electrons were analyzed by a cylindrical mirror electron spectrometer. The outgoing H⁰ atoms were separated from the protons by electrostatic deflection. At higher impact energies the atoms were detected by a surface barrier silicon detector. For low-energy detection a special particle detector has been developed. Electron spectra belonging to the single, coincidence+random, and random events were recorded simultaneously (Fig. 1).

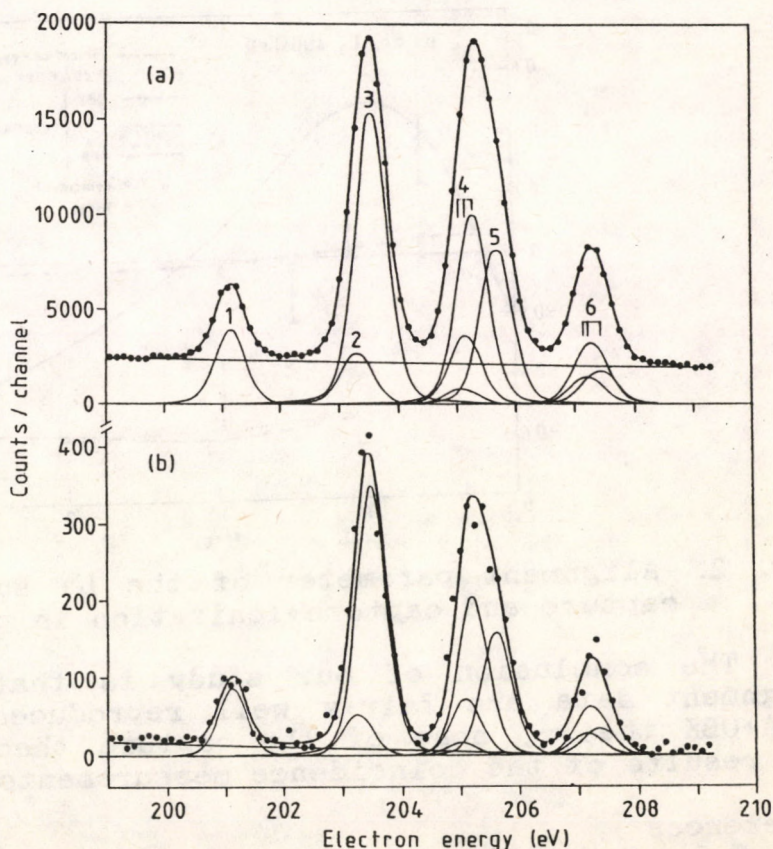


Fig. 1. Single (a) and coincidence (b) Auger electron spectrum measured at 0.7 MeV proton impact. The observation angle is 163°. The notations of the peaks are: 1, $L_{3}-M_{2,3}^2(1S_0)$; 2, $L_{2}-M_{2,3}^2(1S_0)$; 3, $L_{3}-M_{2,3}^2(1D_2)$; 4, $L_{3}-M_{2,3}^2(3P_{0,1,2})$; 5, $L_{2}-M_{2,3}^2(1D_2)$; 6, $L_{2}-M_{2,3}^2(3P_{0,1,2})$.

The anisotropy parameter of three L₃ lines (transitions 1,3,4 in Fig. 1) have been determined measuring the intensity ratios of the anisotropic L₃ lines and the sum of all the isotropic L₂ lines (transitions 2,5,6 in Fig. 1), at two electron emission angles near 90° and 180°. It was assumed that the angular distribution is described by the P₂ Legendre polynomial. The alignment parameter was calculated from the measured L₃-M_{2,3}²(¹S₀) anisotropy parameter using the known angular momentum couplig coefficient(a_2) for this transition.

As a further result of our present work we could determine the so far unknown a_2 values for the L₃-M_{2,3}²(¹D₂) and L₃-M_{2,3}²(³P_{0,1,2}) transitions applying the measured alignment parameters. In Fig. 2 results of the single (ionization+capture) and coincidence (capture) measurements are compared with the predictions of the plane wave Born approximation (PWBA)[1], OBK [1], the impulse approximation (IA)[4], and the strong potential (transverse peaking) Born approximation (SPB)[4].

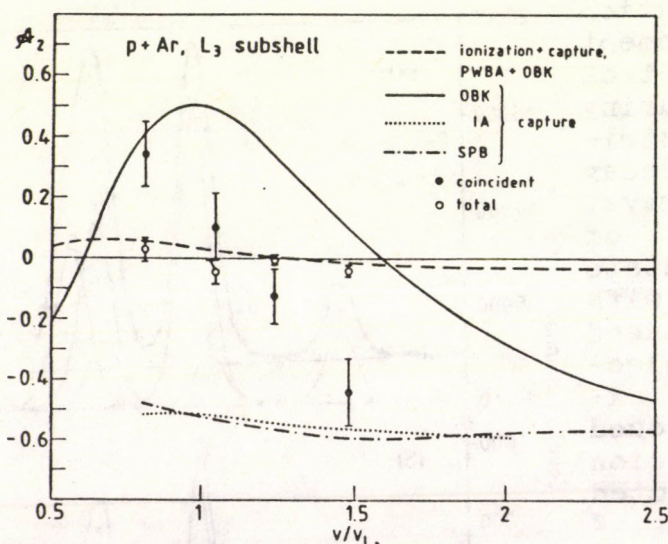


Fig. 2. Alignment parameter of the L₃ subshell excited by capture and capture+ionization in p-Ar collision.

The conclusion of our study is that while the total alignment data are fairly well reproduced by the combined PWBA+OBK theory, none of the capture theories can describe the results of the coincidence measurements.

References

- [1] E.G. Berezhko, N.M. Kabachnik and V.V. Sizov, Phys. Lett. 77A (1980) 231 and J. Phys. B 14 (1981) 2635.
- [2] R. DuBois, L. Mortensen and M. Rodbro, J. Phys B 14 (1981) 1613.
- [3] W. Menzel and W. Mehlhorn, J. Phys. B 20 (1987) L277.
- [4] D.H. Jakubassa-Amundsen, J. Phys. B 14 (1981) 2647 and private communication.

*On leave from Technical University for Heavy Industry, Miskolc, Hungary

EVIDENCE FOR DOMINANCE OF LONGITUDINAL ELECTRON EJECTION IN ELECTRON LOSS PROCESS

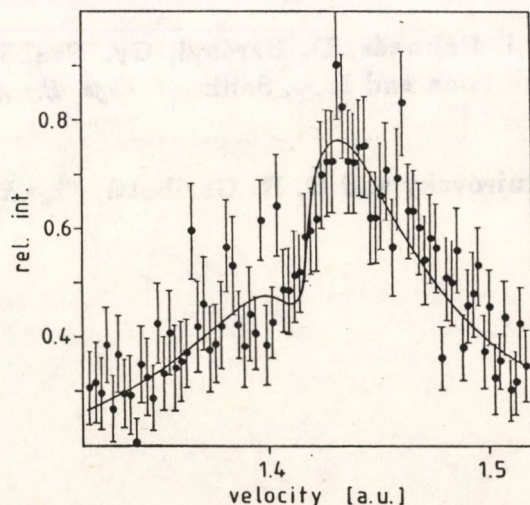
L. Gulyás, L. Sarkadi, Á. Kövér, T. Vajnai, D. Berényi, and S. B. Elston †

For structured light projectiles (like H^0 , He^+) the electron transfer into the projectile's ion continuum (Electron Loss, ELC) exhibits a cusp-shaped spectrum of the electron velocity distribution when the electron velocity matches the ion velocity.

According to the recent ELC theories the cusp can be described by a series expansion [1-3]:

$$\frac{d\sigma}{d\vec{v}} = \sum_{j=2}^{2n} \frac{1}{\vec{v}^j} (1 + \beta_j P_j(\cos\theta')), \quad j \text{ even,}$$

where $d\sigma/d\vec{v}$ is the double differential cross section in the laboratory frame, \vec{v}' and θ' are the velocity and emission angle of the ejected electron in the projectile frame, respectively, n is the principal quantum number of the active electron, P_j are the Legendre polynomials. β_j are the expansion coefficients depending on the collision velocity and the initial state of the projectile.



ELC cusp for 50 keV/amu He^+ -He collisions ($\theta_0 = 1^\circ$).

Experiment: • ; Fitted curve: —

† University of Tennessee and Oak Ridge National Laboratory, Oak Ridge, Tennessee, USA

Generally, the β_j describe the anisotropy of the electron ejection in the projectile frame. Regarding the first non-vanishing coefficient β_2 , the emission pattern (referred to the beam direction) changes from a preferred longitudinal ejection to a transversal one as β_2 changes its sign from positive to negative. The anisotropy character reflects a drastic variation in the shape of the peak, measured in the laboratory frame. In the case $\beta_2 < 0$ the electron distribution has a singular behaviour (sharp peak) at $v'=0$, while in the second case, $\beta_2 > 0$, a dip appears at the top of the peak (inverse cusp).

Up to the present study nobody could demonstrate this dip experimentally because at low projectile velocities the electron capture to continuum process dominates the ELC process [4].

We studied the shape of the ELC cusp in the 50-150 keV/amu He^+-He collision system measuring the ejected electrons in coincidence with the outgoing He^{2+} projectiles. The spectra were fitted to a generic expression of Meckbach et. al.[5]. To describe possible second order effects (e. g. simultaneous capture and loss) further terms (B_{10}, B_{11}, B_{12}) missing from the above expression were also incorporated in the fitting. The determined β_2 values are positive indicating the existence of the cusp inversion (see the dip at velocity 1.41 a.u. in the fitted curve on the figure).

References

- [1] J. S. Briggs and M. H. Day, *J. Phys. B.: At. Mol. Phys.* **13** (1980) 4797.
- [2] J. Burgdörfer, M. Breinig, S. B. Elston and I. A. Sellin, *Phys. Rev. A* **28** (1983) 3277.
- [3] Gy. Szabó, J. Burgdörfer, Á. Kövér, *ATOMKI Annual Report*, 1989,
- [4] Á. Kövér, L. Sarkadi, J. Pálinkás, D. Berényi, Gy. Szabó, T. Vajnai, O. Heil, K. O. Groeneveld, J. Gibbons and I. A. Sellin, *J. Phys. B.: At. Mol. Phys.* **22** (1989) 1595.
- [5] W. Meckbach, I. B. Nemirovsky and C. R. Garibotti, *Phys. Rev. A* **24** (1981) 1793.

TESTING THE FITTING PROCEDURE USED FOR STUDYING THE 'CUSP' SPECTRA

L. Gulyás, A. Kővér, Gy. Szabó, T. Vajnai, D. Berényi

A number of publications have been appeared about the fitting of the observed 'cusp' spectra for electron transfer to the projectile's continuum (ETC) to a generic expression of Meckbach et al.[1-5]. The method based on the series expansion of the cross-section [5]:

$$U = \sum_{n,j} B_{nj} \int (v')^{(n-1)} P_j(\cos\theta') S(v, \theta) d\vec{v}$$

where U is the measured intensity, P_j is the Legendre polynomials. v and θ are the velocity and angle of the ejected electron in the laboratory frame, the prime labels the same values in the projectile system. B_{nj} are the fitting parameters and $S(v, \theta)$ is the transmission function of the spectrometer.

The detailed examination of the above evaluation method show the crucial role of the spectrometer transmission function in the result of the fitting. The different authors use different type of spectrometers and all of them use approximations in determining the $S(v, \theta)$ function. The errors introduced by these approximations might be the explanation of the relatively large discrepancies among the B_{nj} values published by different authors [1,3].

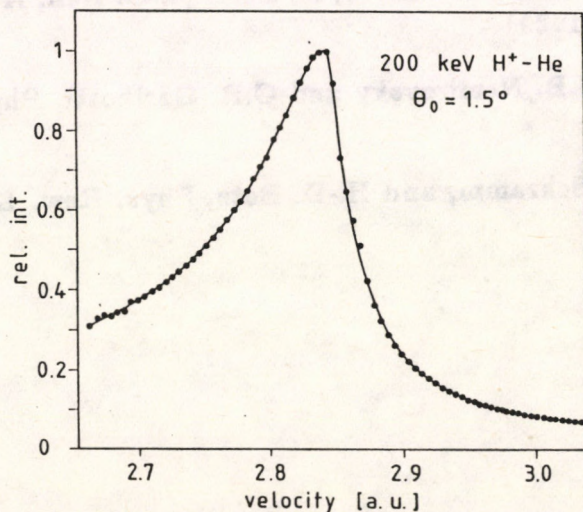


Figure: Measured (•) and fitted cusp yield (—)

The present study is a part of a joint effort of our group and the corresponding group in Bariloche, Argentina. In this we measured the same process on different spectrometers but otherwise at the same experimental conditions. Namely the cusp yield (electron capture to the projectile continuum) were measured in the 200-300 keV $H^+ \rightarrow He$ collision systems at 0° ejection angle. The angular resolution were

$\theta_0 = 0.2^\circ - 2.5^\circ$. The electron spectra measured at the different spectrometers are being analysed separately by the fitting routine used in the two group. In this way we can get information about the errors introduced by the approximations of the $S(v, \theta)$ functions and we can check the fitting procedure.

The figure shows the spectra measured by the ESA-13 spectrometer (Debrecen) and the result of the fitting with six B_{nj} ($n=0,1; j=0,1,2$) parameters.

The spectra measured at different spectrometer acceptance angles make possibility to study the cusp asymmetry ratio (Γ_L/Γ_R) as a function of the spectrometer acceptance angles. According to our preliminary evaluation the Γ_L/Γ_R ratio seems to be constant in the $\theta_0 = 0.2^\circ - 2.5^\circ$ region, which is in contradiction with the paper of Oswald et al [6]. The measurement on the other spectrometer (in the group of Prof. Meckbach) are running now and the detailed results will be published in the near future.

References

- 1 . D. Berényi, L. Gulyás, Á. Kövér, J. de Phys. 48, C9-231., (1987)
- 2 . Y.C. Yu and G. Lapicki, Phys. Rev A 36, 4710., (1987)
- 3 . M. W. Lucas and W. Steckelmacher, / Proceedings of the 3rd Workshop on High-Energy Ion-Atom Collisions, Debrecen/, Springer Vlg., Berlin 1988, p. 229
- 4 . L. Gulyás, Gy. Szabó, Á. Kövér, D. Berényi, O. Heil, K.O. Groeneveld, Phys. Rev. A39, 463., (1989)
- 5 . W. Meckbach, I.B. Nemirovsky and C.R. Garibotti, Phys. Rev. A 24, 1793., (1981)
- 6 . W. Oswald, R. Schramm, and H.-D. Bets, Phys. Rev. Lett. 62, 1114, (1989)

COUPLED-STATES CALCULATIONS FOR L-SHELL IONIZATION OF THORIUM INDUCED BY HEAVY IONS

L. Sarkadi and T. Mukoyama*

Recently Berinde et al. [1] have investigated the vacancy sharing processes occurring in L-shell ionization of atoms at heavy-ion impact. They measured the subshell ionization cross section ratios of thorium bombarded by 0.5-2.5 MeV/amu Be, C, F, Mg, Si and S ions. They compared their results to the predictions of first-order SCA calculations [2]. The observed large deviations indicated a considerable amount of vacancy transfer between the subshells in these collisions. The authors could give a qualitative interpretation of their data performing coupled-channel calculations.

For a quantitative analysis we have made calculations applying the coupled-states model described in [3]. The model gave a reasonable description of the dependence of the subshell ratios on the the atomic number of the projectile and on the collision velocity (as an example, see Fig. 1).

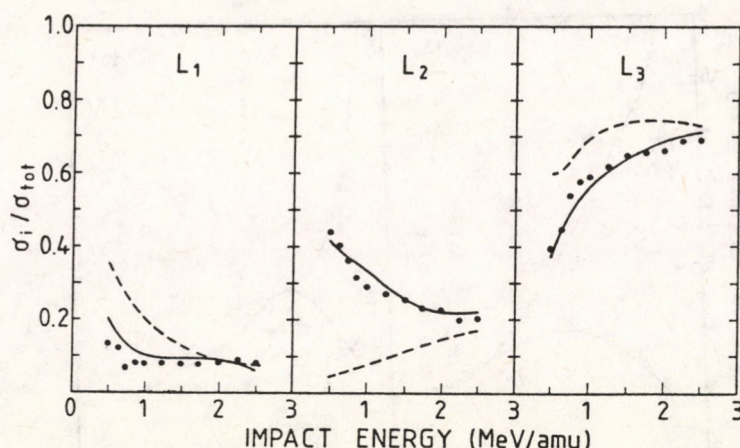


Fig. 1. Contributions of the subshells to the total L-shell ionization for Mg on Th. The experimental points [1] are compared to results of SCA [2] (dashed curve) and coupled-states model [3] (full curve) calculations.

References

- [1] A. Berinde, C. Ciortea, A. Enulescu, D. Flueraşu, I. Legrand, I. Piticu and V. Zoran, Proc. of 3rd Workshop on High-Energy Ion-Atom Collisions, Debrecen, Hungary, 1987, Lecture Notes in Phys. 294 (Springer-Verlag, 1988) p.107.
- [2] F. Rösler, D. Trautmann and G. Baur, Nucl. Instr. and Meth. 192 (1982) 43.
- [3] L. Sarkadi, J. Phys. B: At. Mol. Phys. 19 (1986) L755.

*Institute for Chemical Research, Kyoto University, Kyoto, Japan

L-SHELL IONIZATION BY ANTIPROTONS

L. Sarkadi and T. Mukoyama*

The significance of the theoretical studies of atomic collisions involving antiprotons has largely increased since the recent construction of the low-energy antiproton ring (LEAR) at the CERN. The experimental possibility to change the sign of the electric charge of the projectile provides a sensitive test of the theoretical descriptions.

We have analysed theoretically the particle-antiparticle differences which may occur in L-shell ionization. In addition to the binding- and Coulomb distortion effect discussed by Brandt and Basbas for the K shell [1], for the L shell a further effect due to couplings between the different subshells may also contribute to the differences [2].

To the present analysis we applied the coupled-states model described in [3]. The calculations have been made for gold target in the energy range 0.15-3 MeV. As an example, Fig. 1. shows our results obtained for the L₃- to L₂-subshell cross section ratios.

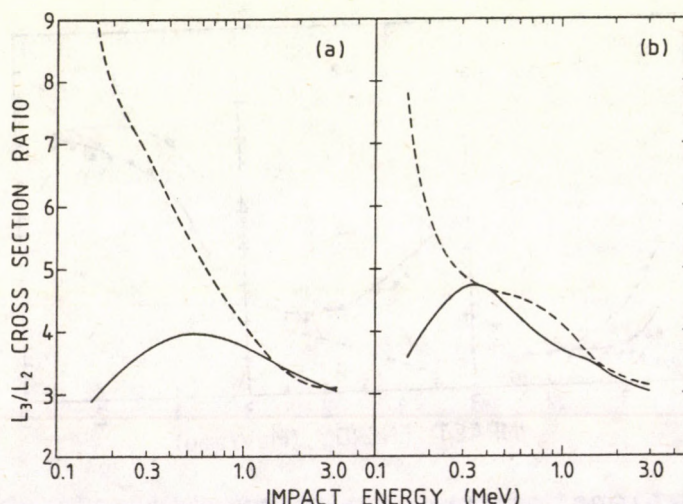


Fig. 1. L₃- to L₂-subshell ionization cross section ratios for proton (dashed curve) and antiproton (full curve) impact. The sources of the the differences for the two kinds of excitation: binding- and Coulomb effect (a); additional subshell coupling effect (b).

References

- [1] W. Brandt and G. Basbas, Phys. Rev. A 27 (1983) 578.
- [2] L. Sarkadi, Acta Physica Hungarica 65 (1989) 201.
- [3] L. Sarkadi, J. Phys. B: At. Mol. Phys. 19 (1986) L755.

*Institute for Chemical Research, Kyoto University, Kyoto, Japan

ELECTRON CAPTURE TO THE CONTINUUM AND SIMULTANEOUS TARGET EXCITATION (OR IONISATION) IN $He^{2+} \rightarrow He$ COLLISION SYSTEM

L. Gulyás, Gy. Szabó

Much attention has been paid in recent years to atomic collision where multielectronic processes are involved, i.e. simultaneous capture and excitation /or ionisation. In the present paper a two-electronic process, namely the electron capture into the continuum state of the projectile ion (ECC) and the simultaneous target excitation (TE) or ionisation (TI) are studied in $He^{2+} \rightarrow He$ collision system.

A theoretical calculation are made which is based on the first Born approximation with asymptotically correct boundary conditions (CB1) [1]. The initial electronic state of the He atom were described by a Roothaan-Hartree-Fock orbital [2] and hydrogenic wave functions were used for final states.

In the CB1 model the long range nature of the Coulomb interaction brings logarithmic phases in the asymptotic wave functions. This factors for the above process are $\frac{Z_P(Z_T-2)}{v} \ln(vR - \vec{v}\vec{R})$ in the entrance and $-\frac{(Z_P-1)(Z_T-1)}{v} \ln(vR + \vec{v}\vec{R})$ in the exit channels [3], which cause mathematical difficulties in calculating the transition amplitudes (Z_P and Z_T are the nuclear charge of the projectile and the target, \vec{v} and \vec{R} are the relative velocity and coordinate of the aggregates).

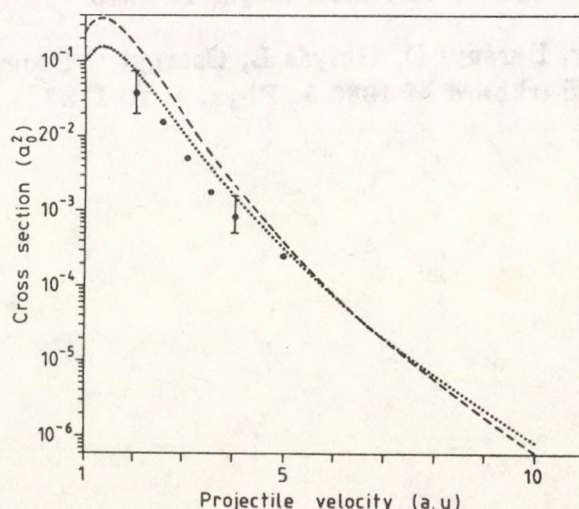


Figure: Single differential cross sections for electron capture to the continuum and simultaneous target excitation or ionisation processes in $He^{2+} \rightarrow He$ collision system. Theory: present result; --- First Born approximation only for ECC process, Ponce et al 1981 [5]. Experimental data: • Kövér et al. 1986.[7]

Avoiding the above difficulties the Coulomb distortion effect of the electron-electron interaction in the exit channel was neglected. This term was calculated on the

way as it is treated in the Brinkman-Kramers approximation [4]. As a result of the above modification, the calculation of the transition matrix element reduce essentially because of the Coulomb phases belong to the asymptotic states cancel each other. The further detail of the calculation are similiar to that ones used in full first Born approximation [5,6]. The averaged transition matrix element was used for comparison.

The result for the single differential cross-section are plotted on the figure (dotted line). The final state of the second electron (excited or ionised) are summed up via the closure approximation. As a comparison the figure show the result for ECC process calculated in the first Born approximation after the paper of Ponce [6] (the active target electron was described by hydrogenic orbital with a 1.7 nuclear charge).

References

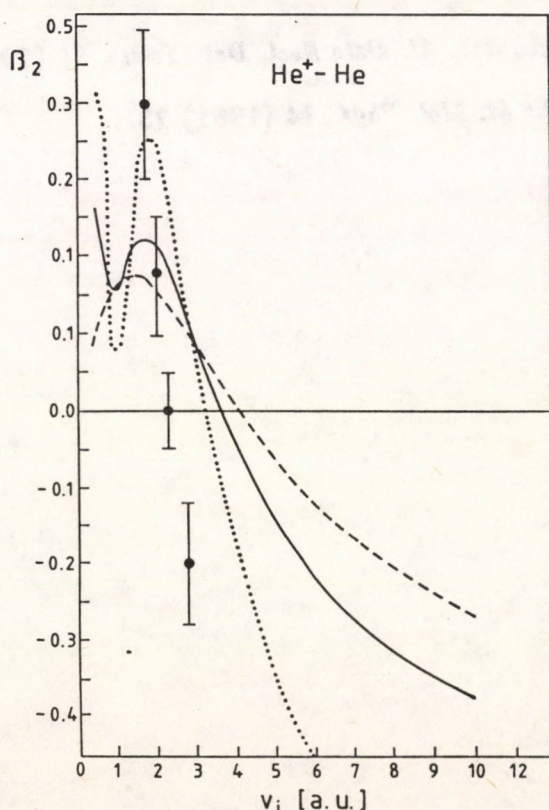
- 1 Belkić Dž, Gayet R and Salin 1979 A Phys. Rep. 56 279
- 2 Clementi E and Roetti C 1974 At. Data Nucl. Data Tables 14 177
- 3 Belkić Dž and Janev R K 1972 J. Phys. B: At. Mol. Phys. 6 1020
- 4 Brinkman H C and Kramers H A 1930 Proc. Acad. Sci Amsterdam 33 973
- 5 McDowell M R C and Colemann J P, 1970 Introduction to the Theory of Ion-Atom Collisions (Amsterdam:North-Holland)
- 6 Ponce V H 1981 J. Phys. B: At. Mol. Phys. 14 3643
- 7 Kövér Á, Szabó Gy, Berényi D, Gulyás L, Csernyi I, Groeneveld K O, Hofmann D, Koschar P and Burkhard M 1986 J. Phys. B 19 1187

CALCULATION OF THE β_2 PARAMETERS FOR ELECTRON LOSS PROCESS IN THE CASE of He^+-He COLLISIONS

Gy. Szabó, J. Burgdörfer † and Á. Kövér

Recently the second order anisotropy parameter (β_2) of the ELC cusp (ELC = Electron Loss to Continuum) was determined experimentally for the He^+-He collision system [1-2] as a function of the projectile velocity. The existing theories, however, determined this parameter only for the He^+-H^0 collision system [3-4].

In this paper we present theoretical β_2 values for the He^+-He collision system in order to compare them with the experimental results. The calculations were performed in the PWBA approximation with analytic Roothaan-Hartree-Fock wavefunctions [5] for the He target electrons. The excitation of target electrons was taken into account with closure approximation developed by Day [6]. The calculations were performed for $1s$, $2s$ and $1s + 10\% 2s$ initial states of the projectile ion. The reason of



Comparison of the calculated and measured β_2 values
Theory: - - - : $1s$; ... : $2s$; — : $1s + 10\% 2s$

† University of Tennessee and Oak Ridge National Laboratory, Oak Ridge, Tennessee, USA

the calculation for the mixture state is that a part of the He^+ projectiles can be excited to $2s$ metastable state by either the ion source or the collisions with residual gas atoms before interacting with the target.

Figure shows the theoretical and experimental β_2 parameters as a function of the projectile velocity. The slope of the experimental and theoretical data are similar but their absolute values differ from each other.

References

- [1] L. Gulyás, L. Sarkadi, Á. Kövér, T. Vajnai, D. Berényi and S. B. Elston, *ATOMKI Annual Report*, 1989,
- [2] L. Gulyás, D. Berényi, Á. Kövér, Gy. Szabó, L. Sarkadi, J. Pálinkás and T. Vajnai, *3rd European Conference on Atomic and Molecular Physics (ECAMP-3)*, Bordeaux, France, April 3-7, 1989.
- [3] J. S. Briggs and M. H. Day, *J. Phys. B.: At. Mol. Phys.*, **13** (1980) 4797.
- [4] J. Burgdörfer, M. Breinig, S. B. Elston and I. A. Sellin, *Phys. Rev.*, **A28** (1983) 3277.
- [5] E. Clementi and C. Roetti, *At. Data Nucl. Data Tables*, **14** (1974) 177.
- [6] M. H. Day, *J. Phys. B.: At. Mol. Phys.*, **14** (1981) 231.

M2/E1 MIXING IN L₃ X-RAY TRANSITIONS

T. PAPP, and I. TOROK

Thin Ba, Sm, and Er targets were bombarded by protons, at 0.23, 0.28, and 0.35 MeV bombarding energies respectively. These energies were chosen so, that the velocities of the protons relative to that of the L₃ electrons were the same.

Using such low energy protons as projectiles the magnetic subshells ($m=1/2$, $m=3/2$) of the L₃ subshell have different ionization probabilities, the L₃ subshell will be aligned. This alignment is reflected in the anisotropic angular distribution of the x-rays. If the final state of the x-ray transition is anisotropically populated by a specific process, and the initial state is statistically populated, the angular distribution of the x-ray transition can be expressed as

$$I(\theta) = I_0[1 + \beta P_2(\cos\theta)], \quad (1)$$

where I_0 is the total intensity, $P_2(\cos\theta)$ is the second order Legendre polynomial. The β anisotropy parameter is related to the A_2 alignment parameter of the final state through $\beta = \alpha A_2$, where α depends on the angular momentum of the initial and final states of the electromagnetic transition and on the M2/E1 mixing ratio (δ) [1].

The ratio of the β anisotropy parameters of different x-ray transitions, having the same final states, does not depend on the alignment parameter and is independent of the ionization process (as far as the single ionization is the dominating ionization process). Using Si(Li) detectors for the detection of the x-rays, several L₃ lines, e.g. the L₁ (L₃-M₁) and L _{α} (L₃-M_{4,5}) lines could be well resolved. The ratio of the anisotropy parameters of these lines can be written [1] as

$$\frac{\beta(L_1)}{\beta(L_\alpha)} = \frac{\alpha(L_1)}{\alpha(L_\alpha)} = \frac{0.5 - \sqrt{3} \delta(L_1)}{[0.1 + \sqrt{7/5} \delta(L_{\alpha 1}) - 0.4R]/(1+R)} \quad (2)$$

where R denotes the intensity ratio of the L _{$\alpha 2$} and L _{$\alpha 1$} lines. (In the L _{$\alpha 2$} transition magnetic term can not occur.[2]) From the measured angular distribution of the L x-rays from Ba, Sm, and Er targets, we determined the above (2) anisotropy parameter ratios, extending our earlier study on Au, Th, and U [3].

The obtained results are represented in fig. 1. as a function of the atomic number (Z). The full dots are the results of the present measurement, while the open circles were taken from ref.[3]. The dashed line represents the theoretical anisotropy parameter ratio, when the M2/E1 mixings are neglected. The full line was obtained with the values of δ and R of ref.[2].

It is surprising, that the deviation between the experimental and theoretical values does not decrease with decreasing Z , since the presence of the M2 component

comes partly as a relativistic effect. The experimental data show, that the knowledge of the mixing ratios is necessary at the inner shell alignment studies. The experimentally determined higher order multipole terms (e.g. M2,E2, etc.) provide a sensitive test of the theoretical radiation transition probabilities and the applied wavefunctions used at the calculations.

References

- [1] T. Papp, Proc. of 3rd International Seminar on High Energy Ion-Atom Coll. Debrecen, Aug. 2-5, 1987, in Lecture Notes in Physics 294, Eds. D. Berényi and G. Hock, Springer-Verlag, Berlin-Heidelberg 1988,p. 204.
 - [2] J. H. Scofield, Phys. Rev. 179(1969)9.
 - [3] T. Papp, J. Pálinkás and L. Sarkadi, in Abstracts of Contributed posters of Eleventh International Conference on Atomic Physics - ELICAP -, Paris, July 4-8, 1988. Abstract No XI-16.
- T. Papp and J. Pálinkás, Phys. Rev. A 38(1988)2686.

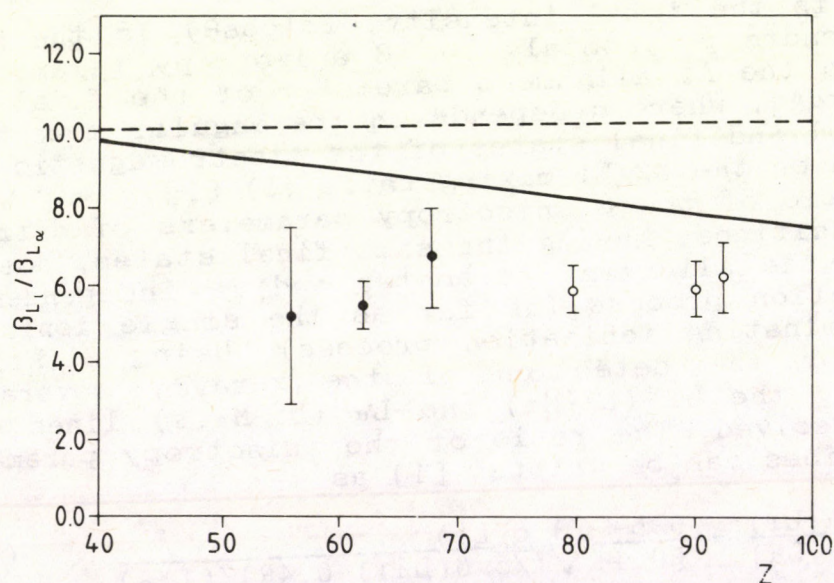


Fig. 1. The ratios of the anisotropy parameters of the L_1 and $L_{\alpha 1,2}$ transitions as a function of target atomic number. Full dots: present work; open circles: former measurements [3]; dashed line: theoretical values with neglect of the M2/E1 mixing; full line: theoretical values using δ and R values of ref.[2].

ON THE SATELLITE STRUCTURE OF Ta M α AND M β X-RAY LINES

I. TOROK, B. SULIK, L. SARKADI and J. VEGH

The MN α satellite lines are unresolvable from the diagram line and from each other, because of the comparable natural line-widths and spacings. Anyhow, it is possible to study the widening and asymmetry of the strongest M-lines, as a function of the excitation mode and energy, using a crystal spectrometer. Approximating the low-energy slope of experimental lines with a Voigt-shaped peak of the width equal to the combination of natural width and instrumental width, a satellite-to-diagram line area ratio can be estimated.

The accepted atomic theories need a lot of complicated calculations, using many parameters which are not known yet with high accuracy; so these theoretical estimations are rather uncertain. A recently developed simple calculation method [1], the so called geometrical model, offers a procedure to predict approximate satellite-to-diagram line area ratios relatively easily. The model works rather well in the case of K-L and L-M-N satellites [1-5]. It is interesting to test it in the range of M-lines. Searching the recent literature it is very rare to find measured M satellite-to-diagram ratios [6, and references therein], but the different modes of excitation and X-ray measurement modes make them ambiguous.

Using an ADP analyzer crystal the Ta M α and M β lines were measured. The excitation was provided by different ion beams (H $^+$, He $^+$) from the Van de Graaff generator of the ATOMKI, at different bombarding energies. About 1 μ A ion beam currents were used. All the spectra were taken in several (3-30) scans, and were summed up channel by channel, after "deglitching". Fig. 1. is a typical proton induced M α -M β spectrum. An X-ray induced spectrum also was taken, and we could compare our spectra also to a Ta M spectrum, obtained by 84 MeV N ion bombardment by Awaya et al. [7]. Table 1. lists the preliminary results, the experimental and calculated satellite-to-diagram ratios.

Table 1.

Excitation		Satellite-to-diagram ratio			
mode	energy	M α		M β	
		exp.	calc.	exp.	calc.
X-ray	<50 keV	0.178	-	0.072	-
H $^+$	0.8 MeV	0.405	0.272	0.807	0.272
H $^+$	2.0 MeV	0.478	0.140	0.740	0.140
H $^+$	3.2 MeV	0.411	0.100	0.707	0.100
He $^+$	1.6 MeV	1.109	1.833	1.581	1.833
He $^+$	3.2 MeV	1.183	1.381	1.602	1.381
N	84 MeV	>3	6.575	>3	6.575

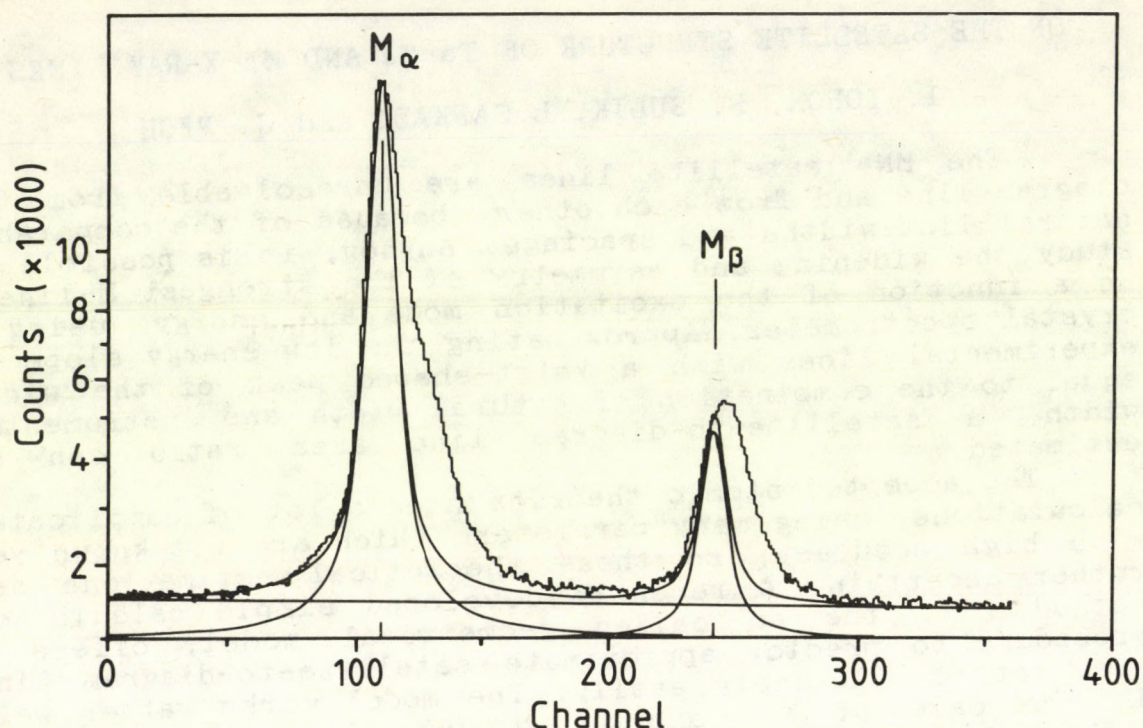


Fig. 1. Ta $M\alpha$ and $M\beta$ X-ray lines, induced by 3.2 MeV protons. (Vertical axis: the square-root of the channel content.)

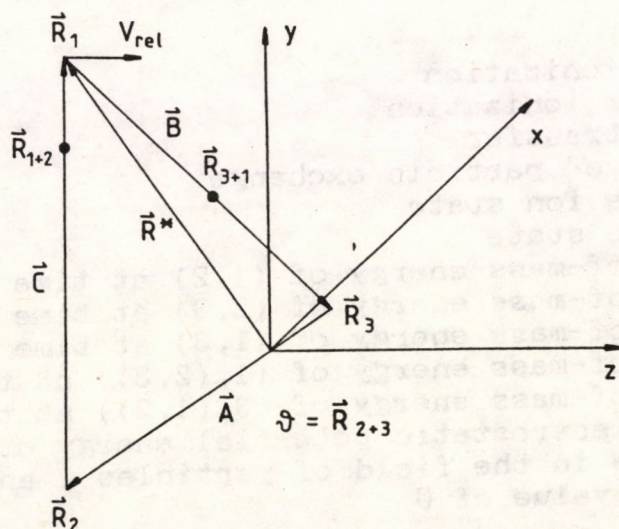
References:

- [1] B. Sulik, I. Kádár, S. Ricz, D. Varga, J. Végh, G. Hock, D. Berényi, Nucl. Instrum. Meth. B28(1987)509.
- [2] I. Kádár, S. Ricz, B. Sulik, D. Varga, J. Végh, D. Berényi, Nucl. Instrum. Meth. B40/41(1989)60.
- [3] I. Kádár, S. Ricz, V. A. Shchegolev, D. Varga, J. Végh, D. Berényi, G. Hock, B. Sulik, Phys. Lett. A115 (1986)439.
- [4] Y. Awaya, Y. Kanai, T. Kambara, T. Mizogawa, A. Hitachi, B. Sulik, in: Spectroscopy and Collisions of Few-Electron Ions. Proc. of the Study Conf. SCOFEL '88, Bucharest, Romania, Aug. 29.-Sept. 2. 1988. Ed. M. Ivascu, V. Florescu, V. Zoran, World Scientific, Singapore, etc., 1989, p.462.
- [5] A. Berinde, C. Ciortea, A. Enulescu, D. Flueraşu, G. Hock, I. Piticu, L. Sarkadi, B. Sulik, V. Zoran, J. Phys. B:At. Mol.Phys.20(1987)L481.
- [6] A. Laakkonen, G. Graeffe, J. de Physique 48(1987)12,C9-605.
- [7] Y. Awaya, T. Tonuma, Y. Tendow, H. Kumagai, T. Katon, K. Izumo, A. Hashizume, A. Hitachi, M. Nishida, A. Yagishita, T. Hamada, ICPR Cyclotron Progress Report 1980, p. 67.

CTMC CALCULATIONS FOR COULOMB 3-BODY COLLISIONS

K. Tökési and G. Hock

During the last months a CTMC code has been developed and tested in order to investigate diverse full 3-body collisions. The calculations involve the experiences acquired in earlier CTMC studies [1-5] and are furnished with appropriate exit channels (see Table). The versatility of the developed CTMC code, in accordance with the corresponding sets of the exit channels, is achieved by immediate re-specification of the pure Coulomb particles ($e\pm$, $p\pm$, $\mu\pm$, etc.) which take part in the full 3-body collisions, giving rise to direct, breakup, transfer, exchange and binding processes, if any.



The geometry of the 3-body collisions is shown in Fig.1. Projectile \equiv (1); Target \equiv (2,3)

This CTMC code will be developed in the future to the case of more complex (screened) potentials.

Table 1

Test	D	DI	TI	CT	EK	NI	Mo
A<C	0	+	-	0	0	0	0
Epe>0	+	+	+	0	0	-	-
ETe>0	0	+	+	+	+	0	-
Epe<UO	0	0	0	+	0	0	0
ETe<UO	+	0	0	0	0	0	0
AVA>0	0	+	+	0	0	0	0
BVB>0	+	0	0	+	0	0	0
CVc>0	0	+	+	0	+	0	0
B<A	0	0	0	0	+	0	0
ETp<UO	0	-	-	0	+	0	0
Ep(Te)<0	0	0	0	0	0	0	+
ET(pe)<0	0	0	0	0	0	0	+
ETp<0	0	0	0	0	0	+	0

A plus sign means that the test must be passed, a minus sign that it must not be passed, and a zero that it is not made.

The undefined quantities of Table 1 are as follows:

D:= direct
 DI:= direct ionization
 TI:= transfer ionization
 CT:= charge transfer
 EK:= "negative" particle exchange
 NI:= negative ion state
 Mo:= molecule state
 Epe:= centre-of-mass energy of (1,2) at time $t=+\infty$
 ETe:= centre-of-mass energy of (2,3) at time $t=+\infty$
 ETp:= centre-of-mass energy of (1,3) at time $t=+\infty$
 Ep(Te):= centre-of-mass energy of (1,(2,3)) at time $t=+\infty$
 ET(pe):= centre-of-mass energy of (3,(1,2)) at time $t=+\infty$
 U:= total electrostatic potential energy of the electron in the field of particles 1 and 3
 UO:= maximum value of U

References

- [1] R. Abrines and I.C. Percival, Proc. Phys. Soc. 88 (1966) 861-872
- [2] J.S. Cohen, Phys. Rev. A26 (1982) 3008-3011
- [3] R.E. Olson, and A. Salop, Phys. Rev. A16 (1977) 531-541
- [4] G. Schiwietz and W. Fritsch, J. Phys. B:At. Mol. 20 (1987) 5463-5474
- [5] V. J. Montemayor (private communication)

**MATERIALS SCIENCE
AND ANALYSIS**

A STUDY OF CURRENT CONDUCTION MECHANISM IN $\text{YBa}_2\text{Cu}_3\text{O}_{7-x}$

K. Vad, S. Mészáros and G. Halász

Electric field generation due to transport current was investigated experimentally in high T_c $\text{YBa}_2\text{Cu}_3\text{O}_{7-x}$ ceramic superconductors. External magnetic field and transport current density dependence of resistivity-temperature characteristics, as well as external magnetic field and temperature dependence of current-voltage characteristics were investigated. The resistivity of a ceramic sample is the sum of the resistivity of grains and grain boundaries. The separation of these two parts can be made on the basis of the measured quantities mentioned above. Resistivity-temperature curves of a semiconductor type $\text{YBa}_2\text{Cu}_3\text{O}_{7-x}$ sample measured with different measuring currents are shown in Fig.1. The sharp drop just below the onset temperature originates from the superconducting grains and it appeared in the characteristics of both metallic and semiconductor type ceramic samples at the same temperature. At lower temperatures the resistance originates from the grain boundaries. At temperatures close enough to the onset temperature we analysed the shape of current-voltage curves. We found linear dependence in $\log V - \log(I - I_c)$ scale up to voltages of 5 mV (corresponding to 5 mV/cm electric field) using I_c as a fitting parameter, i.e. the $V = K(I - I_c)^{a(T)}$ formula describes the voltage-current curves in this voltage range. 'K' coefficient depends on the magnetic field and ' $a(T)$ ' linearly depends on the temperature: $a(T)$ increases with a slope of $\sim 0.3/\text{K}$ from 1 at T_c as the temperature decreases.

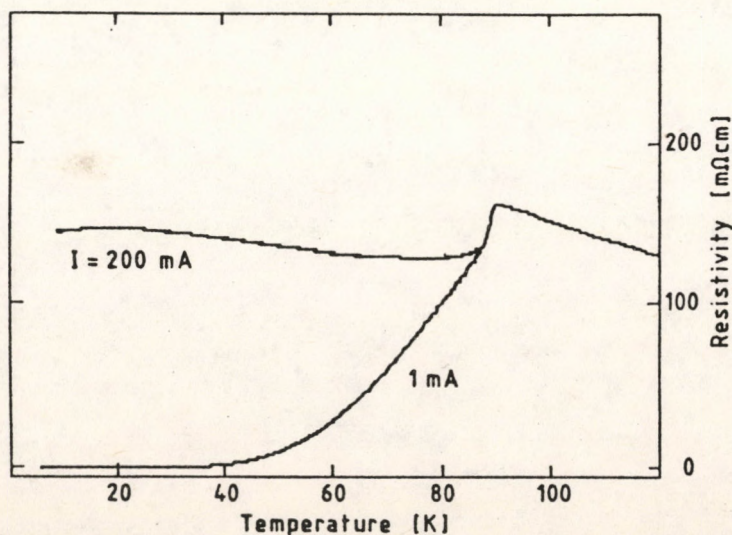


Fig.1 Resistivity-temperature curves of an $\text{YBa}_2\text{Cu}_3\text{O}_{7-x}$ semiconductor type sample with different measuring current.

Using constant measuring current the dependence of electric voltage on the external magnetic field was measured, as well (Fig.2). At temperatures above ~ 80 K the curves show flux flow state in the Abrikosov medium inside superconducting grains, and do not show hysteresis.

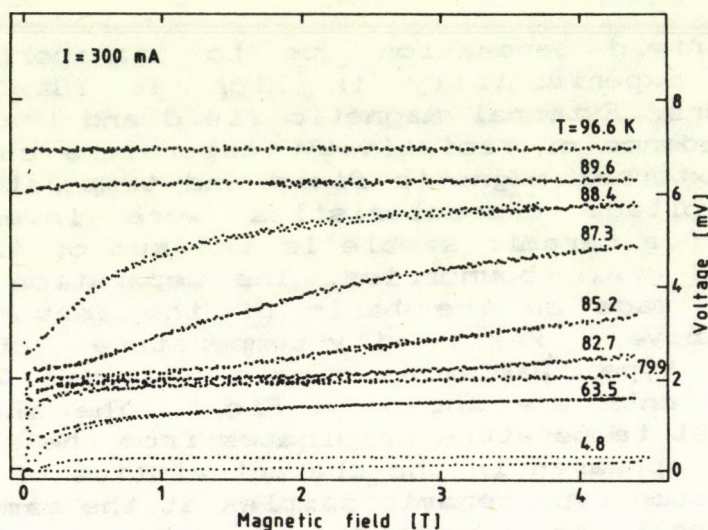


Fig.2 Magnetic field and temperature dependence of voltage drop on a metallic type $\text{YBa}_2\text{Cu}_3\text{O}_{7-x}$ sample using constant measuring current.

AC SUSCEPTIBILITY MEASUREMENTS ON HIGH T_c SUPERCONDUCTORS

S. Mészáros, N. Hegman, G. Halász and K. Vad

We present low field ac susceptibility measurements on polycrystalline $\text{YBa}_2\text{Cu}_3\text{O}_{7-x}$ and BiCaSrCuO high T_c superconductors made by solid state reaction method. Real (χ') and imaginary (χ'') parts of the ac susceptibility and magnetization curves were studied in the temperature range of 4.2-100 K and in different external magnetic fields up to 5 T. Ac excitation fields of 10^{-3} mT to 1 mT amplitude at a frequency of 1 KHz have been used and the measurements of the induced magnetic response were carried out on a dual coil mutual inductance device.

The diamagnetic susceptibilities at 4.2 K were found to be about 80-80 % of the value expected for a bulk superconductor. While at temperatures near T_c supercurrents in individual grains dominate in diamagnetic properties, at temperatures far below T_c intergrain Josephson type supercurrents dominate. If a dc magnetic field is applied coaxially to the ac field, Josephson currents decrease even at low fields. The imaginary part starts to increase just below T_c and shows a peak or peaks representing a hysteretic energy loss in the sample. The loss rapidly increases with the superconducting transition of intergrain junctions and goes to zero when the coherence state extends to the whole sample. The energy dissipation originates from the irreversible flux motion in the three dimensional Josephson junction network and the intragrain motion of

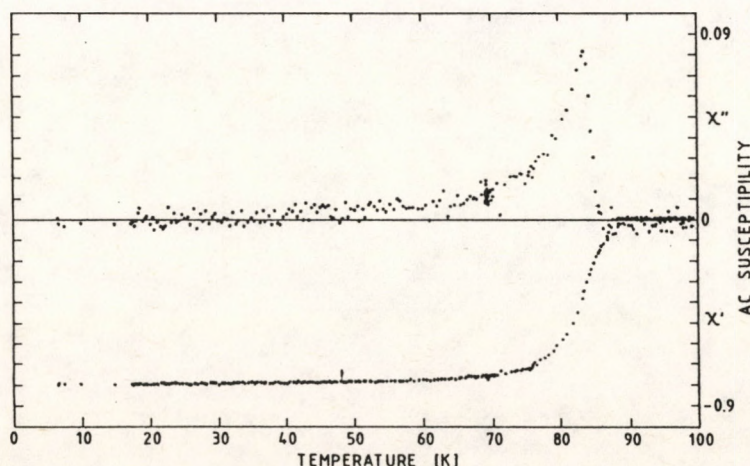


Fig.1 Susceptibility versus temperature on an $\text{YBa}_2\text{Cu}_3\text{O}_{7-x}$ sample. The amplitude of the alternating magnetic field is 7×10^{-3} mT.

Abrikosov vortices. The two contributions can be separated on the basis of their different sensitivity to external dc magnetic fields and ac excitation amplitudes. According to ac susceptibility measurements BiCaSrCuO granular superconductors have different superconducting phases depending on local oxygen density variation in the sample.

Figs.1 and 2 show susceptibility versus temperature curves for YBa₂Cu₃O_{7-x} and BiCaSrCuO (1% Fe impurity) ceramics respectively.

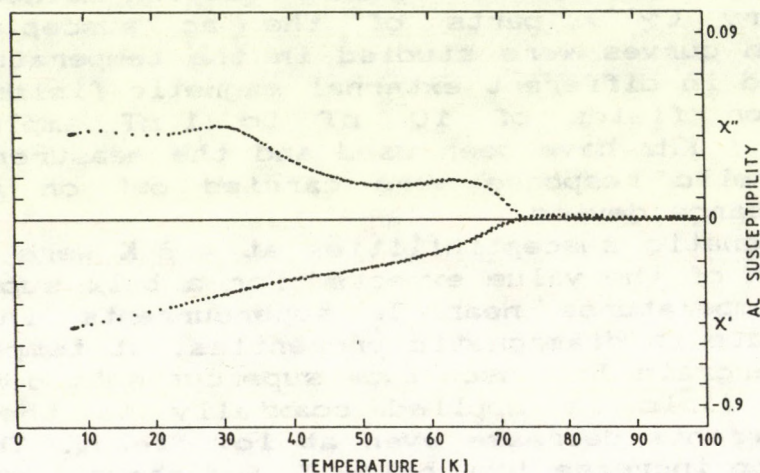


Fig.2 Susceptibility versus temperature on an BiCaSrCuO sample
The amplitude of the alternating magnetic field is 1.4×10^{-1} mT.

TRANSPORT CRITICAL CURRENT MEASUREMENTS IN YBa₂Cu₃O_{7-x} CERAMICS

S. Mészáros, K. Vad and G. Halász

One of the most important parameters characterizing ceramic superconductors is the transport critical current density. Experimental values of critical current densities were obtained by a contactless method based on the flux conservation capability of a superconducting ring. We studied the temperature and magnetic field dependence of YBa₂Cu₃O_{7-x} high T_c materials both in low and high magnetic fields in the temperature range between T_c and 5 K.

It was shown that in zero-field-cooled state at 77 K the critical current shows hysteresis at magnetic fields higher than ~ 3 mT. At lower temperatures this threshold field producing irreversibility in critical current density versus magnetic field curves is higher. The critical current density versus external magnetic field curves in zero-field-cooled state are shown in Fig.1. Supposing that the weak links between superconducting grains are Josephson junctions, a theoretical curve was fitted to the experimental values. This curve was calculated on the basis of a simple model of N Josephson junction connected parallelly with critical current

$$I_c(B) = I_c(0) \frac{1}{N} \sum_{i=1}^N \left| \frac{\sin(\pi B / B_0 F_i)}{\pi B / B_0 F_i} \right|$$

, where $F_i = 0.5 + 0.05i$ ($i=0,1,\dots,N=25$) was chosen.

Temperature and magnetic field dependence of the critical current of an YBa₂Cu₃O_{7-x} ring near critical temperature can be seen in Fig.2. The inset shows the $[\log I_c - \log(1-T/T_c)]$ curve, where T_c was chosen as a fitting parameter to be T_c = 88 K and it is regarded as the transition temperature to coherence state. The curves merge into the temperature axis. This supports the conclusion that the Josephson junctions in YBa₂Cu₃O_{7-x} material are mainly S-N-S type and not S-I-S. The temperature dependence of critical current density in YBa₂Cu₃O_{7-x} bulk material was found to be $j_c = K(1-T/T_c)^m$. We have got from the slope of the line in the inset of Fig.2 that $m = 2.1$. The theoretically expected value for bulk superconductors is $m = 1$ [1].

In field-cooled-state magnetic flux lines are trapped in the material with low pinning forces. The material remembers the magnetic field in which it was cooled down (memory effect) and the critical current values depend sensitively on it. The decay of trapped flux shows logarithmic time dependence.

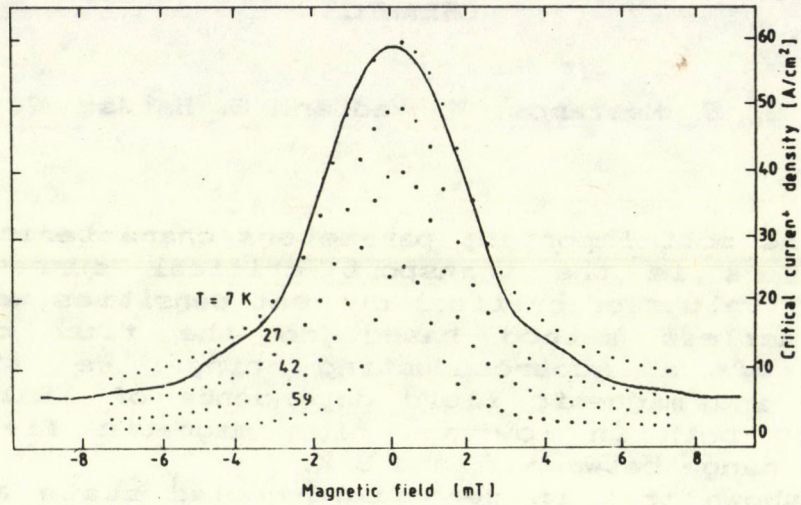


Fig.1 Magnetic field dependence of the critical current density at different temperatures

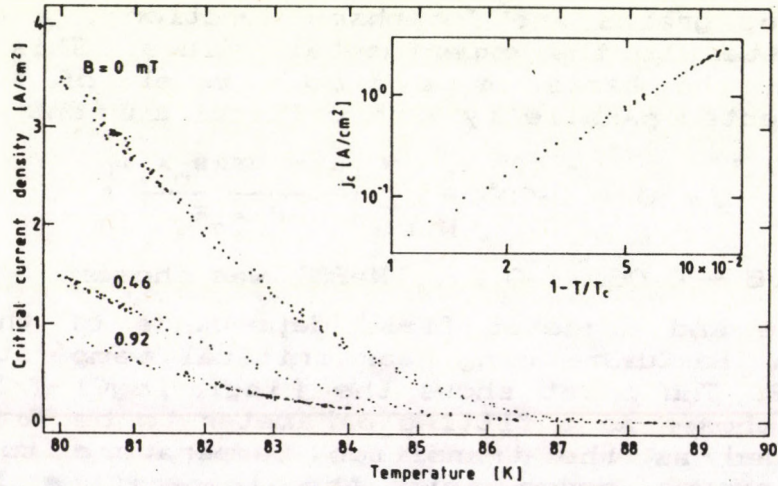


Fig.2 Temperature and magnetic field dependence of the critical current density at temperatures near T_c .

Reference

- [1] S. Han, Physica C 156 (1988) 765.

XPS STUDY OF THE $\text{YBa}_2\text{Cu}_3\text{O}_{7-x}$ SUPERCONDUCTOR CERAMICS

Z. Tóth, J. Tóth

The mechanism of superconductivity of high temperature superconductor ceramics (HTSCs) has not been cleared up. It was shown that in the Cu based superconductors the average valency of Cu should be higher than two [1].

We studied polycrystalline $\text{YBa}_2\text{Cu}_3\text{O}_{7-x}$ ceramics by the home made XPS instrument of ATOMKI [2],[3],[4]. Sintered sample pellets were prepared in the usual way in KÖPORC Ceramic Works, Budapest.

Before the measurements the surfaces of the pellets were cleaned by scraping with a stainless steel knife in air. Then the pellets were inserted in a minute into the chamber of vacuum of 10^{-6} Pa. For cleaning we have not made Ar^+ -ion etching to avoid the destruction of the crystal structure [6].

In the wide scan spectra, not only the photoelectron lines of the components Y, Ba, Cu, O of the ceramics, but the C lines coming from the surface contamination were detected as well.

The unusually wide Ba $3d_{5/2}$ line was fitted with two peaks, at an energy distance ~ 1 eV (Fig 1). One of these lines was interpreted [8] as Ba^{2+} ions coordinated completely to O^{2-} ions (Fig 1, peak a)) and the other one due to the Ba^{2+} sites coordinated partly to O^{2-} ions and partly to O vacancies (Fig 1, peak b)). In our case the concentration of O vacancies seems to be lower than in the case of Steiner et al. [8].

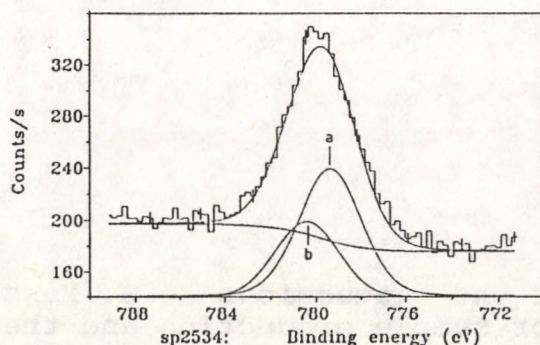


Fig 1.

XPS spectrum of $\text{Ba}3d_{5/2}$ of an $\text{YBa}_2\text{Cu}_3\text{O}_{7-x}$ sample:
Peak a): Ba^{2+} ions fully bound to O^{2-} ions.

Peak b): Ba^{2+} ions partly bound to O vacancies.

Having examined different ceramics we have found difference between the Cu 2p spectra of which showed good Meissner effect (Fig 2 a)) and which showed bad Meissner effect (Fig 2 b)). It is also well known that after removal of O from the crystal, the charge balance can be restored partly by the reduction of the Cu^{3+} to Cu^{2+} and partly by the oxidation of the O^{2-} to O^- [5]. These processes determine the $\text{Cu}^{2+}/\text{Cu}^{3+}$ ratio. From studying the spectra of the different valence Cu one can see, that the chemical shift between di- and trivalent copper is 1.2 eV [8], this shift was used in our fitting procedures.

If we study the shake up satellite structure of the lines Cu 2p we can find satellite lines only in the case of Cu^{2+} [8]. So if we measure the satellite to main peak ratio, we can determine the average charge of Cu or the concentration of

holes in O 2p band as a function of the concentration of oxygen vacancies (x) [5].

From the measurements of the photoelectron lines Ba 3 d_{5/2} and Cu 2p of the ceramics one can conclude for the oxygen vacancy concentration, which is one of the most important parameters from the point of view of the superconducting properties of HTSCs.

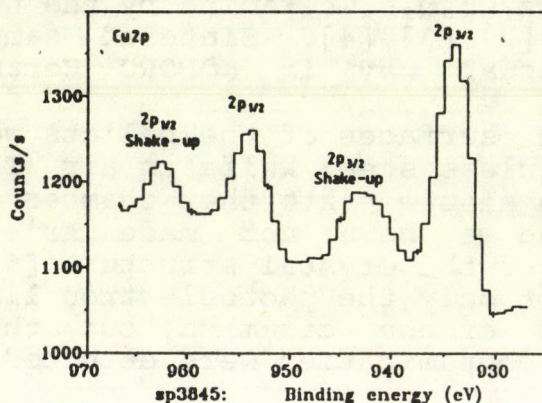


Fig 2 a)
XPS spectrum of Cu 2p
of an YBa₂Cu₃O_{7-x}
sample with good
Meissner effect.

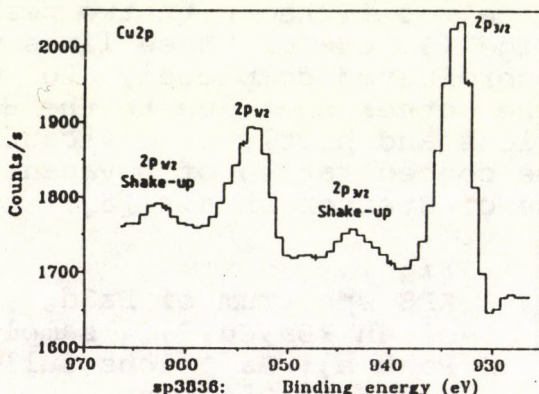


Fig 2 b)
XPS spectrum of Cu 2p
of an YBa₂Cu₃O_{7-x}
sample with bad
Meissner effect.

Acknowledgement:

The authors are indebted for the discussions to S. Mészáros, K. Vad and G. Halász; and for sample production and the test of Meissner effect to co-workers of KÖPORC Sz. Balanyi and L. Balázs.

References:

- [1] S. Kohiki et al., Phys. Rev. B **38** 9201-9204 (1988)
- [2] D. Varga et al., Nucl. Instr. and Meth. **154** 477 (1978)
- [3] I. Cserny et al., Proc of the 5th Semin of Electr Spectr p.29-30, 26-29 Aug 1984, Dresden, GDR
- [4a] J. Végh, Abstrs of the 7th Seminar of Electron Spectr, p. 93; 20-24 Sep 1988, Bourgas, Bulgaria
- [4b] J. Végh, Users' Manual of EWA Computer Program, Version 2.08, unpubl.
- [5] Z.-X. Shen Phys. Rev. B **38** 11820-11823 (1988)
- [6] F.C. Brown, J. of Low Temp. Phys. **69** 151-156 (1987)
- [7] P. Steiner et al., Z. Phys. B **69** 449-458 (1988)
- [8] P. Steiner et al., Z. Phys. B **67** 497-502 (1987)

SEPARATION OF FLUORINE-18 FROM METALLIC GALLIUM

P. Mikecz, Gy. Tóth¹, A. Páli², J. Vitéz²

¹ Medical University of Debrecen

² Aluminious Earth Factory and Aluminium Foundry , Ajka

At the determination of oxygen content of high purity gallium metal using the CPAA method with the $^{16}\text{O}(^3\text{He},p)^{18}\text{F}$ and $^{16}\text{O}(^3\text{He},n)^{18}\text{Ne} \rightarrow ^{18}\text{F}$ nuclear reactions [1,2] it is necessary to separate the ^{18}F isotopes from the matrix because of the interference of positron emitting arsenic isotopes coming from nuclear reactions on gallium.

For the separation the following wet chemical method was chosen. The surface of the irradiated sample was etched in a concentrated $\text{HNO}_3:\text{HCl}$ mixture (ratio: 20 to 1) at 0 °C. The thickness of removed layer was calculated from the gallium content of the etching solution determined on atomic absorption spectrophotometer. The average etching speed was found to be 0.4 micron/min. Then the remained gallium was electrochemically dissolved from the copper backing in concentrated hydro-chloride acid. The solution was transferred into a special polyethylene vessel containing 25 microlitre concentrated hydrofluoric acid as carrier of the fluorine. A stream of nitrogen gas was bubbled through the solution and hexamethyldisilazane was added. This compound reacts with fluoride ions resulting volatile fluorotrimethylsilane (FTMS) [3]. After acidification of the solution with concentrated sulphuric and phosphoric acid mixture the $^{18}\text{FTMS}$ was removed by the gas stream, and adsorbed on solid sodiumhydroxide and silicagel. The separation yield of the ^{18}F - determined in preliminary experiments by using non activated gallium samples and ^{18}F with known activity - was found to be 65 +/- 15 %.

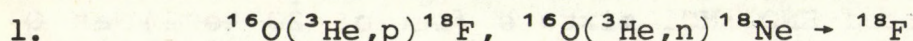
- [1.] I. Mahunka, F. Ditrői, S. Takács, ATOMKI Annual Report 1989. (to be published)
- [2.] F. Ditrői, I. Mahunka, S. Takács, Korszerű Techn. 16 (1988) 23.
- [3.] H. Kvaternik, P. Angelberger, K. Buchtela, Proc. of 7th Int. Symp. on Radiopharm. Chem. (1988) 456

DETERMINATION OF BULK OXYGEN CONTENT IN HIGH PURITY GALLIUM

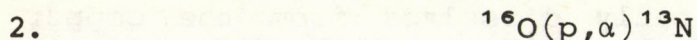
I. Mahunka, F. Ditrói and S. Takács

High purity gallium is used by the modern semiconductor industry (e.g. for GaAs production). Oxygen is the most undesirable trace element in the high purity gallium. Its concentration is decreased during the purification process by several methods, and the residual concentration must be well known. One of the most powerful method for oxygen determination in gallium is the charged particle activation analysis (CPAA).

Two possible nuclear reactions were studied for oxygen determination;



reactions [1,2] yield positron-emitter ^{18}F radioisotope. The half-life of ^{18}F is 110 min. which allows comfortable processing between the irradiation and the gamma measurement.



reaction [3,4] yields also a positron-emitter radioisotope with considerable cross-section. Its half-life is 10 minutes. The matrix material is also activated because of the high threshold energy ($Q = -5.2$ MeV). In this case chemical separation of ^{13}N isotope is demanded, and because of the relatively short half-life of it a fast processing is needed.

Comparing the two methods and our possibilities the ^3He irradiation were chosen for oxygen determination. Irradiating the gallium with a ^3He beam above 6.5 MeV the matrix material itself is also activated and positron-emitter As isotopes are produced. In this case chemical separation of the ^{18}F is necessary [5]. When the incident energy is under 6.0 MeV the gallium is not activated, but the yield of ^{18}F is high enough.

An other important problem should be solved, that on the surface of gallium there is always a thin oxide-layer which must be removed after the irradiation and before the gamma measurement. The removal can be done mechanically or by chemical etching.

Special sample handling is demanded during sample preparation, irradiation and mechanical and chemical processing because of the low melting point of the gallium.

The gallium was melted and loaded under nitrogen atmosphere into a copper container which could be cooled down by the vapour of liquid nitrogen. After freezing again the samples were placed into a vacuum chamber and two 13 μm thick kapton foils were placed in front of the target to monitorize the beam. The bombarding energy of the $^3\text{He}^{++}$ beam was chosen so that the incident energy on the gallium surface was 6.0 MeV. The irradiation time was 30 minutes and the beam current did not exceed 200 nA. The irradiations were done at the horizontal

beam line of the MGC cyclotron in Debrecen [6].

After the irradiation the surface oxide-layer was removed by step-by-step etching, by using a mixture of HNO_3 and HCl at 0°C [5]. Between two etching the residual activity of the sample was measured. The removed thickness was calibrated by using inactive material and the removed amount of the gallium was measured by using Atomic Absorption Spectrometry (AAS).

After perfectly removing the surface oxid-layer the bulk oxygen concentration could be determined by using absolute or relative method.

The experimental data were processed and evaluated by computer codes developed by us.

In this recent work three samples were investigated by using the absolute method. The measured concentrations of oxygen are shown in table 1.

Table 1. Determination of oxygen concentration in gallium

Sample No	Oxygen Concentration (ppm)
1.	131 ± 21
2.	70 ± 11
3.	81 ± 13

To summarize, it was shown that ^3He charged particle activation followed by surface etching and gamma-ray spectrometry is a rapid and reliable method for determination of bulk oxygen concentration in gallium. However, it is necessary to mention that the surface etching usually not uniform, so the real surface of the sample after etching not equal with the geometrical one. This nonuniform feature of the surface can cause systematic error in the calculation of the thickness of the removed layer and through this in the final result.

REFERENCES

- [1] P. Misalides, J. Krauskopf, G. Wolf, K. Bethge, NIM B18(1987)281
- [2] H.L. Rook, E.A. Schweikert, Analytical Chemistry 41(1969)958
- [3] J.L. Debrun, Private communication
- [4] J. Fitschen, R. Beckmann, U. Holm, H. Neuert, Int. J. Appl. Radiat. Isot. 38(1977)781
- [5] P. Mikecz, Gy. Tóth, A. Páli, F. Vitéz, ATOMKI Ann. Rep., 1989 (to be published)
- [6] F. Szelecsényi and F. Tárkányi ATOMKI Annual Report 1988 p.116

X-RAY FLUORESCENCE ANALYSIS OF BRONZE OBJECTS FROM THE AVAR AGE

M. Kis-Varga, Institute of Nuclear Research Debrecen Pf. 51.
4001 Hungary

L. Költő, Rippl-Rónai Museum Kaposvár, Május 1. u. 10.
7400 Hungary

More than 2000 bronze objects from the Avar Age has been analysed by energy dispersive XRF method. The weight percentage of elements Fe, Cu, Zn, Ag, Sn, Sb and Pb has been measured by using I-125 radioisotope excitation and the spectrometer made by ATOMKI. The concentration values were determined by the fundamental parameter method described in [1].

Processing the data by cluster analysis we attempted to use the composition of objects to analyse the burial sites. It was found that the intrinsic relationships within each burial site were easily detected.

The comparison of various burial sites was attempted on the basis of frequency histogrammes and dendogrammes. From these it is assumed that the Avar Empire was possibly supplied with belt ornaments by several workshops servicing larger areas.

In the comparison of mounting buds of belts it was possible to show that the mounts of various belt sets were fixed at the same time. The method proved viable to separate from the belt set pieces that originated from a different period or were of uncertain origin.

Alloys used for jewellery and belt ornaments were found to differ in composition thus offered the conclusion that they must have been made of different materials and technologies.

The composition of bronze objects from the Avar and Roman Ages so far has allowed us to believe that the recasting of Roman bronzes was not a widespread practice of the Avar Smiths even in the region of one-time Pannonia.

Reference

- [1]. M. Kis-Varga, X-Ray Spectrometry, Vol. 8, No. 2. (1979) 73.

**EARTH AND COSMIC SCIENCES,
ENVIRONMENTAL RESEARCH**

MARINE PHOTOSYNTHETIC CARBON ISOTOPIC FRACTIONATION REMAINED CONSTANT IN THE EARLY OLIGOCENE

E. Hertelendi, I. Vető*

Pre-Neogene marine kerogens reveal much lighter carbon isotopic composition than do Neogene-Quaternary marine kerogens [1]. Recent studies [2] suggest that isotopic reversal is due to an Oligocene-Miocene drop in atmospheric carbon dioxide level caused by a decrease of marine photosynthetic carbon isotopic fractionation (MPHCF). Our results show that the Early Oligocene marine kerogens from Hungary and the Carpathians belong to the light pre-Neogene kerogen group and they do not show a stratigraphic trend toward less negative $\delta^{13}\text{C}$ values. This finding makes unlikely that a decrease of fractionation would have begun during the Early Oligocene. The large non-stratigraphic variation of the kerogen $\delta^{13}\text{C}$ value revealed by our samples reinforces ideas about importance of local, environmental constraints [1,3,4] on carbon isotopic composition of marine kerogen.

Formation of kerogens lighter than average can be explained by the contribution of some very light carbon. This carbon can be introduced into the process of photosynthesis as CO_2 derived by bacterial oxidation of the sedimentary organic matter or it can be added to the sedimentary organic matter during the very early burial as cell material of metanotrophic bacteria. Since the carbon of the cell material of these bacteria can be significantly lighter than that of the substrate methane, in the case of the oxidation of biogenic methane with a $\delta^{13}\text{C}$ of at about -60 ‰, even minor contribution of the corresponding cell material can cause a large negative shift in the isotopic composition of the sedimentary organic matter.

Heavy kerogen found in a layer represents only 1 ky long time interval does not give a convincing evidence for a long-standing change in isotopic fractionation. This nanno marl layer witnessed anannofrorial bloom so it can not be excluded that during its formation carbon dioxide acted as the limiting nutrient what is known to cause an enrichment of the heavy carbon isotope in the marine kerogen.

REFERENCES

- [1] M.D. Lewan, *Geochim. Cosmochim. Acta* 50, 1583-1591 (1986)
- [2] B.N. Popp, R. Takigiku, J.M. Hayes, J.W. Louda, & E.W. Baker, *Am. J. Sci.* 289, 436-454 (1989)
- [3] W. Küspert, in *Cyclic and Event Stratification* (eds. Einsele & Seilacher) 482-501 (Springer, 1982)
- [4] J.M. Hayes, R. Takigiku, R. Ocampo, H.J. Callot, & P. Albrecht, *Nature* 329, 48-51 (1987)

* Hungarian Geological Survey, Budapest

GEOCHRONOLOGICAL STUDIES WITH THE K/Ar METHOD

K. Balogh, E. Árva-Sós, Z. Pécskay

In 1989 appeared a number of publications which were based on experimental results obtained in the previous years.

A summary of bio- and chronostratigraphy of the Carpathians during the period of Main and Late Alpine Molasses has been prepared in a cooperation with the Geol. Ust. D. Stura, Bratislava [1], the age of metamorphism and uplift has been established in the Little Plain (coop.: Geochem. Res. Lab. of Hung. Acad. Sci., Budapest) by dating $< 2\mu\text{m}$ K-white micas [2], the K/Ar age of a new basalt occurrence has been measured (coop.: Hung. Nat. Mus., Budapest; Geochem. Res. Lab. of Hung. Acad. Sci., Budapest) [3]. The reliability of K/Ar ages obtained on Pliocene basalts has been considered and it has been pointed out that the too old age of the Somoska basalt could not be explained by isotopic fractionation of atmospheric argon (coop.: Geol. Ust. D. Stura, Bratislava; Hung. Geol. Inst., Budapest) [4]. New chronologic results on the covered Neogene volcanites in the Great Hungarian Plain have been presented (coop.: Dept. Miner. Geol., Kossuth L. Univ., Debrecen) [5]. Age of magmatism and partly that of alteration has been established for the Mesozoic volcanites south of the Mecsek Mts. (coop.: Hung. Geol. Inst., Budapest; Ore Mining Comp. at Mecsek, Pécs) [6]. Jurassic age has been measured for an andesite reached by borehole Nagybatony-324, North-Hungary (coop.: Hung. Geol. Inst., Budapest) [7].

In 1989 continued the study of anomalously old ages obtained on Pliocene basalts. It has been pointed out that the too old age of the Somoska basalt was caused likely by the positive correlation of K and excess Ar content of this rock. (Coop.: Geol. Ust. D. Stura, Bratislava; Hung. Geol. Inst., Budapest) It has been demonstrated by recording Ar release spectra that the argon retentivity of cryptomelene is superior to that of the clayey crust of manganese nodules at Urkut. On this ground an age of 85-90 Ma has been established for the oxidization of manganese carbonates at this locality (coop.: Dept. Miner. Geochem. and Petrogr., József A. Univ., Szeged; Geochem. Res. Lab. of Hung. Acad. Sci., Budapest). Badenian andesites have been detected south of the Balaton (coop.: Hung. Geol. Inst., Budapest). Middle Oligocene age has been established for the volcanic rocks of Central Rodope, Bulgaria (coop.: Geol. Inst. Bolg. Acad. Sci., Sofia). Continued the chronologic study of Mesozoic magmatic rocks in the Transdanubian Central Mts. and in North Hungary. (coop.: Dept. of Petrogr. and Geochem., Eötvös L. Univ., Budapest; Hung. Geol. Inst., Budapest). Dating of Miocene tuffs and tuffites in the Western Mecsek Mts. started (coop.: Ore Mining Comp. at Mecsek, Pécs).

REFERENCES

- [1] D. Vass, Kad. Balogh (1989): Z. Geol. Wiss., Berlin, 17 No.9. pp. 849-858.
- [2] P. Árkai, Kad. Balogh (1989): Acta Geol. Hung.: 32/1-2, pp. 131-147.
- [3] A. Embey-Isztin, G. Dobosi, G. Noske-Fazekas, E. Árva-Sós (1989): Miner. Petrol., 40, pp. 183-196.
- [4] Kad. Balogh, L. Ravasz-Baranyai, M. Nagy-Melles, D. Vass (1989): 14th Congress CBGA, Sofia, 1989. Extended Abstracts, pp. 1182-1185.
- [5] V. Széky-Fux, Z. Pécskay (1989): 14th Congress CBGA, Sofia, 1989, Extended Abstracts, pp. 1194-1197.
- [6] E. Арва-Шов, Л. Равас-Бараньяи (1989): 14th Congress CBGA, Sofia, 1989, Extended Abstracts, pp. 1158-1161.
- [7] Árváné Sós E., Balogh Kad., Ravaszné Baranyai L. (1988): Ann. Rep. Hung. Geol. Inst. on 1986. pp. 117-120.

WATER TRANSPORT MEASUREMENTS ON OAK (*Quercus petraea*) TREES
BY ^{24}Na TRACER TECHNIQUE

Cs. Béres¹, A. Fenyvesi, T. Molnár², P. Jakucs¹, I. Mahunka,
P. Mikecz, Z. Kovács

¹Institute of Ecology, L. Kossuth University, Debrecen

²Biomedical Cyclotron Laboratory, Medical University School,
Debrecen

Radioecological experiments at the research forest area of the Sikfőkut Project of the Kossuth University [1] were continued for clearing the mechanism of the new type of early and sudden death of trees of the most wide-spreaded kind of oaks (*Quercus petraea*) in Hungary.

^{24}Na was produced via the $^{27}\text{Al}(n,\alpha)^{24}\text{Na}$ reaction at the intense fast neutron source of the MGC-20 cyclotron. The activity needed for one experiment (cca. 20 MBq) was prepared in carrier-free form in 5 ml of distilled water. The active solution was injected into the tracheas of healthy and sickened *Quercus petraea* trees. Gamma radiation of ^{24}Na moving in the tree by the water stream was measured by a minicomputer based system consisting four scintillation counters fitted onto the trunk at different height.

Velocities of the water stream in the penetratable (or working) tracheas of the tree were calculated from the time dependences of the counting rates of the detectors. The measured values were in the range of 5 - 350 cm/min dependent upon the external abiotic conditions (meteorological situations, soil humidity, hour of the day, etc.). The velocity of the water stream could as well be the same in the working tracheas of healthy and sickened trees.

The rate of the water transport is decreasing with decreasing number of working tracheas. The chance of injecting into working tracheas and measuring nonzero velocity is depend on their percentage in the tree consequently our experimental technique is capable of detecting the presence of unpenetratable tracheas even at the early stages of the disease [1]. The percentage of working tracheas in the sickened trees is smaller than that in the healthy trees as it has been verified by other investigations, too [2].

The other important factor is the water uptake of the tree. In this connection the role of micorrhisas of oaks is crucial. In the soil of the test fields pH=4.8-3.9 values were measured. The ecological limit for the micorrhisas of oaks is at pH=4.5 under forest circumstances. At this critical pH value the quantity of micorrhisas of oaks decreases dramatically [3]. As results of that the water uptake of the tree is blocked and the working tracheas become plugged up even in the middle of the vegetation

period. The last stage of this progress is the death of the tree.

It seems to be proved that the primary reason of this disease is the increasing human activity and resulting increased acidity of soil by pollution and acidic deposits [4].

REFERENCES

- [1] Cs. Béres, A. Fenyvesi, P. Jakucs, I. Mahunka, Z. Kovács, T. Molnár, L. Szabó, Nucl. Instr. and Meth. in Phys. Res. B43 (1989) 101-103
- [2] P. Jakucs and J.A. Tóth, Az erdő, 28(8)(1988) 358-361. in Hungarian
- [3] L. Hóles, I. Berki, Acta Bot. Hung. 34(1988)
- [4] P. Jakucs, Ambio. 17(4)(1988) 267-274

RADON MEASUREMENTS IN HUNGARIAN CAVES PERFORMED BY SOLID STATE NUCLEAR TRACK DETECTION TECHNIQUE

I. Hunyadi and J. Hakl

Starting from 1978 in as many as 17 caves of Hungary regular radon observations were carried out at 146 different measuring places performed with monthly changed integrating radon detectors. The shortest observation was near two years long, while the longest is still going on from the beginning.

The first dozen radon measuring sites were set off in the Hajnóczy cave. Later the radon observations in caves were extended to the majority of the Hungarian karstic regions. (Fig.1.).

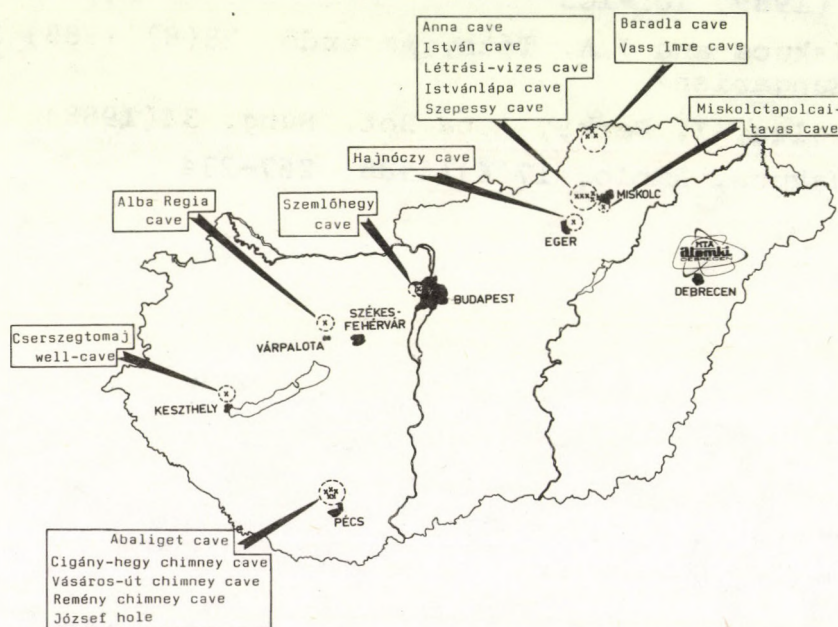


Fig. 1. The location of the caves where regular radon measurements have been performed by solid state nuclear track detectors in the last decade in Hungary.

The underground cavities investigated by us show a wide variety according to the form, extensions, depth, origin,... starting from smaller chimney-caves and ending at big complicated systems. However these differences are reflected partly in the measured radon activity concentrations the mean values do not differ one from the other more than a factor of 30.

It was recognized that in every caves more or less periodical fluctuations of smaller or larger amplitude can be found around the mean value of the radon activity concentration (Fig.2.). The frequency and amplitude distribution of the observed radon data are characteristic for the cave and its environment, for the uranium (radium) content of the enclosing rocks and stones and for the extension of that porous surroundings which is in correspondence with the cave air by the intrusion of atmospheric air and radon traced subsurface fluids.

The direct radon emanation from the wall surface of the known cave labyrinths cannot account either for the maximal values or for the variations occurring in the radon activity concentration of the cave air or other substances.

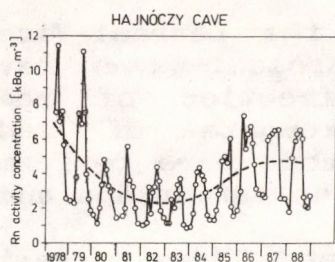


Fig. 2. The seasonal variation with one year periodicity in the radon activity concentration measured in the Great-hall of the Hajnóczy cave. Dashed line resulted in a low pass filter procedure with one year moving average (MA).

The most common and the most apparent phenomenon which takes place in the majority of the investigated caves is the periodically formed, temperature gradient forced air flow of a seasonally reversed direction resulting in a typical radon distribution pattern (Fig. 2.). In some cases less regular water inflows are the determining factors in the formation of the radon concentration in caves.

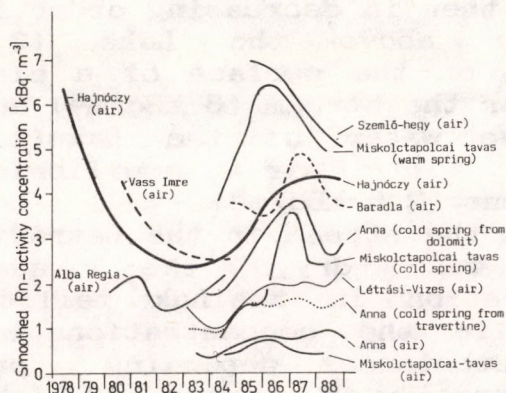


Fig. 3. Long term variation obtained by a low pass filter procedure from the one month integrated data of the caves involved into the radon studies by SSNTDs.

In spite of the great variety in the geographical situation of the caves and even for different substances similar basic tendency manifests itself in the longterm behaviour (Fig.3.): rapidly decreasing values in the late 70-s are joining through a definite minimum to increasing curves which have a broad maximum around 1986 and decreasing again in the present days. Further research are in progress to look for intermediate environmental processes which may help to understand this tendency.

This work was supported in part by the Research Fund of the Hungarian Academy of Sciences, contract No. AKA 1-3-86-185.

REFERENCES

- G. Somogyi, I. Hunyadi and J. Hakl: Historical review of one decade radon measurements in Hungarian caves performed by solid state nuclear track detection technique, Proc. of the 10th Int. Conf. of Speleology, Aug 13-20, Budapest
- G. Géczy, I. Csige and G. Somogyi: Air circulation in caves traced by natural Radon, *ibid.*

RADON TRANSPORT BY WATERS IN CAVES OF EASTERN BÜKK REGION

J. Hakl, I. Hunyadi and L. Lénárt*

Radon mapping has been performed in the Létrási-Vizes, Anna, Istvánlápá, Szepessy and Miskolctapolcai-tavas caves (Lénárt et.al. 1989). To study the direction of radon transport processes simultaneous measurements of radon activity concentration in different substances were performed at 6 places, 2 in the Létrási-Vizes, 1 in the Istvánlápá and 3 in the Szepessy caves.

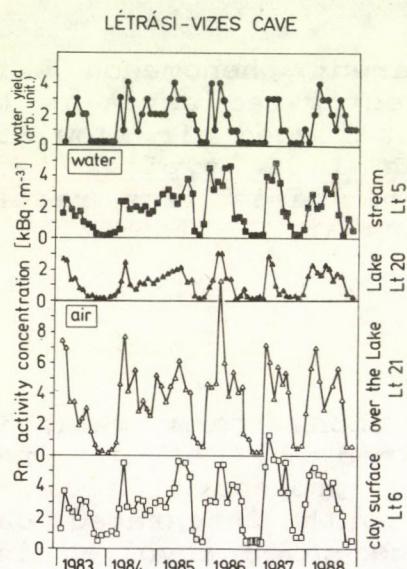


Fig. The radon activity concentrations in different substances and water yield of the feeding stream at the Lake in the Létrási-Vizes cave

The longest time series obtained are at the Lake in the Létrási-Vizes cave (see Fig.), where the radon activity concentration varied strongly with time. The highest average radon activity concentration was found in the stream (2.0 kBq/m^3 , in air equilibrium equivalent = 5.1 kBq/m^3) then in decreasing order in the air above the Lake (3.4 kBq/m^3), on the surface of a clay hang near the stream (3 kBq/m^3) and in the water of the Lake (1.0 kBq/m^3 , in air equilibrium equivalent = 2.6 kBq/m^3).

When the stream in the Létrási-Vizes was dry, the radon concentration in the Lake fell to zero, while the concentrations in other substances depending on season were low in winter and high in summer. In case of active stream, elevated radon levels were always measured in the surrounding of the Lake. The radon concentration

found in stream showed a good correlation with the water yield of the stream. It follows that radon is essentially carried to the Lake by the stream. These observations can be explained by the way, that subsurface waters permeating porous rocks can significantly be enriched in solved radon, so then entering the cave they may increase the radon concentrations by degassing inside the cave.

At each site in the Szepessy and Istvánlápá caves we always measured low radon activity concentrations with only a slight change in time. The sequence of the averaged data showed another character than those observed around the Lake in the Létrási-Vizes cave. The highest mean values were found in soil and air (900 Bq/m^3). The concentration values found in stagnant waters are lower and similar to that measured in

* Technical University for Heavy Industry, Miskolc

dropping waters of the Létrási-Vizes cave (200 Bq/m^3 , in air equilibrium equivalent = 500 Bq/m^3).

The difference between the values of mean radon concentrations in different caves is apparent. From the summarized data we can conclude that from the point of view of ventilation the Szepessy and Istvánlápa caves can be regarded much more closed than the Létrási-Vizes cave. The form of these caves (more than 100 m deep narrow vertical entrances) also gives a good support for the latest statement. In these caves there are also the clastic deposits of non karstic origin among the sources of radon, which were transported into the caves by late waters. However in the lack of strong fluid motions, which can significantly influence the radon levels in caves, the formed radon concentrations are lower, than in the nearby Létrási-Vizes cave.

This work was supported in part by the Hungarian Academy of Sciences, Research Fund contract No. AKA 1-3-86-185.

REFERENCE

L. Lénárt, G. Somogyi, J. Hakl and I. Hunyadi: Radon mapping in caves of Eastern Bukk region, Proc. of the 10th Int. Conf. of Speleology, Aug. 13-20, 1989, Budapest

RADON AS A NATURAL TRACER OF CAVE AIR CIRCULATION

G. Géczy*, I. Csige

We have been performing continuous radon concentration measurements with solid state nuclear track detector in the Szemlo-hegy Cave since 1985. The passages of the cave are nearly horizontal, their total length is 2200 metres. The radon concentration shows seasonal variation with summer maxima and winter minimum at each measuring site and increases moving on towards the end point of the cave. These changes of the radon concentration can be interpreted with the help of a simple air circulation model of the cave (Géczy et al. 1989).

During 4 years the mean radon concentration decreased at each measuring points by cca. 20%. Depicting the radon concentration of the cave air as the function of the external temperature we get curves with hysteresis (see Fig.).

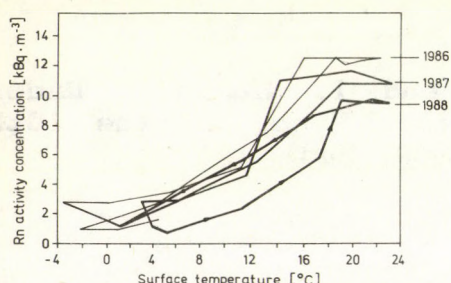


Fig. Relation between the radon concentration and external temperatures changing with years

The shape of the curves becomes flatter and flatter during the observation, that is, less and less radon enters the cave at the same external temperature. Since the radon concentration of the cave air is determined by the porosity of the rock and the surface/volume ratio of the fractures, the reasons of the decrease can be the following:

1. The water content of the rock has been changed, which implied a change in the porosity.

2. A part of the fractures has become plugged, therefore the surface/volume ratio of the fracture system decreased.

3. The fractures have been widened out thus the surface/volume ratio of the fracture system decreased.

On the basis of the available data there cannot be detected a longterm unidirectional variation either in the external precipitation, or in the rock dilatation. Therefore we can assume that the radon concentration decreases as the effect of the plugging of the microfractures. This hypothesis is supported by the fact that during the air circulation of the cave, the pollution of several ten thousand cubic metres air yearly and of the infiltrated external waters are deposited in the cave and in the fracture system.

This work was supported in part by the Research Fund of the Hungarian Academy of Sciences, contract No. AKA 1-3-86-185.

REFERENCE

G. Géczy, I. Csige and G. Somogyi : Air circulation in caves traced by natural radon. Proc. of the 10th Int. Conf. of Speleology, Aug. 13-20, 1989, Budapest.

* Eötvös Lóránd University, Budapest, Hungary

XPS STUDY OF THE SURFACE COMPOSITION OF AMBIENT AEROSOLS SIZE-SEGREGATED BY CASCADE IMPACTORS

J. Tóth, L. Kövér, I. Vajasy-Perczel*, P. Mikecz,
T. Tarnóczy*

* Dept. of Atomic Phys., Lab. of Surface Phys., TU, Budapest

During 1989 the XPS investigations of size-segregated ($<0.5 \mu\text{m}$, $0.5-1 \mu\text{m}$, $1-2 \mu\text{m}$, $2-4 \mu\text{m}$, $4-8 \mu\text{m}$, $8-18 \mu\text{m}$) ambient aerosol particles were continued to get new data for surface nitrogen and sulfur compounds on the surfaces of aerosols stucked on teflon (TFE) samplers and to reveal the distribution of carbon contamination and silicon originated from the particles vs. size fractions. For the reliable data interpretation AES, SAM, SEM methods were also used to check our earlier statements [1], [2], [3] concerning to the correlation between elemental concentrations of carbon/sulfur. The SAM was introduced to get lateral distribution of S, C, O on the surface of Cu samplers. Model experiments in atmospheric conditions, reaction of SO_2 and H_2S gases with Cu and Ni surfaces were made as well [4].

In the XPS spectra the very large intensity C 1s peak originated from contaminations (e.g. soot particles) decreased sharply when we went from the small particle size fraction ($<0.5 \mu\text{m}$) to the larger ones ($1-2 \mu\text{m}$). The intensity of Si 2s peaks sharply decreased, when we went from the larger fractions to the lower ones. The systematic study of this preliminary indications is in progress.

In our model experiments the reaction of SO_2 with Ni and Cu surfaces resulted $\text{SO}_4^{2-}/\text{SO}_3^{2-}$ peak, with H_2S we have got S^{2-} peak. After 5 keV, $\theta_i=45^\circ$, $20 \mu\text{A}/\text{cm}^2$ Ar^+ ion bombardment for 5 minutes the $\text{SO}_4^{2-}/\text{SO}_3^{2-}$ peak was reduced to S^{2-} in the case of Cu, while in the case of Ni it was reduced only partly to S^{2-} [4].

New experiments by the help of teflon samplers in the Battelle type cascade impactor are in progress to investigate the more final details of representative sampling vs. time region of the part of the day.

Studying of the combination of different surface methods from methodical point of view for the investigation of surfaces of ambient aerosol particles is continued also to get more reliable information on chemical composition and morphology of the particle surfaces.

References:

- [1] L. Kövér, J. Tóth; Atmospheric Environment **18** (1984) 2135
- [2] L. Kövér, J. Tóth, J. B. Schág, I. Borbély-Kiss,
P. B. Barna, I. Pozsgai, F. Medve; Vacuum **37** (1987) 175
- [3] L. Kövér, J. Tóth, J. B. Schág, I. Borbély-Kiss;
Surface and Interface Analysis (SIA) **14** (1989) 217
- [4] To be published in SIA

**BIOLOGICAL
AND
MEDICAL RESEARCH**

CORRELATIONS BETWEEN HAIR BIOELEMENTS AND CLINICAL PARAMETERS IN HUNGARIAN DIABETIC CHILDREN.

J. Bacso and I. Uzonyi

Inst. Nucl. Res. Hung. Acad. Sci. (ATOMKI), Debrecen

M. A. Cser

Dept. Child. Health N°II of Semmelweis Med. Univ.,
Budapest.

In twenty diabetic children (3-15y) and in other members of their family (8 healthy siblings and 15 healthy parents) micro elements were analyzed in hair samples by XRFA. Patients and family members were taking the same quality food containing 40% carbohydrate of their total calorie needs. Patients were on NOVO Actrapid (0.39 ± 0.21 IU/kg/d) and Monotard (0.54 ± 0.17 IU/kg/d). In the patients there were measured the urinary glucose excretion and the glycosilated haemoglobin (HbA_1), too.

The hair samples were cut near to skin from the occipital region of head, and the first section of a few cm was used for analysis. The measurements were carried out using an ATOMKI-type Si(Li) X-ray spectrometer of FWHM=165 eV resolution for MnK line. The characteristic X-ray lines of elements with low atomic numbers ($Z \leq 24$) and with higher atomic numbers ($Z > 24$) were excited by ^{56}Fe and ^{125}I annular radioisotope sources, separately. Evaluation of characteristic x-ray spectra were performed using measured counts in fixed energy windows for each x-ray line. In case of ^{56}Fe excitation the background at each x-ray peak position was calculated as a linear function of the unresolved Compton- and Rayleigh-peak area. In case of ^{125}I excitation the background was determined quite similarly, but instead of the backscattered peak the counts measured in the 4.2-5.2 (KeV) energy interval were used. After background subtraction the peak overlap was corrected by predetermined peak interference factors. Calculation of elemental composition was carried out with an X-ray fluorescence method elaborated for any thickness biological samples. The method is based on the use of a calibration standard, which is similar in composition to the unknown, applying the following equation system for the concentration calculation: $W_i^x = W_i^o \times G_i^{st} / G_i^x$. W_i^x, W_i^o denotes the concentration of element i and the apparent concentration, respectively. The difference in matrix absorption and sample thickness between the unknown and the standard are taken into account by the G_i^{st} / G_i^x function which had been derived from the Shiraiwa-Fujino equation in parametral form. For calibration the H-8 animal kidney standard was applied in the present work.

Results: The elements: P, S, Cl, K, Ca, Mn, Fe, Ni, Cu, Zn, Hg, As, Se, Br, Pb, Rb, Sr, Zr, Mo, Cd were measured in hair samples of diabetic children and healthy members of their family. On the basis of statistical evaluation of results, at the first glance, the hair-K, -Cl, -Ca and -Zn concentrations are remarkable:

K and Cl: The mean values and standard errors are: K(650 ± 130) ppm, Cl(2830 ± 480) ppm for diabetic children and K(250 ± 58) ppm, Cl(1310 ± 22) ppm for members of families and the regression equation between K and Cl are: $K(\text{ppm}) = 0.2347 \times Cl(\text{ppm}) - 15.38$,

$r=0.8694$ $p<0.001$ $N=25$ for diabetic children and $K(\text{ppm})=0.2479 \times \text{Cl}(\text{ppm})-36.78$, $r=0.8409$ $p<0.001$, $N=28$ for members of family. It is seen from the figures that the K and Cl excretion into hair (probably the metabolic rate of K and Cl) is two times higher for diabetic children than the other members of the family. Supposing further that Cl is excreted mostly in form of KCl and NaCl, the Na excretion is higher in the members of family than in diabetic children.

Ca and Zn: Positive linear correlations were observed between hair Ca and urinarie glucose excretion (see fig. 1a) $r=0.92$ $p<0.001$, duration of diabetes $r=0.77$ $p<0.01$ and glycosylated Hb (fig. 1b) $r=0.74$ $p<0.01$. Hair-Ca and hair-Zn show a non linear positive correlation (see fig.2a diabetic, fig.2b family). It should be mentioned that the saturation value for hair Zn (~300 ppm) is ~50% higher in both group than for the healthy adults. Further although impaired relationship was observed between hair-Zn and urine glucose $r=0.49$ $p<0.01$ $N=25$ duration of diabetes $r=0.53$ $p<0.01$ and HbA₁, $r=0.39$ $p<0.05$. The physiological evaluation of figures observed will be detailed in other paper.

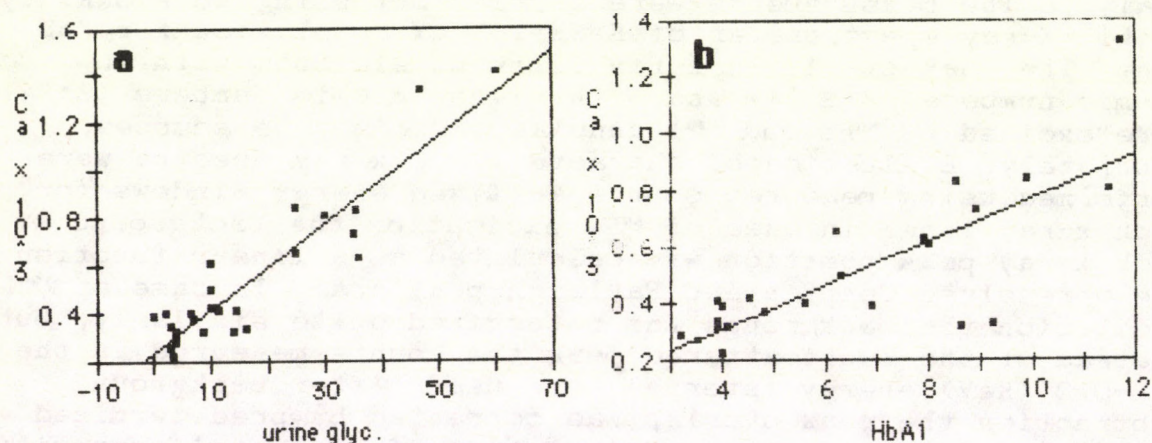


Fig.1 Hair-Ca vs. urinary glucose excretion (1a) and glycosylated haemoglobin (1b).

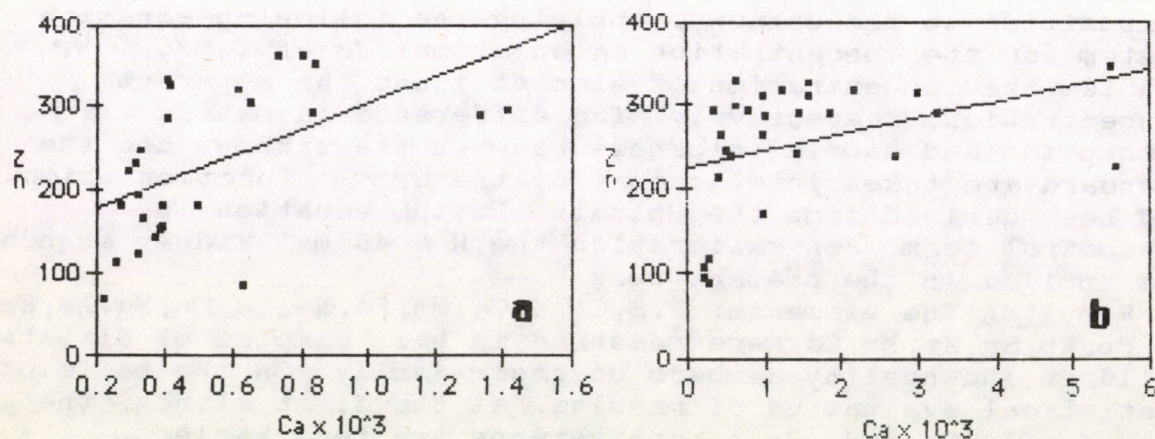


Fig.2 Hair-Zn vs. hair-Ca. 1a/diabetic, 1b/healthy.

PRODUCTION OF ^{110}In VIA $\text{Cd}(^3\text{He},\text{xn})^{110}\text{Sn} \rightarrow ^{110}\text{In}$ REACTION WITH LOW ENERGY CYCLOTRON FOR PET INVESTIGATION

F. Szelecsényi, Z. Kovács, F. Tárkányi, Gy. Tóth⁺

The ^{110}In is a positron emitting (62%) radionuclide with a half-life of 69 m. With the increasing use of positron emission tomography in nuclear medicine, compounds labelled with ^{110}In could be potentially useful for imaging with PET scanners, for example for diagnosing the rejection of transplanted organs, when repeated investigation with short interval is necessary to see the effect of the used therapy.

The only practical way to produce ^{110}In without producing its 4.9 h half-life, non-positron emitter isomeric state leads through its parent nuclei, the ^{110}Sn ($T_{1/2} = 4.11$ h) which decays only to the ground state of ^{110}In . Until now the ^{110}Sn has been produced by proton particle irradiation of natural In target (1). However, this method of production demands a high energy cyclotron ($E_p = 80$ MeV). With low and middle energy cyclotrons for practical production two other possibilities exist: the (p,xn), (p,pxn) reactions on Sn above 20 MeV and the (^3He ,xn), (^4He ,xn) reactions on Cd for lower energy accelerators. In this work we investigated the $\text{Cd}(^3\text{He},\text{xn})^{110}\text{Sn}$ process which can be performed using our low energy cyclotron.

Excitation function was measured by stacked-foil technique for the reaction of $\text{Cd}(^3\text{He},\text{xn})^{110}\text{Sn}$ on natural Cd in the energy range of 16.3 to 27 MeV using the MGC-20 cyclotron of ATOMKI, Debrecen. Commercially available high purity cadmium foils (Goodfellow, Cambridge, England) and samples prepared via electrolytic deposition of Cd on Ni foils were used as target materials. The excitation function measurement was carried out by activation method using gamma-ray spectroscopy. The experimental technique and the data evaluation were similar to (2). The cumulative cross sections obtained are shown in Fig.1. The abundance of the target material and the Q-values of the contributing nuclear reactions are summarized in Table 1. In the investigated energy range the $^{110}\text{Cd}(^3\text{He},3\text{n})^{110}\text{Sn}$ reaction appears to be dominant. The calculated thick target yield of ^{110}Sn amounts to 1860 MBq/C ($\sim 180 \mu\text{Ci}/\mu\text{Ah}$) in the energy range of 16.3 to 27 MeV. The levels of the radioactive impurities of ^{108}Sn , ^{109}Sn , ^{111}Sn , ^{113}Sn and ^{115}Sn at EOB depend on the irradiation time and the isotopic abundance of the target.

For production the irradiated Cd of 0.1 g/cm^2 target was dissolved in 9 M HBr, evaporated to dryness and picked up in 5 ml 9 M HBr. After an optimal cooling period of ~ 3 h, the main part of the contaminating Sn isotopes decayed out except ^{113}Sn ($T_{1/2} = 115$ d). For separation of the directly produced and decay product In isotopes from Cd matrix and Cd and Sn radioisotopes cation exchange method was chosen (3). DOWEX 50 WX-2 (100-200 mesh) resin was used to select the In isotopes from Cd and from the main parts of the Sn isotopes. The solution was led through

⁺ Biomedical Cyclotron Laboratory, University of Medical School Debrecen, Hungary, H-4012

the column of 4 mm i.d. and 4 cm length with 1 ml/min volume speed. The column was washed with 10 ml of 9 M HBr to remove the Sn remained on the resin as much as possible and without removing In isotopes. Because of the not too low distribution coefficient of Sn(IV) at this molarity we reduced it to Sn(II) where this coefficient is smaller therefore no significant part of Sn remained on the column. 174 min later when the ^{110}In activity reached the maximal value in the filtrate, the solution was led again through another column. To remove the ^{110}In activity the resin was eluted with 3 M HBr and the filtrate was evaporated to dryness. The ^{110}In activity (A) at the end of the radiochemical process can be given by

$$A = bC$$

where C is the EOB activity of ^{110}Sn and $b = 0.35$ which includes the cooling times and the efficiency of the radiochemical separation. ^{110}In -oxine was prepared using the method of Thakur (4) for labelling cellular blood components.

This method for producing ^{110}In with low energy cyclotron seems to be simple and quick. The shape of the excitation function for ^{110}Sn and the isotopic abundance of the target used suggest that yield could be significantly increased using higher entrance energies and enriched target.

References

- 1 H. Lundqvist et al., Abstract of the Fifth Symposium on Medical Application of Cyclotrons, Turku, Finland, ISBN-952-90095-9-3. p.14.
- 2 F. Tárkányi et al., to be published in Radiochimica Acta, 1990
- 3 F. Nelson, D.C. Michalson, J. of Chromatog. 25 414 (1966)
- 4 M.L.Thakur et al., J. Lab. Clin. Med. 89 217 (1977)

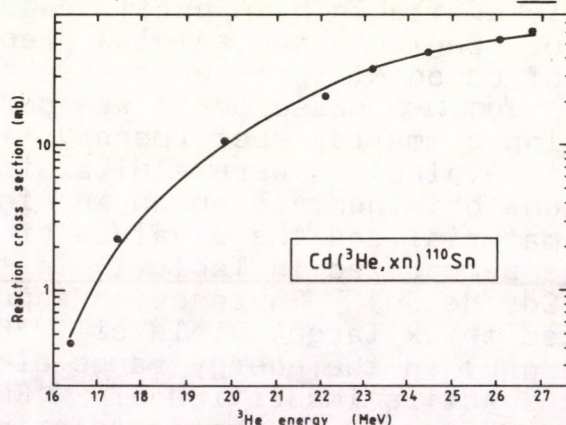


Fig.1. Excitation function of $\text{Cd}(^3\text{He}, xn)^{110}\text{Sn}$ reaction measured on natural Cd.

Table 1. Nuclear processes contributing to the formation of ^{110}Sn .

Reaction	Q (MeV)	Isotopic Abundance of the Target (%)
$^{108}\text{Cd}(^3\text{He}, n)^{110}\text{Sn}$	+ 3.4	0.89
$^{110}\text{Cd}(^3\text{He}, 3n)^{110}\text{Sn}$	-13.8	12.5
$^{111}\text{Cd}(^3\text{He}, 4n)^{110}\text{Sn}$	-20.8	12.8

PRODUCTION OF PURE IODINE-123

P. Mikecz, L. Andó, I. Mahunka, J. Tóth, A. N.Chelcov¹,
I. A. Suvorov¹

¹ Kurchatov Atomic Energy Institute, Moscow USSR

One of the most important medical radioisotopes is the ^{123}I . However, up till now the Debrecen cyclotron produced ^{123}I was not pure enough because of the poor enrichment of ^{123}Te in our target material [1]. To solve this problem a new method had been developed in the Kurchatov Atomic Energy Institute to produce a higher enriched material. The isotopic compositions of this and the earlier used tellurium-dioxide are given in Table 1.

Table 1. Isotopic compositions of enriched tellurium samples

^{120}Te	^{122}Te	^{123}Te	^{124}Te	^{125}Te	^{126}Te	^{128}Te	^{130}Te
in %							
a <0.01 2.86	1.62	73.4	11.5	3.1	3.71	3.81	
b <0.1 <0.1	1.6	95.6	2.7	<0.1	<0.1	<0.1	

a: from Technabexport b: from Kurchatov Ins.

The high enriched [^{123}Te]tellurium-dioxide material of the Kurchatov Institute was tested by XPS. The chemical composition was found to be $2\text{TeO}_2 \cdot \text{SO}_3$. This compound was transformed into TeO_2 by heating up to 600 °C for 5 minutes, then it was melted onto platinum backings. In this way two targets were made with 102 and 115 mg/cm² thickness.

The yield and the purity of the ^{123}I produced from this material were determined at different proton beams using the horizontal isotope production beam-line of the MGC-20E cyclotron [2]. The bombarding energies were 12, 15 and 18 MeV at a beam current of 200 nA. The obtained results are shown in the Table 2.

Our results are comparable with the earlier published data of Scholten et al. [3], and Barral et al. [4]. On the basis of our measurements the ^{123}I produced from the new TeO_2 at 15 MeV or lower bombarding proton energies is suitable for medical purposes because of the reduced level of undesired iodine isotopes.

Table 2. Experimentally determined ^{123}I yields and impurity levels

Bomb. energy [MeV]	^{123}I -yields [GBq/C]	Impurities in % at EOB		
		^{121}I	^{124}I	^{130}I
12- 9.6	23.7	n.d.	0.33	n.d.
12- 9.45	27.1	n.d.	0.31	n.d.
15-13.0	22.8	1.5	0.26	n.d.
15-12.8	27.6	1.4	0.27	n.d.
* 15-10.6	20.5	1.2	2.2	1.1
18-16.3	6.67	34.2	0.30	n.d.
18-16.1	7.7	31.6	0.27	n.d.

*: TeO_2 from the Techsnabexport
n.d.: not detectable

References

- [1.] Z. Kovács, P. Mikecz, I. Szabó, Nucl. Med. 26. (1987) 197
- [2.] F. Szelecsényi, F. Tárkányi, ATOMKI Annual Report 1988 p. 116
- [3.] B. Scholten, S. M. Qaim, G. Stöcklin, Appl. Radiat. Isot. 40 (1989) 127
- [4.] R. C. Barral et al., Eur. J. Nucl. Med. 6 (1981) 411

PRELIMINARY REPORT ON THE PRECLINICAL EXPERIMENTS REQUIRED FOR NEUTRON THERAPY

A. Csejtej¹, A. Fenyvesi, L. Trón²

¹Radiological Clinic, Medical University School, Debrecen

²Biomedical Cyclotron Laboratory, Medical University School, Debrecen

Nowadays application of fast neutrons in cancer therapy is considered as a standard treatment modality in highly developed countries [1]. According to international comprehensive statistics neutron therapy would be absolutely indicated in case of about ten percent of all cancer patients.

The compact MGC-20 cyclotron in Debrecen might offer new dimension for radiation treatment by making possible to use high LET particles. Though application of fast neutrons in cancer treatment has a long history, a lot of theoretical and practical questions of this treatment modality are not solved in a satisfactory way. This can be explained basically by the fact that each cyclotron and each neutron sources have individual dosimetric characteristics having a remarkable impact on the relative biological effectiveness (RBE). Therefore beyond a reliable physical dosimetry a far reaching radiobiological experimentation that is an equally reliable biological dosimetry seems to be absolutely indispensable [2], [3], [4]. Finding proper biological systems showing quantitatively dose dependent reactions we have carried out RBE determinations as the first steps on this way.

Mammalian cell cultures were irradiated by uncollimated beam of fast neutrons produced on thick beryllium target bombarded with 10 MeV deuterons. A Chisobalt standard cobalt unit was used as a reference.

Bone marrow was prepared from (BALB)cXCBA/F1 mice and irradiated. Survival fraction of granulocyte-macrophage colony forming units in culture (GM-CFUc) was plotted against absorbed dose of fast neutrons and Co-60 gamma ray. [5]. RBE was defined as the ratio of D₀ values of the appropriate survival curves and proved to be as much as 2.5.

Finding the colony forming technics too troublesome and time-consuming not to speak about statistical difficulties, the more flexible method of flow cytometric analyses of the DNA content of single cells was employed using Becton-Dickinson FACS III device. SP/2, V79 and DD cell lines were irradiated and G2 phase block was determined after 24 h incubation time. An excellent correlation was found between survival measured by the classical colony forming technics and the extent of G2 phase block in the studied range. This modern, reliable and

fast method seems to be an effective way to investigate most questions related to the dose, dose rate and spectrum dependence of the RBE as well as the oxygen enhancement ratio (OER).

In conclusion it can be stated that our cyclotron offers a real alternative in radiation treatment of cancer patients. We do believe, the preclinical experimental work just started serves the purpose of the subsequent human therapy.

REFERENCES:

- [1] Wambersie, A., Battermann, J.J., Strahlentherapie 161, 746(1985)
- [2] Fletcher, G. et al., Biological basis and clinical implications of tumor radioresistance, Masson Publ. Inc., New York 1983
- [3] Higgins, P.D. et al., Radiation Research 95, 45(1983)
- [4] Magdon, E., Radiobiol. Radiother. 26, 27(1985)
- [5] Metcalf, D., The hemopoietic colony stimulating factors, Elsevier, Amsterdam, 1984

INVESTIGATION OF BIOSYNTHETICAL FORMATION OF p-OH-V-PENICILLIN
BY TRITIUM LABELLED PRECURSOR

I. Kovács⁺, B. Palotás⁺, Z. Kovács

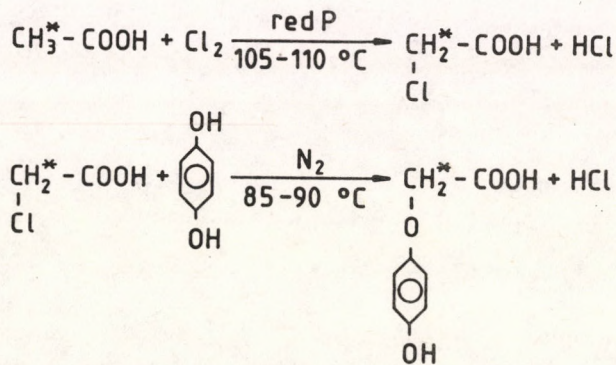
The tracer technique is very frequently used in the investigation of biosynthesis of antibiotics. The type of penicillin formed depends on the structure of precursor, added during the fermentation.

During the V-penicillin fermentation a part of the phenoxyacetic acid (POAA) undergoes hydroxylation forming p-OH-phenoxyacetic acid (p-OH-POAA) and paralelly about 5% p-OH-V-penicillin also appears (Fig.1.). It finally results in lower yield of V-penicillin because many cleaning steps are required to eliminate the contaminating product below the permitted level.

There are 3 possible ways of p-OH-V-penicillin formation (Fig.2.). According to the results of fermentation experiments the possibility of way I was excluded.

At way II the POAA, while at way III the p-OH-POAA, formed previously from POAA, is the precursor. Fermentation experiments did not give unambiguous answer for these two cases therefore we investigated the appearance (way III) or absence (way II) of T-labelled p-OH-POAA precursor added to the broth during fermentation.

The labelled p-OH-POAA was prepared according to the following reactions:



The final product was cleaned in many recrystallization steps to obtain pure precursor. The overall yield was 12%, with 0.5 MBq/g specific activity.

The sterilized solution of the labelled p-OH-POAA was added to the broth at 48 h of fermentation. Two parallel shaken fermentations were carried out: one was running with POAA, the other with p-OH-POAA precursor. The fermentations were stopped at 72 h and after the filtration and separation of broth the activity of penicillin and precursor fractions were measured with LKB liquid scintillator.

⁺BIOGAL Pharmaceutical Factory, Debrecen

In the case of POAA precursor all the activity remained in the precursor fraction and no activity appeared in the penicillin fraction, while at p-OH-POAA precursor 22% of the activity was measured in the penicillin fraction. Therefore the p-OH-V-penicillin is formed only on way II during the V-penicillin fermentation.

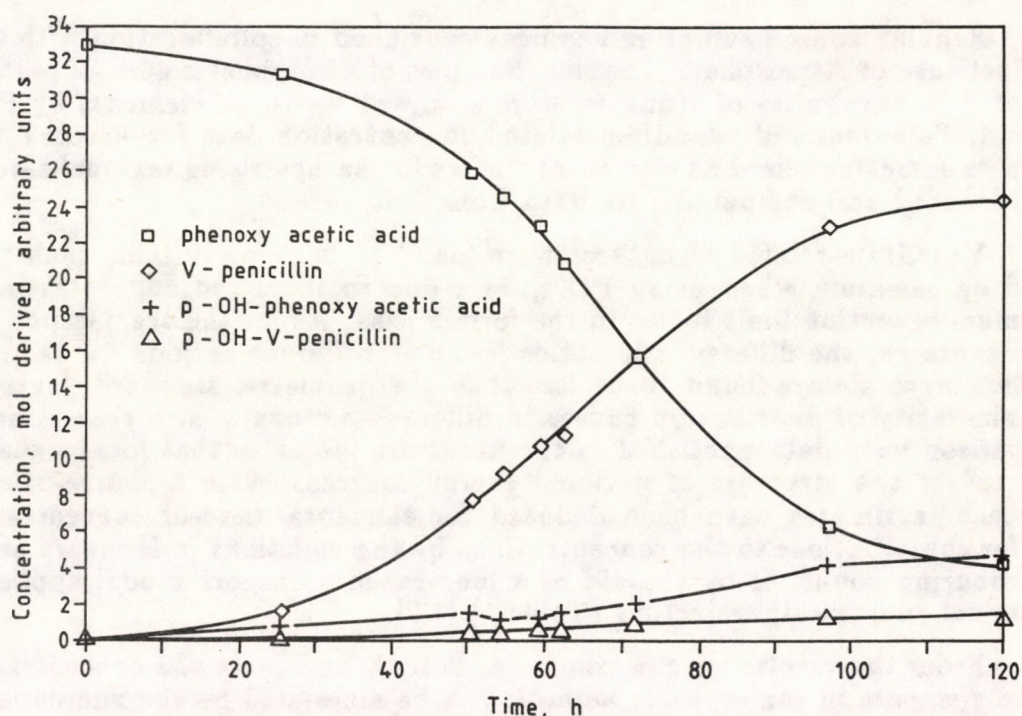


Fig.1. Formation of p-OH-V-penicillin during V-penicillin fermentation with phenoxyacetic acid precursor

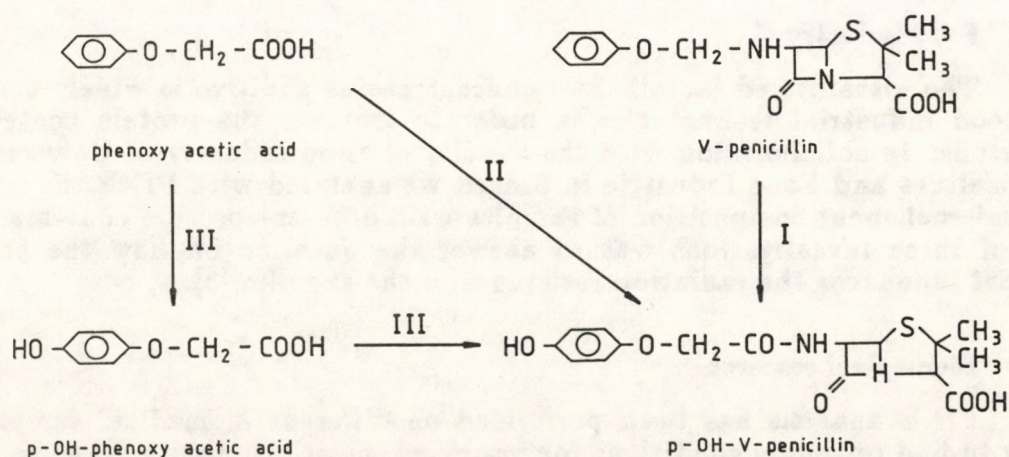


Fig.2. Theoretical possibilities of p-OH-V-penicillin formation

THE ANALITICAL APPLICATION OF CHARGED PARTICLE INDUCED X-RAY EMISSION METHOD

I. Borbély-Kiss, E. Koltay, Gy. Szabó

Aerosol research

Regular aerosol sampling has been continued in collaboration with Central Institute of Atmospheric Physics. Samples of atmospheric aerosol particles collected in rural sites of Hungary were analysed up to 21 elements by PIXE method. Selenium and vanadium related concentration data for selected trace elements sometimes used as elemental tracers in characterising regional aerosols were deduced and compared with data from literature.

Vanadium-related signatures were found to be more reliable than those based on selenium when using PIXE data due to increased concentration to minimum detection limit ratios in the former case. As for the tracing power of the signatures, the difference in ratios found in different periods for the same location were always found to be less than the geometric standard deviation. The similarity of distribution curves in different periods is also reassuring. A comparison with data published in the literature indicates that local signature data reflect the structure of national energy sources. With a source-oriented approach, estimates have been deduced for elemental aerosol concentrations and for contributions to the concentrations by the emissions in Hungary and in neighbouring countries by the aid of a long-range transport model applied to an annual average air trajectory (Table 1) [1,2].

From the results we can conclude that, by and large the concentrations of the elements in atmospheric aerosols can be simulated by the simple model applied. The evaluation gives a guess on the dry deposition velocities as well. To perform a more consequent averaging for yearly data the model requires some further improvement.

Food industry

The ultrafiltered lactalbumin concentrate as additive is widely used by the food industrial technologies in order to increase the protein content of foodstuffs. In collaboration with the Faculty of Food Industry of University of Horticulture and Food Industrie in Szeged we analysed with PIXE the macro- and microelement composition of samples with different protein contents. The aim of these investigations was to answer the question on how the protein content influences the radiation resistance of the samples [3].

Biomedical research

PIXE analysis has been performed on different biomedical samples in order to find optimum conditions for improved sensitivity limits for some trace element. Among other the case of selenium has been carefully studied due to an increased role of selenium in biomedical processes.

Element	Dry depo- sition velocity cm sec ⁻¹	Concentration		Hungarian contri- bution %	(wet total) depo- sition %
		calculated ng/m ³	measured ng/m ³		
V	0.10 [25] 2.70 [25]	13.08 3.51	2.4	79	30
Cr	0.32 [25] 6.80 [26]	6.93 0.80	4.6	34	80
Mn	0.40 [25] 2.20 [25]	5.68 2.01	10.7		
Co	0.3 [26] 2.8 [25]	0.76 0.23	1.6	38	80
Ni	0.13 [25] 2.0 [26]	5.54 1.93	2.3	36	90
Cu	0.18 [25] 1.78 [25]	9.0 4.9	2.9	90	40
Zn	0.25 [27] 4.5 [26]	26.11 1.68	26.4	13	85
As	0.1 [25] 2.3 [25]	1.75 0.37	2.5	24	90
Se	0.1 [26] 0.79 [25]	0.19 0.11	1.2		
Pb	0.06 [28] 0.30 [29]	28.0 22.0	20.6	32	95

Table 1.

References

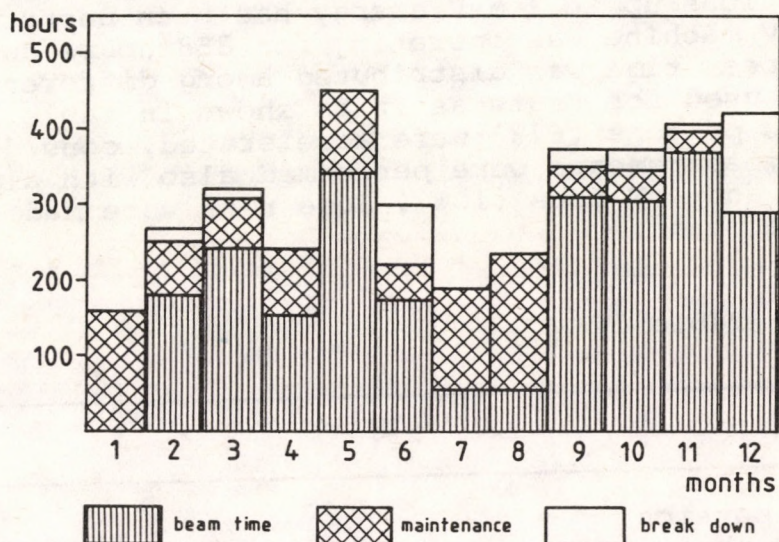
- [1] I.Borbély-Kiss, E.Koltay, Gy.Szabó, L.Bozó, E.Mészáros, Á.Molnár: in press in Nucl. Instr. Meth. in Phys. Res.
- [2] I.Borbély-Kiss, L.Bozó, E.Koltay, E.Mészáros, Á.Molnár, Gy.Szabó: Submitted to the journal Atmospheric Environment.
- [3] J.Kispéter, J.Beczner, I.Borbély-Kiss, L.Horváth, A.Novák: ESNA XXth Annual Meeting, Oct. 16-20 1989. Lunteren/Wageningen, the Netherlands. Book of Abstracts p.

**DEVELOPMENT OF METHODS
AND INSTRUMENTS**

STATUS REPORT ON THE CYCLOTRON

Z. Kormány, A. Valek

The overall working time of the MGC cyclotron was 3753 hours with monthly distribution shown in Figure. The utilization of the cyclotron was mainly concentrated to 9 months and the remaining ones were reserved for maintenance and developments. The cyclotron was available for the users 2535 hours; the effectively used beam time is summarized in the Table



Projects	Beam time in hours
Nuclear spectroscopy	528
Nuclear reaction studies	387
Nuclear life-time studies	185
Isotope production	416
Neutron source	186
Material investigation	124
Charged particle irradiations	225
Total	2051

As developments, the prototype of the rotating wire scanner head has been built in to the transport channel; a big vacuum chamber has been installed for irradiation of foils used to investigate the foil-filter production technology; an irradiation process has been worked out to manufacture masks from chemical resisting material (Melinex) to mark industrial goods.

ACTIVITIES AT THE VAN DE GRAAFF ACCELERATOR LABORATORY

L. Bartha, Á.Z. Kiss, E. Koltay, A. Nagy and Gy. Szabó

During 1989 the beam time of the VDG-1 machine amounted to 783 hours and its proton and helium beams fulfilled the total need of electron spectrometry group working in atomic physics, the only user this time. The construction and manufacturing of a new analysing magnet having a possibility to analyse $Z \leq 10$ ions up to 1 MeV energy has been performed.

The 5 MV machine was operating for 858 hours during this period. Its beam time was distributed among different research subjects and used for tests as it is shown in table 1. Although in most cases protons (67%) were accelerated, considerable part of the measurements were performed also with alpha particles (16%) and ^{15}N ions (10%). Some runs were made with C, ^{14}N , F and He beams.

Table 1.

Field	Hours	%
Atomic physics	106	12
Nuclear physics	125	15
Analytical studies	404	47
Accelerator physics	208	24
Machine test	15	2
Total	858	100

The developement around the accelerator concentrated to the test of a radio-frequency ion source of probeless extraction geometry as a possible source of light heavy-ions and molecular beams in different charge states. It has been proved in Rutherford scattering analysis of the magnetically resolved beam components that the high energy double charged beam is mixed with a beam of low energy molecular fragments of the same momentum. Results of such measurements are shown for illustration in Figs. 1 and 2, for the cases of He and N beams, respectively. Conclusions have been drawn on how such sources can be applied in ion-atom collision physics and nuclear microanalysis.

A three port switching magnet of 1 MeV. Amu/e² mass - energy product together with a 1.8 kW high stability power supply has been developed and manufactured upon the order of IAEA. The system delivered will be used in the beam transport system of a neutron generator at the Advanced Institute for Nuclear Science and Technology, Havana, Cuba.

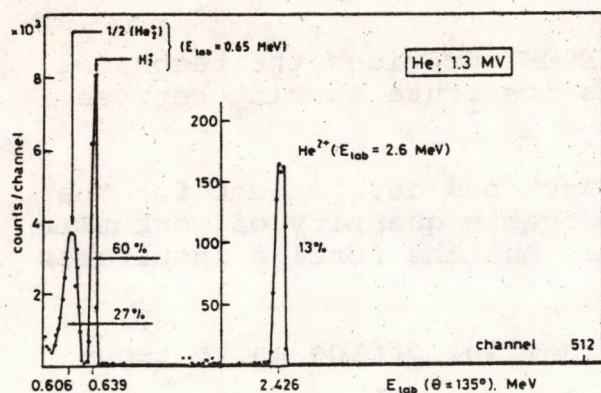


Fig. 1. Energy spectrum observed for helium as source gas when deflecting He^{2+} component and molecular fragments of the same momentum at a terminal voltage 1.3 MV. Intensity ratios for the components given in percentages were calculated from peak areas and Rutherford cross sections.

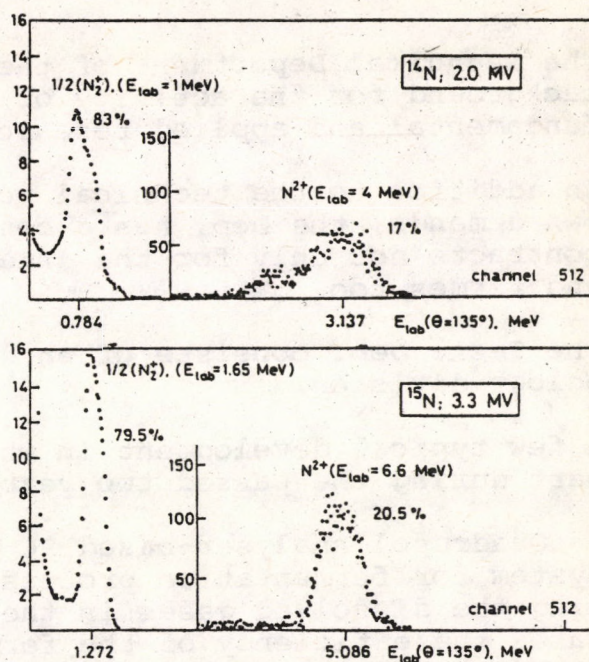


Fig. 2. Same as in fig. 1. for ^{14}N and ^{15}N gases, at terminal voltages of 2.0 and 3.3 MeV, respectively.

REFERENCE

L. Bartha, Á.Z. Kiss, E. Koltay and Gy. Szabó: Nucl. Instr. Meth. in Phys. Res., in print.

TECHNICAL DEPARTMENT

I. Gál

The Technical Department of the ATOMKI provides the technical background for the activity of the institute sharing between fundamental and applied research.

In addition to the technical research and development for the own demands, the Dep. has a considerable quantity of work under contracts not only for the internal but the foreign institutes and firms, too.

The Tech. Dep. consists of an engineering office and a technology division.

A few typical development in which the Tech. Dep. has taken part during the passed two years:

- Quadrupol analyser-based PC controlled automatic monitoring system for fermentation processes. By monitoring and analysing the dissolved gases in the fermentation liquid, the system makes the efficiency of the fermentation process optimum. This work has been supported by national advanced research program.

- A complete surface-analytical system is under testing now. The system based on a high resolution electron spectrometer is equipped with sample-transport and preparation devices, 30 kV X-ray tube, ion-gun, electron-transport lens-system and hemispherical analyser. The data acquisition and evaluation are computerized.

- General arrangement of an MI-1309 soviet made spectrometer was reconstructed and modernized by changing vacuum valves, pumps, ion source, etc. As a result of this development, better ultimate vacuum level, higher ion-current, more stable ion-beam and increased resolution, and higher precision in the determination of isotope ratio should be expected. Due to the new multi-sample ion source, a significant time saving could be achieved because the change of samples will be carried out without opening and baking the vacuum system after every single sample change.

- A new mass spectrometer (QMS) system had been constructed to investigate the gas-metabolism of plants. In vivo, multi-component measurements of gases in plants are carried out with an unique analyser system, consisting of a quadrupole mass spectrometer, a sampling unit with ten membrane probes, and a growth chamber. The microprocessor controlled quadrupole mass spectrometer makes it possible to measure gas concentrations simultaneously and quickly. The vacuum for the QMS and sampling unit is produced by full-automatic diffusion pump systems. The membrane probes are stainless steel perforated capillaries covered by 0,15 mm thick silicone rubber membrane. These sampling

capillaries are directly put into the stem of the plants hermetically. The gases in tissues, liquids and hollows of the plant diffuse across the membrane of the capillary and get into the QMS. In vivo, continuous and multicomponent analysis is achieved in this way. The illumination and temperature of the plants are controlled in the growth chamber. Environmental effects on the internal gas composition of wheat stalk are observable.

- Industrial design has been completed of the newest member of existing oil diffusion pump-family. The expectable pumping speed is 5000 ls^{-1} and the ultimate vacuum level is about 10^{-8} mbar using Santovac-5 oil filling.

- A coupled GC-MS measuring system is under development. This indispensable arrangement is spreading quickly in the up-to-date organic chemistry. The developing process includes a new quadrupole analyser of 1-500 a.m.u. with ion transport system and closed ion source.

- A superconducting gravimeter was designed and produced to measure the time-dependence of gravitational field on a fixed location. A superconducting ball is levitated in a stable magnetic field generated by a superconducting magnet. The position of the ball is continuously recorded by SQUID-based detection system. The whole probe is housed in a He gas filled temperature controlled chamber.

- A susceptometer has been put in operation to measure low-field magnetic susceptibility of small-size samples. The magnetic field is provided by a superconducting magnet. The samples are introduced into a temperature controlled He gas filled chamber. The magnetic moment of the sample is measured by SQUID detector. Special vibration-free mechanics was designed to move the samples between the detector coils.

THE EFFECT OF REAL GAPS IN ELECTROSTATIC SPECTROMETER

K. Tökési, A. Kövér, D. Varga

The calculations used generally for the determination of the electron trajectories in an electron spectrometer do not take into account the distortion of the electrostatic potential caused by the gaps located in the inner and outer electrodes for the entrance and exit of electrons and particles. We investigate this effect for our ESA-13, "box" type distorted field cylindrical mirror electron spectrometer. The main parameters of this analyzer can be found in ref. [1]. The radius of the inner cylinder is $R_1=32\text{mm}$. A computer program [2] is used to determine the distortion of the electrostatic field around the gaps.

Schematic diagram of the spectrometer with the location of the gaps can be seen in Fig.1. The size of the gaps are the followings:

- 1.gap: 3 mm of diameter aperture from 6.4 mm of the spectrometer wall for the entrance electrons and particles
- 2.gap: 9 mm of diameter aperture from 41 mm of the spectrometer wall for the outgoing particles
- 3.gap: gap between the two spectrometer electrodes

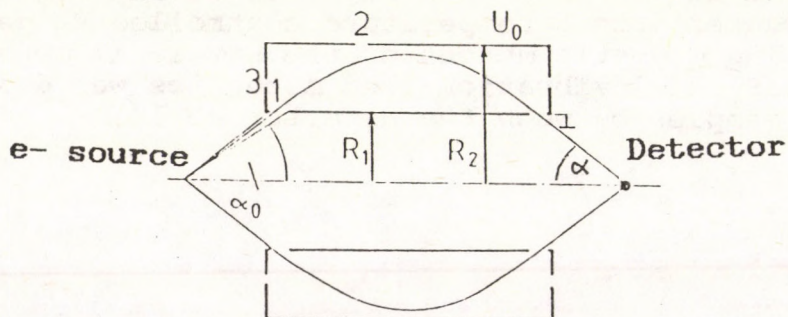


Fig 1. Schematic diagram of the "box" type distorted field cylindrical mirror electron spectrometer [ESA-13] with the location of the gaps.

In this paper we demonstrate the effect of the gaps by comparing the electron trajectories in the analyzer with and without the gaps. The electrons enter the analyzer with 490 relative to the analyzer axis and the initial start point (source point) is 20 mm from the spectrometer wall on the spectrometer axis.

The table shows the characteristic parameters of the electron trajectories in the analyzer.

Table

Characteristic parameters of the electron trajectories.

gaps	alpha	rmax(mm)	Z(mm)
without gaps	50.541687	61.50	112.92685
1	50.312679	61.27	112.91848
2	50.957566	62.10	114.22672
3	50.148507	60.32	111.84008
1,2	50.729839	61.86	114.15366
2,3	50.574448	60.88	113.29214
1,3	49.905723	60.07	111.64336
1,2,3	50.320145	60.60	113.10890

Marks of the table are:

alpha: angle of the outgoing electrons
 rmax: maximum radial range from the spectrometer axis
 for the electron inside the analyzer; (R2=64mm)
 Z: Z coordinate of the focal point

References

- [1]. D. Varga, A. Kövér, L. Kövér, and L. Redler, Nucl. Instrum. Meth. A238(1985)393.
- [2]. N.G. Shakun, M. Rysavy, Nucl. Instrum. Meth. A281 (1989) 37-42

MODEL CALCULATION OF X-RAY TUBE

K. Tökési, M. Rysavy*

* Nuclear Physics Institute, Czech. Acad. Sci.; 25068 Rez
Czechoslovakia

The development of the computers has opened the possibility to calculate the properties of bigger and more complicated electrostatic arrangement. By the help of the Shakun program, described in [1], the potential distribution of an X-ray tube and the trajectories of the charge particles in the calculated potential space have been calculated.

The Figure 1 shows the schematic cross section of the X-ray tube with a typical electron trajectory.

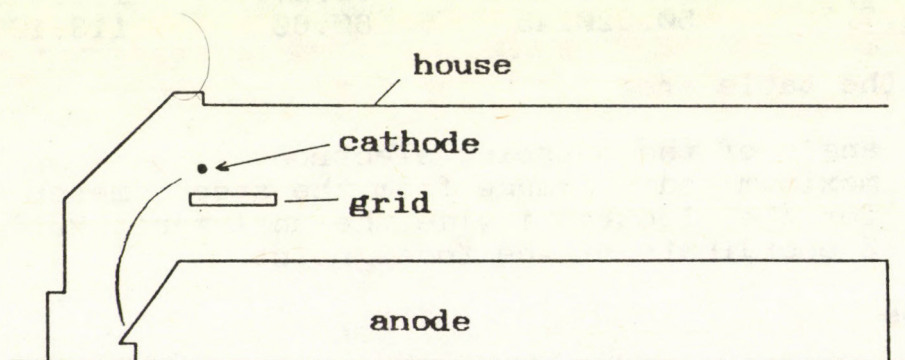


Fig. 1 Schematic cross section of the X-ray tube with a typical calculated electron trajectory

The position, where the electrons hit the anode (which is an important parameter when the X-ray tube is used in an XPS instrument) strongly depends on the position of the grid at a given electrode potential arrangement.

References

- [1]. N.G. Shakun, M. Rysavy, Nucl. Instrum. Meth. A281 (1989) 37-42

DOUBLE FOIL ASSEMBLY FOR A HIGH PRESURE DEUTERIUM GAS TARGET

T. Molnár¹, A. Fenyvesi, I. Mahunka, F. Tárkányi

¹Biomedical Cyclotron Laboratory, Medical University School,
Debrecen,

Biomedical neutron irradiations and especially human cancer treatments need high mean energy and intensity neutron sources. In the case of small cyclotrons ($E_p \leq 20$ MeV) the optimal solution is a high pressure deuterium gas target [1], [2]. Such a type of sources was constructed by Schraube [3] for the German Cancer Research Institute (Heidelberg) and now it has been installed at the MGC-20E cyclotron in Debrecen [4].

Increasing the pressure in the target volume a more defined and point like neutron source is resulted but this is limited by the mechanical strength of the entrance foil. A good way of lowering the danger of a foil eruption is the use of a double foil system and a helium flow between them at half pressure of the target gas with the same beam energy loss. A puffer volume in the closed helium gas cooling circuit gives the possibility of collecting and recovering the expensive enriched target material in the case of failure of the internal foil. A realization of this concept is shown in Fig. 1. Detailed studies are in progress on the optimalization of the rate of the diameter of the beam to the diameters of the foils, foil materials, their thicknesses and cooling parameters.

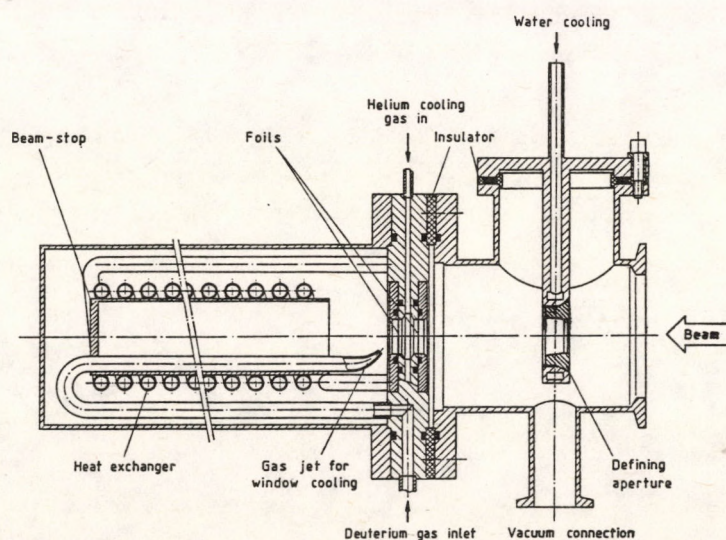


Figure 1. The high pressure deuterium gas target with the double foil assembly.

REFERENCES

- [1] G.J. Batra, D.K. Bewley, M.A. Chaudri, Nucl. Instr. and Meth., 100(1972), pp. 135-139
- [2] M.A. Chaudri, Nucl. Instr. and Meth., 120(1974). pp. 357-358
- [3] H. Schraube, GSF-Bericht S 465
- [4] A. Fenyvesi, I. Gál, I. Mahunka, T. Molnár, F. Tárkányi, A. Csejtej, Magyar Radiológia 63(1989), pp. 166-176

BEAM SPLITTING FOR PARALLEL IRRADIATIONS

S. Takács, F. Tárkányi, I. Gál, L. Andó

The radioactive isotopes produced by charged particle irradiation are usually more expensive than those made in nuclear reactors, mainly because of the lack of parallel irradiation possibility at accelerators. For this reason there is a renewal interest for simultaneous experiments dividing the primary beam into two or more parts. There are several type of the beam splitter based on different phenomena [1,2].

In this paper we report a new type of beam splitter. The technical arrangement of it is shown in Fig.1.

The beam coming from the accelerator goes through a rotating magnetic field produced by a three-phase electric motor stator mounted on the beam line. As the results of the interaction of the charged particles in the beam and the magnetic field the beam is diverted from its original direction. The shape of the time integrated distribution of the particles in the beam perpendicular to their original direction is a ring with a radius which depends on the strength of the applied magnetic field. The time integrated intensity distribution of the beam can be seen on Fig.2. in the case of Gaussian shaped primary beam[3].

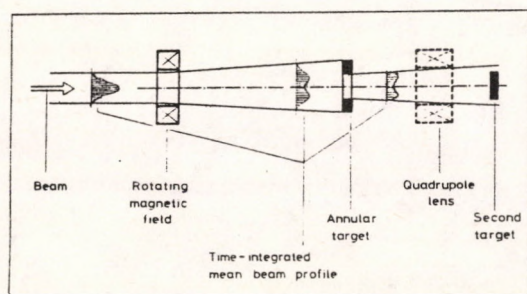


Fig.1. Two simultaneous irradiations using rotating magnetic field

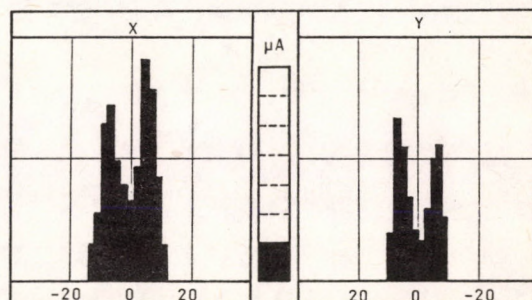


Fig.2. The beam profile measured by rotating scanner

Applying an annular target after the rotating magnetic field the beam can be divided into two parts. The main part is used to activate the annular target while the particles going through it after necessary focusing can be used to irradiate a second target.

In this arrangement both targets are free from destructive hot-spots. The beam intensity ratio on the two targets can be changed continuously by changing the strength of the magnetic field. Stronger the magnetic field lower the intensity on the second target. Applying this arrangement the original time structure of the beam remains unchanged and there is no shadow effect as in the case of the electrostatic splitter which can cause intensity loss.

However, it should be mentioned that using this method at an accelerator having a macro pulsing system a synchronisation must be used for uniform thermal load of the targets. The method requires an annular target which means more complicate target preparation. Because of the loading limit of the stator this method applicable only at a low energy accelerators.

References

1. M. Olivo, H.W. Reist, Proc. of European Particle Accelerator Conference, Rome, June 7-11, 1988
2. W.C. Edwards, Annual Research and Development Report 1982 Medical Research Council Cyclotron Unit, Hammersmith Hospital, London, pp. 58-59
3. Z. Kormány, T. Lakatos, A. Valek, Proc. of 12th International Conference on Cyclotrons and Their Applications, West-Berlin, May 8-12, 1989

DETERMINATION OF EFFECTIVE BOMBARDING ENERGIES AND TARGET FLUXES IN MEASUREMENT OF EXCITATION FUNCTIONS BY MEANS OF STACKED-FOIL TECHNIQUE

F. Tárkányi, F. Szelecsényi, S. Takács, J. Végh

Cross section and production yield data of charged particle induced nuclear reactions play important role in the production of medical radioisotopes. The stacked-foil technique in which several foils or gas cells are placed in a series and irradiated in one step is one of the most frequently used methods for excitation function measurements. The main advantages of this method are that it gives very good relative accuracy; gives possibility for simultaneous irradiation; correction for recoil losses is usually not necessary; and it is economical. The weak points of the stacked-foil technique are that large uncertainties appear in the calculated incident energies because of the superimposed errors of the foil thicknesses; there is variation in particle flux along the thickness of a long stack; and cooling problem exists at low melting point of the target and higher beam intensities.

These disadvantages could be eliminated significantly by the new approach of monitor reactions in which: the energy scale, the effective bombarding energy and the cross section values at each samples of the stack are determined relative to the monitor reactions. The fluxes in the stack are determined more accurately using more monitor foils, and the beam intensity reduction can be followed along the stack.

The basic principles of the proposed method are as follow:

When the beam energy in a given monitor foil is well estimated, the fluxes calculated from different monitor reactions are the same (provided that the cross sections of the monitor reactions at least relatively correct).

If the whole beam entering the first foil goes through the whole stack and the thicknesses and energies are well estimated for each foil, then the calculated flux in every monitor foils using the same monitor reaction must be the same.

The proposed method is illustrated by proton bombardement of a stack with natural copper monitor foils. In practice the bombarding beam intensity is determined with the first few monitor foils using all the measured reaction channels (ABCD points on Fig.1.). The next monitor foils give same flux values only at the right energy position (EF). In the energy region where only one reaction channel is open using the flux constancy principle, the energy can also be estimated (G). At many open reaction channels the beam divergency could be also followed.

Our experiences show that in a stack having many foil after 8-10 MeV energy absorption using even the best estimation of sample thicknesses, the experimentally "measured" energy may shift 1-2 MeV [3]. In the case of a long stack of gas cells where the beam divergency plays an important role the flux lowering could be simply followed. The method defines new

conditions for the monitor reactions and demands new and more precise nuclear data.

References

- [1] A. Gütter, Nucl. Phys. A383(1982)98
- [2] P. Kopecký, Int. J. Appl. Radiat. Isot. 36(1985)657
- [3] F. Tárkányi, F. Szelecsényi, Z. Kovács, S. Sudár, Radiochimica Acta (accepted), ATOMKI Preprint 5-1989P

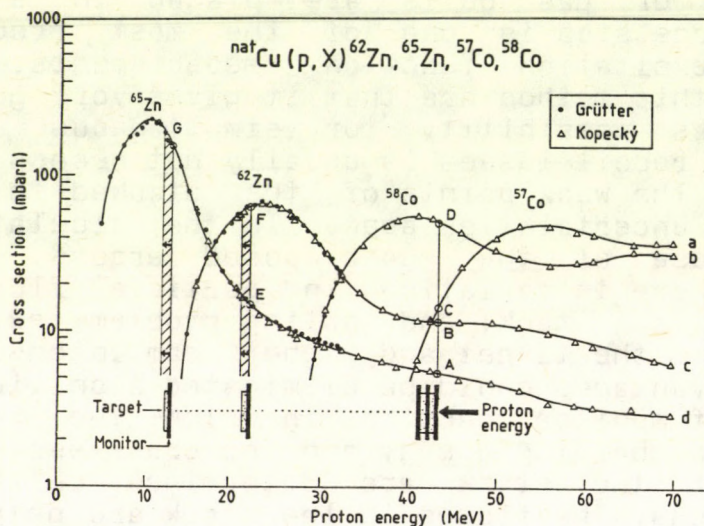


Fig.1. Illustration of the method using proton induced monitor reactions on natural Cu.

A CHARGED PARTICLE BEAM ROTATOR FOR UNIFORM THERMAL LOADING OF TARGETS

L. Andó, B. Tóth, F. Tárkányi

High intensity irradiations or targets with a low melting point need "hotspot-free", uniformly distributed thermal loading of the irradiated targets. The uniform heat dissipation could be achieved by defocusing the beam, or by moving periodically the target or the beam.

At most of the existing beam lines the beam is swept by periodically changed perpendicular dipole magnetic fields. An other applied solution is the beam rotation using a motor stator.

At our cyclotron for high intensity irradiations (used mainly in applied fields) the beam rotation method was chosen and installed because of the simplicity.

In accordance with the basic operation principle the beam spot on the target of the charged particle beam, coming from the MGC-20E compact cyclotron, is translated along a circle due to the spinning dipole magnetic field. The magnetic field is produced by a three-phase electric motor stator mounted on the beam lines at 2-3 meters from the targets.

For the beam spinning magnets a special power supply has been built.

It has two operation modes:

- circular with variable radius,
- a pulsing spiral with variable maximum diameter, where the ramp time is changing in accordance a special function to get uniform thermal loading of the target.

For the necessary synchronisation to the macro-pulsing system of the cyclotron the power supply has two controll modes:

- own independent time base with independent regulation,
- synchronised direct control from the cyclotron.

It is easy to see that an inhomogen rotating dipole magnetic field can focus the beam. Such an unnecessary effect has to be avoided therefore the magnetic field of the used motor stator (typ. KMERa 100 L 2/1, VEB Elektromotorenwerke Thurm/GDR) was measured in detail. For the magnetic field measurements static condition was performed by DC power supplies. Small volume, sensitive Hall-probe (Lake Shore Cryotronics, USA) have been used for mapping. The typical distribution of the magnetic field in the middle plane perpendicular to the axis of the stator is presented in the Fig.1. As it is shown the magnetic field is dipole and uniform in the interested central region.

Our experiences with high intensity beams show that the beam rotator could be used effectively. The effect of the rotator in circular mode is illustrated in Fig.2.

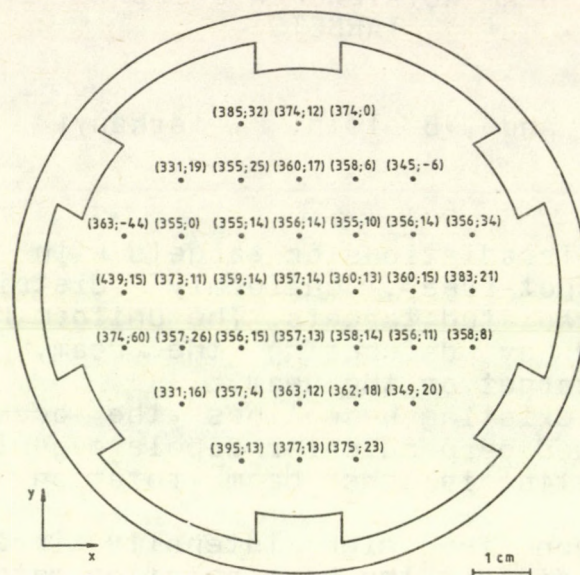


Fig.1. The Hall-voltages of the probe (U_x , U_y in relative units) in the middle plane perpendicular to the axis (z) of the stator

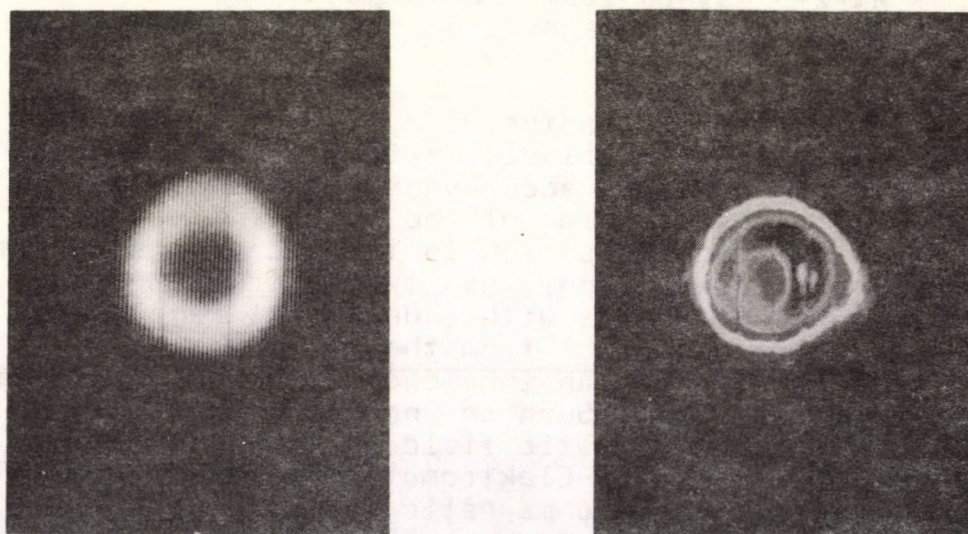


Fig.2. Thermographic pictures of the rotated beam

SECONDARY TARGET EXCITATION SOURCE FOR X-RAY FLUORESCENCE ANALYSIS USING ANNULAR ^{241}Am ISOTOPE

G. Kalinka

Despite the popularity of X-ray tubes for X-ray fluorescence analysis as flexible, intense excitation sources, radioisotopes are still being in use due to their compactness and relatively low prices. Considering, however, the half-lives of the most frequently used isotopes (^{55}Fe : 2.7 y; ^{109}Cd : 1.27 y; ^{125}I : 60 d; ^{241}Am : 433 y; ^{57}Co : 270 d) the idea of low price turns to be an illusion - except for ^{241}Am .

The applicability of ^{241}Am as direct exciter is however, strongly limited (mainly to lighter rare earth elements) because of the intense backgrounds in the 0-15 keV and 45-60 keV regions due to 60 keV γ Compton scattering in detector (especially in low atomic number Si detector) and specimen respectively.

A better solution is to use ^{241}Am in secondary target arrangement [1-5], transforming it into a "tunable" excitation source, but at a sacrifice of significant intensity reduction [6].

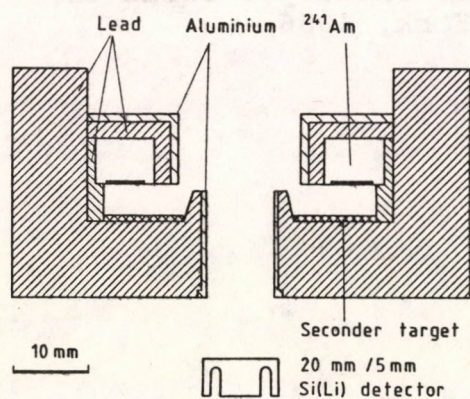


Fig. 1. Sketch of the secondary target excitation arrangement.

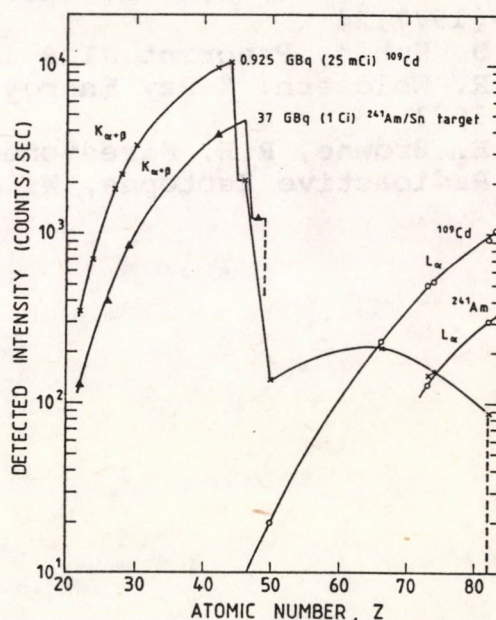


Fig. 2. Comparison of excitation efficiencies of 0.925 GBq ^{109}Cd and 37 GBq $^{241}\text{Am}/\text{Sn}$ target by excitation of thick pure elements and detection with 50 mm²/4 mm Si(Li) detector.

The assembly designed in our laboratory (Fig.1.) exhibits the following features:

- the secondary spectrum "quality" (regarding higher energy γ -scatter and fluorescent contamination from assembly materials) compares to that of ^{109}Cd
- the secondary to primary intensity ratio is about 1: 100, at maximum spectral purity, using medium atomic number pure element (Mo-Dy) secondary targets (Fig.2.)
- from the point of view of radiation safety the γ -ray attenuation of the whole assembly in side and downward directions are $\sim 10^{-20}$, 10^{-5} , 10^{-2} , 10^{-1} for ≤ 100 , 200, 300, 700 keV photon energies respectively, which means a total photon emission of $\sim 10^{-5} \text{ s}^{-1}$ in the 200-800 keV region due to high energy γ -rays from ^{241}Am [7], assuming $3.7 \times 10^{10} \text{ Bq}$ (1 Ci) source activity.

REFERENCES

- [1] R.D. Giaque, Anal. Chem. 40(1968)2075
- [2] C. Shenberg, S. Amiel, Anal. Chem. 43(1971)1025
- [3] C. Shenberg, M. Boazi, J. Radioanal. Chem. 27(1975)457
- [4] J.W. Rowson, S.A. Hontzeas, Can. J. Spectroscopy 22 (1977)24
- [5] D. Rubio, Preprint JINR 18-81-506, 1981
- [6] R. Woldseth: X-Ray Energy Spectrometry, KEVEX, Burlingame, 1973
- [7] E. Browne, R.B. Firestone (Ed: V.S. Shirley): Table of Radioactive Isotopes, Wiley, New York, 1986

PREPARATION OF THE ASTATOACETIC ACID AND DETERMINATION OF ITS DISSOCIATION CONSTANT

Z. Szűcs, Yu.V. Norseev¹, D.D. Cuong¹, L. Vasáros²

1., Joint Institute for Nuclear Research, Dubna, USSR

2., Central Institute of Physical Research, Budapest, Hungary

Astatine has only short-lived radioactive isotopes. The astatine isotopes, with sufficiently long half-lives for chemical experiments, can be produced only by cyclotron. For this reason our knowledge about the chemical behaviour and the physical properties of this very rare element and its compounds is limited.

The preparation of astatoacetic acid could be performed by the following exchange reaction:



The dissociation constant (K_a), one of the most important data of acids, can be determined by the radioactivity of the dissociated and undissociated acids distributed between an organic and aqueous phase at different pH values. The distribution coefficient (D) can be described by the following equation:

$$1/D = 1/D_o + 1/D_o \frac{K_a}{[\text{H}^+]}$$

where D_o is the distribution constant of the undissociated acid. From the plot of $1/D$ versus $1/[\text{H}^+]$ the K_a value can be calculated.

²⁰⁹⁻²¹¹At isotopes were produced by bombarding metal thorium with 660 MeV protons in the syncrocyclotron of the JINR in Dubna (USSR). Astatine was separated from other spallation products by thermochromatographic method [1].

The astatine was distilled into $5 \times 10^{-1} \text{ mol dm}^{-3}$ solution of Na_2SO_3 at pH=12. To this solution containing At^- equal volume of aqueous solution of 1 mol dm^{-3} iodoacetic acid was added, and the reaction mixture was heated at 333 K for 20 min. After synthesis the solution was purified from the At^- and I^-

ions by ion exchange chromatography (column: DOWEX 1X8, eluent: $0.1 \text{ mol dm}^{-3} \text{ NaNO}_3$). Yield of the synthesis was higher than 95%. The eluat of the astatoacetic acid was shaken with equal volume of diethyl ether in a sealed pot for 15 min. After separation of the phases their activity and the pH of the anorganic phase were measured. The extraction step and the measurements were repeated several times at different pH varied by addition of $1 \times 10^{-1} \text{ mol dm}^{-3} \text{ HClO}_4$ or NaOH solution to the aqueous phase. The method described above was checked by determination of the pK_a value of the corresponding [^{131}I]iodo compound in the same way. The results of the pK_a measurement of the astatoacetic acid and the [^{131}I]iodo analogue are compiled in the table together with the literature values:

Table: pK_a values of halogeno-acetic acids

HALOGENO-ACETIC ACID	REF. [2, 3]	REF. [4]	THIS WORK
FLUORO	2.59		
CLORO	2.86		
BROMO	2.90		
iodo	3.18		3.17 ± 0.06
ASTATO		3.77	3.63 ± 0.04

As it can be seen from the data, our results are comparable with the literature values.

Reference:

- [1] Norseyev Yu.V.: Thesis., JINR 12-83-387, Dubna (1983)
- [2] Christensen J.J., Izatt R.M., Hansen L.D.: J. Amer. Chem. Soc. 89, 213 (1967)
- [3] Christensen J.J., Oscarson J.L., Izatt R.M.: J. Amer. Chem. Soc. 90, 5949 (1968)
- [4] Samson G.: Radiochimica Acta, 13, 220 (1970)

IBM PC based data acquisition system for electron spectrometers

I. Cserny, J. Végh

The rapidly evolving IBM PC computers provide low cost "host computers" for computer-based data acquisition systems. A simple solution to the problem of recording data measured by (single-channel) electron spectrometers is presented here, which has been installed for a KRATOS ES-300 XPS/UPS apparatus.

The spectrometer is controlled by an IBM PC/XT/AT compatible add-on interface board, which contains a 16-bit digital output register, one 16-bit counter and a timer. The spectrometer voltage is controlled by a 16-bit digital-to-analog converter, which is located outside of the computer, and is driven through opto-couplers in order to eliminate electrical noise problems. The counter input, which accepts the detector pulses, is also isolated using a pulse transformer.

The data acquisition software was written in Turbo Pascal language with few bytes of machine coding. In order to economize memory usage, the software is divided into two components: the data acquisition module and the user interface program.

Data acquisition and recording is performed by a memory resident program, which can communicate with any other (even user-written) software through the MS-DOS multiplex process interrupt (INT \$2F) calls. This program runs entirely on interrupt level thus leaving the CPU free for other tasks. This gives the user the freedom to run any other application program, without affecting the data acquisition in progress.

All data acquired in one experiment are stored in a single ASCII file. The file format conforms to the standard data format suggested by the VAMAS community [1,2] for surface analytical techniques.

The user interface part (which allows setting up various parameters, controlling the measurement, and real-time displaying of incoming data) is a transient program, which may be removed from the memory, if the user has other tasks to do (word processing, program development, data evaluation, etc.). Several energy regions in various sequence can be measured. The program presets default parameter values and retains the last recently used ones.

This software piece can be used either independently or as a part of the evaluation and measurement control program EWA developed by one of the authors (JV). In the latter mode the acquired data can also be accessed from the evaluation program for on-line evaluation.

[1] W. A. Dench, L. B. Hazell, M. P. Seah, *Surface and Interface Analysis*, 13, (1988) 63

[2] "VAMAS Surface Chemical Analysis Standard Data Transfer Format with Skeleton Decoding Programs", National Physical Laboratory Report, DMA(A) 164, July 1988

PUBLICATIONS
AND
SEMINARS

Papers published in 1989

(* denotes co-author from other establishment)

NUCLEAR PHYSICS

Kiss A. Z., Somorjai E., *Raisanen, J., *Rauhala, E.; **Stopping powers of 1.5-7.2 MeV ^4He ions in havar, nickel, kapton and mylar;** Nuclear Instruments and Methods in Physics Research "B" 39 (1989) 15

Tárkányi F., Kovács Z., *Qaim, S. M., *Stöcklin, G.; **Differential production yields of ^{123}I in proton and deuteron induced reactions on natural xenon;** Radiochimica Acta 47 (1989) 25

*Curutchet, P., Vertse T., *Liotta, R. J.; **Resonant random phase approximation;** Physical Review "C" Nuclear Physics 39 (1989) 1020.

Lévai G.; **A search for shape-invariant solvable potentials;** Journal of Physics "A" 22 (1989) 689.

*Rowley, N., Pál K. F., *Nagarajan, M. A.; **Bandcrossings at high spin: level interactions and diabolic points;** Nuclear Physics "A" 493 (1989) 13.

*Keinonen, J., *Tikkanen, P., *Kuronen, A., Kiss A. Z., Somorjai E., *Wildenthal, B. H.; **Short lifetimes in ^{24}Mg for test of rotational collectivity in shell-model wave functions;** Nuclear Physics "A" 493 (1989) 124.

*Schröder, U., *Engstler, S., *Krauss, A., *Neldner, K., *Rofls, C., Somorjai E., *Langanke, K.; **Search for electron screening of nuclear reactions at sub-coulomb energies;** Nuclear Instruments and Methods in Physics Research "B" 40 (1989) 466.

Nyakó B. M., *Gizon, J., *Barnéoud, D., *Gizon, A., Józsa M., *Klamra, W., *Beck, F. A., *Merdinger, J. C.; **Observation of band structures in the odd-odd nucleus ^{126}La ;** Zeitschrift für Physik "A" 332 (1989) 235.

*Cujec, B., Hunyadi I., *Szöghy I. M.; **$^{12}\text{C}(^{12}\text{C}, ^8\text{Be})^{16}\text{O}$ cross-section measurement at sub-barrier energies;** Physical Review "C" Nuclear Physics 39 (1989) 1326.

*Merchant, A. C., Pál K. F., *Hodgson, P. E.; **The alpha-particle structure of ^{44}Ti ;** Journal of Physics "G" 15 (1989) 601.

*Simpson, J., *Riley, M. A., *Sharpey-Schafer, J. F.,
*Bacelar, J., *Cook, A. P., *Cresswell, J. R., *Elenkov, D. V,
*Forsyth, P. D., *Hagemann, G. B., *Herskind, B., *Holm, A.,
*Howe, D., Nyakó B. M.; **The structure of states at very high spin in ^{157}Er** ; Journal of Physics "G" 15 (1989) 643.

*Tikkanen, P., *Keinonen, J., Kiss A. Z., *Wildenthal, B. H.;
Transition strenghts in the mirror nuclei ^{29}Si - ^{29}P ; University of Helsinki, Report Series in Physics (HU-P-251-1989); Proceedings of the XXIII Annual Conference of the Finnish Physical Society March 30-April 1, 1989, Haikko, Finland (1989) 29.

Cseh J.; **Application of the algebraic cluster model to light nuclei**; Journal of the Physical Society of Japan, Suppl.58 (1989) 604.

*Sheikh, J. A., *Nagarajan, M. A., *Rowley, N., Pál K. F.;
Cranked-shell-model calculations in a truncated space; Physics Letters "B" 223 (1989) 1.

Krasznahorkay A., Dombrádi Zs., Timár J., Fényes T., Gulyás J., *Kumpulainen, J, *Verho, E.; **Nuclear structure of ^{108}In** ; Nuclear Physics "A" 499 (1989) 453.

Pál K. F., *Nagarajan, M. A., *Rowley, N.; **On the Bengtsson-Frauendorf cranked-quasiparticle model**; Nuclear Physics "A" 500 (1989) 221.

Gyarmati B.; **Calculation of resonant wave functions in nuclear physics**; Proceedings of the Symposium on "Resonances", Lertorpet, Aug 19-26, 1987; Lecture Notes in Physics, Vol.325, Berlin, etc. Springer Verl. 325 (1989) 153.

Kruppa A. T.; **Resonant states in the microscopic cluster model**; *ibid.* p. 453.

Gyarmati B., Vertse T.; **The regularization method**; *ibid.* p. 544.

Vertse T., *Curutchet, P., *Liotta, R. J.; **The use of gamow functions in nuclear problems**; *ibid.* p. 179.

Tárkányi F., *Qaim, S. M.; **Excitation functions for the formation of some radioisotopes of cesium and iodine in proton and deuteron induced nuclear reactions on natural xenon**; Radiochimica Acta 47 (1989) 169

Máté Z., Szilágyi S., Zolnai L., *Bredbacka, A., *Brenner, M., *Kallman, K. M., *Manngard, P.; **Low energy alpha scattering on ^{62}Ni** ; Acta Physica Hungarica 65 (1989) 287.

Vertse T., *Curutchet, P, *Liotta, R. J., *Bang, J.; **On the role of anti-bound states in the RPA description of the giant monopole resonance**; *ibid.* p. 305.

Kiss A. Z., Koltay E., Somorjai E.: **New data for $^{12}\text{C}(\text{p},\gamma)^{13}\text{N}$ radiative capture process: note on an anomaly in thick target measurements;** *ibid.* p. 277.

Fényes T., Dombrádi Zs.; **Nuclear structure of ^{116}In ;** *ibid.* p. 295

Krasznahorkay A., Dombrádi Zs., Timár J., Gácsi Z., Kibédi T., *Passoja, A., *Julin, R., *Kumpulainen, J., *Brant, S., *Paar, V.; **Nuclear structure of ^{110}In ;** *Nuclear Physics "A"* 503 (1989) 113

Tárkányi F., *Qaim, S. M., *Stöcklin, G.; **Cross sections and yields relevant to radioisotope production;** Progress Report on Nuclear Data Research in the FRG NEANDC(E)-302u Vol. V., INDC(ger)-34/LN+Special. ed.: W. Scierjacks, Karlsruhe, FRG, Kfk Institut für Material- und Festkörperforschung, (1989) 17

Krasznahorkay A., Dombrádi Zs., Timár J., Fényes T., Gulyás J., *Kumpulainen, J., *Verho, E.; **Nuclear structure of ^{108}In ;** JYFL (Dept. of Phys. Univ. of Jyväskylä), Annual Report 1988 (1989) 62

Lovas R. G., Kruppa A. T.; **Consistent cluster-model description of $A=2$ to 8 nuclei;** Int. Symp. on Developments of Nuclear Cluster Dynamics, Sapporo, 1-3 Aug 1988, Singapore, World Scientific (1989) 39

Cseh J.; **Algebraic approach to the molecular resonances;** *ibid.* p. 255.

Lovas R. G.; **What is a cluster?;** Supplement to Journal of Physical Society of Japan 58 (1989) 288

*Lanen, J. B. J. M., Lovas R. G., Kruppa A. T., *Blok, H. P., *Van den Brand, J. F. J., *Ent, R., *Jans, E., *Kramer, G. J., *Lapikás, L., *Quint, E. N. M., *Van der Steenhoven, G., *Tiemeijer, P. C., *De Witt Huberts, P. K. A.; **(e,e'p) study of triton + deuteron + proton clustering in ^6Li ;** *Physical Review Letters* 63 (1989) 2793.

ATOMIC PHYSICS

Sarkadi L., Pálinskás J., Kövér A., Berényi D., *Vajnai T.; **Observation of electron capture into continuum states of neutral atoms;** *Physical Review Letters* 62 (1989) 527

Végh L.; **Critical angle in double ionisation;** *Journal of Physics "B"* 22 (1989) 35

***Watanabe, T., Végh L.; Scattering correlation in multiple ionization by electron-, proton-, antiproton- and multicharged ion impact; Nuclear Instruments and Methods in Physics Research "B" 40 (1989) 89**

Ricz S., Kádár I., Végh J.; The postcollision interaction observed at high-energy ion-atom collisions; ibid. p. 77.

Kádár I., Ricz S., Sulik B., Varga D., Végh J., Berényi D.; High-resolution target Auger spectroscopy at the impact of energetic heavy ions on Ne; ibid. p. 60.

Kövér A., Sarkadi L., Pálincás J., Berényi D., Szabó Gy., *Vajnai T., *Heil, O., *Groneveld, K. O., *Gibbons, J., *Sellin, I. A.; The contribution of the ECC to the forward electron cusp in 50-150 keV amu⁻¹ He⁺-He, Ar collisions; Journal of Physics "B" 22 (1989) 1595

Kövér A., Sarkadi L., Pálincás J., Gulyás L., Szabó Gy., *Vajnai T., Berényi D., *Heil, O., *Groneveld, K. O., *Gibbons, J., *Sellin, I. A.; ECC and ELC contributions to the "cusp" and its shape at the impact of light ions with accompanying electron(s); Nuclear Instruments and Methods in Physics Research "B" 42 (1989) 463

Végh J., Kádár I., Ricz S., Sulik B., Varga D., Székely G.; A reliability test of measured spectra; Nuclear Instruments and Methods in Physics Research "A" 281 (1989) 605

Szabó Gy., Kövér A., Gulyás L.; Ejected electrons at backward angles from He and Ne by He²⁺ impact; Acta Physica Hungarica 65 (1989) 195

Sarkadi L.; L-shell ionization and L X-ray emission induced by antiprotons; ibid. p. 201

Török I.; Study of the chemical shift of K x-ray lines with a home-built X-ray crystal spectrometer; ibid. p.225

Kádár I., Ricz S., Sulik B., Varga D., Végh J.; The reduction of the systematic error caused by the nuclear background in high resolution electron spectroscopy of high-energy ion-atom collisions; ibid. p. 229

Vatai E.; On the energy dependence of the electron shake processes; ibid. p. 265

Papp T., Pálincás J.; Resolution and detection of weak X-ray lines using a Si(Li) detector combined with absorbers; ibid. p. 209.

***Dubois, R. D., Kövér A.; Single and double ionization of helium by hydrogen-atom impact; Physical Review "A" 40 (1989) 3605**

Pálinkás J., *Schuch, R., *Cederquist, H., *Gustafsson, O.,
Observation of electron-electron scattering in electron capture by fast protons from He; Phys. Rev. Lett. 63 (1989) 2464

Gulyás L., Szabó Gy., Kövér A., Berényi D., *Heil, O.,
*Groneveld, K. O.; **Study of the cusp for H^0 , He^+ , He^{2+} (0.2 MeV/u)-Ne, Ar, Kr collision systems in the angular region from 0 to 4; Physical Review "A" 39 (1989) 4414**

*Heil, O., *Hofmann, D., Kövér A., Szabó Gy., Gulyás L.,
Sarkadi L., Pálinkás J., Berényi D., *Gibbons, J.,
*Sellin, I. A., *Groneveld, K. O.; **Cuspelektronen-verteilungen selektiert nach ECC- und ELC-Prozessen in He^+ (50-150 keV/u)-He, Ar Stößen; Jahresbericht 1988; J. W. Goethe Univ. Frankfurt/m., Inst. für Kernphysik (1989) 34**

Kádár I., Berényi D., Ricz S., Sulik B., Varga D.,
Végh J.; **High resolution target auger spectroscopy of heavy ion-atom-collisions; Proceedings of the Study Conference SCOFEI'88. Bucharest, Romania, Aug 29-Sep 2, 1988; eds.: M. Ivascu, V. Florescu, V. Zoran, Singapore, World Scientific (1989) 434**

Végh L., Sulik B.; **Independence of recoil-ion velocity on the screening effect of the target electrons; ibid. p. 504**

*Awaya, Y., *Kanai, Y., *Kambara, T., *Mizogawa, T.,
*Hitachi, A., Sulik B.; **Multiple inner shell ionization of target atoms by 0.8-26 MeV/u heavy-ion impact; ibid.p.462**

MATERIALS SCIENCE AND ANALYSIS

*Milesz S., Molnár J., *Illés Z., *Sándor A. **Determination of ion mobilities by IBM PC controlled nuclear electro-migratic method, Journal of Radioanalytical and Nuclear Chemistry Letters, 135 (1989) 231**

Tárkányi F.; Kovács Z.; *Qaim, S. M.; *Stöcklin, G.;
Differential production yields of ^{123}I in proton and deuteron induced reactions on natural xenon, Radiochimica Acta 47 (1989) 25

Ditrói F., Mahunka I., Takács S., *Seif el-Nasr, S.A.H.; **Trace element analysis of motor oil by CPAA method on external proton beam, Journal of Radioanalytical and Nuclear Chemistry Articles, 130 (1989) 263**

Takács S., Ditrói F., Mahunka I.; **Investigation of aluminium made by powder metallurgy by using the CPAA method, Nuclear Instruments and Methods in Physics Research "B" 43 (1989) 99**

Kövér L., Tóth J., *Itoh, A.; **An experimental method for resolution calibration of electron spectrometers**; Acta Physica Hungarica 65 (1989) 217

Takács S., Ditrói F., Mahunka I.; **Measurement of oxide-layer thickness of internal granules in high-purity aluminium**; ibid. p. 355

EARTH AND COSMIC SCIENCES, ENVIRONMENTAL RESEARCH

Borbély-Kiss I., Koltay E., Szabó Gy., *Mészáros E.; **Elemental ratios related to selenium and vanadium as regional characteristics in atmospheric aerosols over Hungary**; Időjárás 93 (1989) 36.

Kövér L., Tóth J., *Schäg J. B., Borbély-Kiss I.; **Surface analysis of air pollutants by XPS: problems and experiences**; Surface and Interface Analysis (SIA) 14 (1989) 217.

*Várhegyi A., *Gerzson I., *Baranyi I., *Palyi, A., Hakl J.; **Application of methods based on microbubble radon transport theory for different geological tasks**; XXXIVth Int. Geophys. Symp., Budapest, 4-8 Sep 1989.; Abstracts and Papers of the Technical Program (1989) 713.

*Géczy G., Csige I., Somogyi Gy.; **Air circulation in caves traced by natural radon**; Proceedings of the X. International Congr. of Speleology, Budapest, 13-20 Aug 1989; ed.: Kósa A., Magyar Karszt- és Barlangkutató Társulat 2 (1989) 615.

Hakl J., *Lénárt L., Somogyi Gy.; **Time integrated radon measurements performed in a karstic well water**; ibid. p. 618.

*Lénárt L., Somogyi Gy., Hakl J., Hunyadi I.; **Radon mapping in caves of Eastern Bükk region**; ibid. p. 620.

Somogyi Gy., Hunyadi I., Hakl J.; **Historical review of one decade radon measurements in caves in Hungary performed by solid state nuclear track detection technique**; ibid. p. 631.

Arva-Sós E., *Ravasz-Baranyai L.; **Kalij-argonovaya izotopnaya geohronologiya mezozojskikh magmaticheskikh porod nekotoryh pajonov vengrii**; Carpatho-Balkan Geological Association 14th Congress; Sofia, 1989, Extended Abstracts 4 (1989) 1158.

Balogh K., *Ravasz-Baranyai L., *Nagy-Melles M., *Vass, D.; **Interpretation of K/Ar ages of young basalts: methods for eliminating unreliable ages**; ibid. p. 1182.

*Székyné-Fux V., Pécskay Z.; **New radiometric data to the chronology of covered neogene volcanic rocks from boreholes in the great hungarian plain;** *ibid.* p. 1194.

*Arkai P., Balogh K.; **The age of metamorphism of the east alpine type basement, Little plain, W-Hungary: K-Ar dating of K-white micas from very low- and low-grade metamorphic rocks;** *Acta Geologica Hungaricae* 32 (1989) 131.

*Embey-Isztin, A., *Dobosi G., *Noske-Fazekas G., Arva-Sós E.; **Petrology of a new basalt occurrence in Hungary;** *Mineralogy and Petrology* 40 (1989) 183.

*Uchrin G., *Ormai P., Hertelendi E.; **Local and global impact of tritium and carbon-14 released from Paks nuclear power plant;** *Proceedings of the 30th Anniversary Symposium of Radiation Protection in the Boris Kidric Institute of Nuclear Science, Radiation Protection Selected Topics.* eds.: Minkovic, M. M., Pavlovic, R. S., Raicevic, J. J., Beograd, Boris Kidric Inst. (1989) 358.

Hertelendi E., *Petz R., *Scheuer Gy., *Schweitzer F.; **Radiokarbon koradatok a Paks-Sárközi süllyedők kialakulásához;** *Mérnökgeológiai Szemle* 38 (1989) 137.

*Vass, D., *Balogh K.; **The period of main and late alpine molasses in the Carpathians;** *Z. Geol. Wiss., Berlin* 17 (1989) 849.

BIOLOGICAL AND MEDICAL RESEARCH

Fenyvesi A., Mahunka I., Tárkányi F., *Molnár T.; **Ciklotron neutronforrások és orvosbiológiai alkalmazásuk;** *Automatizálás* 22 (1989) 19.

*Béres Cs., Fenyvesi A., *Jakucs P., Mahunka I., Kovács Z., *Molnár T., *Szabó L., Ditrói F.; **Application of an MGC-20 cyclotron and methods of radioecology in solution of problems of forestry and the wood industry;** *Nuclear Instr. and Methods in Physics Research "B"* 43 (1989) 101.

*Sági F., Langer G., *Mozsik L., Csatlós M.; **Role of internal gas components of the wheat stalk: physical or metabolic?;** *Proceedings of 4th Intern. Conf. on Physical Properties of Agricult. Maters., Rostock, GDR, 4-8 Sep 1989;* ed.: I. Hellebrand, *Academy of Agricultural Sciences of the GDR* 2 (1989) 719.

Kovács A.; **Az élelmiszerfizika hazai műhelyei. Élelmiszerfizika az ATOMKI-ban - eredmények és lehetőségek;** *Kertészeti és Élelmiszeripari Egyetem Közleményei, Élelmiszerfizikai közlemények* 53 (1989) 79.

*Molnár T., Fenyvesi A., Mahunka I., *Csejtei A.; **Dozimetriai mérések nagyintenzitású ciklotron neutronforrásokon**; Magyar Radiológia 63 (1989) 159.
*Csejtei A., *Molnár T., *Marián T., Fenyvesi A., Kovács P., *Ebel Gy.; **Neutronterápiához kapcsolódó első sugárbiológiai kísérletek**; ibid. p. 152.

*Milesz S., *Norseev, Yu. V., Szűcs Z., *Vasáros L.; **Characterization of DTPA complexes and conjugated antibodies of astatine**; Journal of Radioanal. and Nucl. Chem. Letters 137 (1989) 365.

*Shmakova N. L., *Norsejev Yu. V., *Vajnsón A. A., Cyuts Z., *Fadjejeva T. A., *Fomenkova T. E., *Halkin V. A., *Tserevatenko A. P.; **The biological effect of astatine-211 alpha-particles and therapy of ehrlich ascite carcinome**; Preprint of JINR, P19-89-172, Dubna, USSR (in Russian)

DEVELOPMENT OF INSTRUMENTS AND METHODS

Szabó Gy., Zolnai L.; **PIXASE: a computer package for evaluation of PIXE spectrum series. Part II.: calculation of the effective cross sections for x-ray production**; Nuclear Instruments and Methods in Physics Research "B" 36 (1989) 88

Szelecsényi F., Mahunka I., Tárkányi F., Andó L.; **A debreceni ciklotron az izotóptermelés szolgálatában**; Automatizálás 22 (1989) 23

Fenyvesi A., Mahunka I., Tárkányi F., *Molnár T.; **Ciklotron neutronforrások és orvosbiológiai alkalmazásuk**; ibid. p. 19.

Ujhelyi Cs.; **Counting equipment "dead time" independent of net count rate of a radioisotope**; International Journal of Radiation Applications and Instrumentation Part "A": Applied Radiation and Isotopes 40 (1989) 461.

Medveczky L., *Horváth E.; **Personal neutron dosimeters at the paks nuclear power station**; Kernenergie 32 (1989) 283.

Kormány Z., Szűcs I., Valek A., Vámosi J.; **A study of third harmonic mode acceleration for the MGC**; ibid. p. 359.

*Astakhov, A. Ya., *Batusov, Yu. A., *Bencze L., *Faragó I., *Kisvárad A., *Molnár L., *Soroko, L. M., Végh J.; **Meso-optical Fourier transform microscope - a new device for high energy physics**; Nuclear Instruments and Methods in Physics Research "A" 283 (1989) 13.

Medveczky L., *Zsolnay É.; **Hasadó radiátor konverteres szilárdtest-nyomdetektoros neutrondoziméter érzékenységeinek meghatározása**; Izotóptechnika, Diagnosztika 32 (1989) 123.

***Molnár T., Fenyvesi A., Mahunka I., *Csejtei A.; Dozimetriai mérések nagyintenzitású ciklotron neutronforrásokon; Magyar Radiológia 63 (1989) 159.**

Lakatos T.; Extra gyors röntgenfluoreszcencia analízis új típusú spektrométerrel; XXXII. Magyar Szinképelemző Vándorgyűlés, V. Magyar Molekulaspektroszkópai Konferencia, Sárospatak, 1989. jún. 19-22. szerk.: Szilvássy Z., Veszprém, Gépipari Tudományos Egyesület (1989) 191.

Lakatos T.; Adaptive digital filtering for x-ray spectrometry; XIII. International Symposium. on Nuclear Electronics, Varna, 12-18 Sep 1988. eds: E. K. Aksenova, E. V. Ivaskevic, Dubna, OIYAI, d13-88-938 (1989) 343.

Fenyvesi A., Gál I., Mahunka I., *Molnár T, Tárkányi F.; Nagyintenzitású ciklotron neutronforrások; Magyar Radiológia 63 (1989) 166.

Conference contributions and talks

(* denotes co-author from other establishment)

NUCLEAR PHYSICS

Fényes T., Dombrádi Zs.; **Structure of odd-odd In nuclei;** International Conference on Selected Topics of Nuclear Structure, Dubna, Jun 20-24, 1989

Pál K. F., *Rowley, N., *Nagarajan, M. A.; **Bengtsson-Franendorf and exact cranking calculations on a single-j shell;** *ibid.* p.32.

*Rowley, N., Pál K. F., *Nagarajan, M. A.; **Level interactions and diabolic points in the cranking model** *ibid.* p. 31.

Fényes T.; **The cyclotron program in Hungary and the perspectives for the future;** Symposium on "use of cyclotron", Department of Physics, University of Jyväskylä, Jyväskylä, Finland, May 25-26, 1989

Cseh J.; **Interacting boson models for nuclear cluster states;** *ibid.*

Fényes T.; **Structure of odd-odd In nuclei;** *ibid.*

Somorjai E., Józsa M., Kiss A. Z., Koltay E., Keinonen, J., Tikkanen, P.; **The structure of ^{40}Ar studied by $^{36}\text{S}(\alpha, \gamma)^{40}\text{Ar}$;** *ibid.*

Szelecsényi F., Tákányi F., Kovács Z.; **Production of ^{66}Ga and ^{67}Ga at a compact cyclotron;** (abs.: ed.: S. J. Heselius, Turku, 1989, Printed by Gillot OY,, pp. 24-25); 5th Symp. on Med. Appl. of Cyclotrons, Turku, Finland, May 31-Jun 3, 1989

Krasznahorkay A., Dombrádi Zs., Timár J., Fényes T., Gulyás J., *Kumpulainen, J., *Verho, E.; **Nuclear structure of ^{108}In .** (Sbornik Annotatsij Dokladov d4-89-327 p. 42); Int. Conf. on Selected Problems in Nuclear Structure, Dubna, 20-24 Jun 1989

Gulyás J., Dombrádi Zs., Fényes T., Timár J., *Passoja, A., *Kumpulainen, J., *Julin, R; **In-beam spectroscopy of ^{106}In .** *ibid.* p. 41.

Fényes T., Dombrádi Zs.; **Structure of ^{114}In nucleus** *ibid.* p. 44

Fényes T., Dombrádi Zs.; **Structure of ^{116}In nucleus;** *ibid.* p. 45.

Krasznahorkay A., Dombrádi Zs., Timár J., Gácsi Z., Kibédi T.,
*Passoja, A., *Julin, R., *Kumpulainen, J., *Brant, S.,
*Paar, V.; **Nuclear structure of ^{110}In** ; *ibid.* p. 43.

*Gizon, A., *Barci, V., *El-Samman, H., *Weiss, B., *Gizon, J.,
Nyakó B. M.; **π h 11/2 * ν h 11/2 configuration in doubly-odd ^{124}Cs**
(abstr.: contributed papers no page number);
International Conference on the Spectroscopy of Heavy Nuclei,
Crete, Greece Jun 25 - Jul 1, 1989

Nyakó B. M., *Gizon, J., *Barci, V., *Gizon, A., *André, S.,
*Barneoud, D., *Curien, D., *Genevey, J., *Merdinger, J. C.;
Evidence for h 11/2 proton alignment in ^{127}Ce ; *ibid.*

Dombrádi Zs., Fényes T., *Paar, V.; **Structure of odd-odd $^{116-104}\text{In}$ nuclei**; *ibid.*

Szelecsényi F., Kovács Z., *Spett, B., Tárkányi F.; **Production of ^{66}Ga by compact cyclotron for PET studies**; (abstr.: Eur.J. Nucl. Med. 15 (1989) 578) European Association of Nuclear Medicine Congress, Strasbourg, France, 28 Aug 1989

Cseh J.; **Dynamic symmetries in the molecule-like states of atomic nuclei**; (abstr., ed.: Gy. Darvas, D. Nagy, Budapest, pp. 78-80); Symmetry of Structure: Ann Interdisc. Symposium, Budapest, 13-19 Aug 1989.

Dombrádi Zs., Gácsi Z.; **Structure of excited states in ^{116}Sn** ; (abstr.:); International Nuclear Physics Conference, Sao Paulo, Brasil, 20-26 Aug, 1989

*Gizon, J., Nyakó B. M., *Barci, V., *Gizon, A., *André, S.,
*Barneoud, D., *Curien, D., *Genevey, J., *Merdinger, J. C.;
Investigation of collective bands in ^{127}Ce ; (abstr.) *ibid.*

Gácsi Z.; **Branching ratios and monopole strengths in ^{116}Sn** ; *ibid.*

Kruppa A.T.; **Atommagok klasztermodellje az $5 < a < 8$ tömegszám tartományban**; (absztr., Budapest, 1989, OMIKK p.102); Magyarok szerepe a Világ Természettudományos és Műszaki Haladásában II., Tudományos Találkozó., 1989. aug. 21-27

Lovas R. G.; **Nukleoncsomok atommagokban**; *ibid.* p. 101

Kalinka G.; **Új részecske és foton detektálási elvek és módszerek**; Röntgenfluoreszcenciás Ankét, Veszprém, Hungary, 1989. nov. 27-29.

*Dragoun, O., *Brabec, V., *Kovalik, A., *Fiser, M.,
*Novák J., *Rysavy, M., Kövér L., Cserny I.,
*Zashkvara, V. V., *Ashimbaeva, B. U.; **High-resolution spectroscopy of low-energy electrons emitted in nuclear transformation**; VIIIth Intern. Conf. of Hyperfine Interacts., Prague, Czechoslovakia, 14-19 Aug 1989

ATOMIC PHYSICS

*Heil, O., *Keller, N., Kövér A., Szabó Gy., Gulyás L., Sarkadi L., Pálincás J., *Vajnai T., Berényi D., *Groneveld, K. O., *Gibbons, J., *Sellin, I. A.;

A coincidence study of the shape and yield of ECC and ELC at low energies; (abst.: Europhysics Conference Abstracts vol.13c part ii. ed.: A. Salin p. 656); 3rd European Conference on Atomic and Molecular Physics, Bordeaux, France, Apr 3-7, 1989.

Gulyás L., Berényi D., Kövér A., Szabó Gy., Sarkadi L., Pálincás J., *Vajnai T.; **Cusp inversion in the electron loss (ELC) process;** *ibid.* p.653)

Sarkadi L.; **Proton-antiproton differences in L-subshell ionization;** 11th Int. Semin. on Ion-Atom Collision (ISIAC XI), Manhattan, USA, 3-4 Aug, 1989

Sarkadi L., Pálincás J., Kövér A., Berényi D., *Vajnai T.; **Electron capture into continuum states of neutral atoms;** *ibid.*

Végh J., Ricz S., Kádár I., Sulik B., Varga D., Berényi D.; **Angular and Z dependence of Ne K Auger production cross section at the impact of fast ions with different charge states;** *ibid.*

Sarkadi L., Kövér A., Berényi D., Pálincás J., Szabó Gy., *Vajnai T.; **The dependence of the cusp shape on the charge of the incoming and outgoing ions;** (Abstracts of Contr. Papers, p. 590); 16th Int. Conf. on the Phys. of Electronic and Atomic Collisions (XVI ICPEAC), New York, USA, 26 Jul - 1 Aug, 1989

Ricz S., Végh J., Varga D., Kádár I., Sulik B., Berényi D.; **High order multipole contribution (A4) to the Auger angular distributions observed in Ne³⁺-Ne collision;** *ibid.* p. 519);

Sarkadi L., Pálincás J., Kövér A., *Vajnai T.; **L₃-subshell alignment induced by electron capture in H⁺-Ar collision;** *ibid.* p. 516

Papp T., Török I.; **M2/E1 mixing in L₃ X-ray transitions;** *ibid.* p. 520

Papp T.; **Sugárzásos átmenetek magasabb multipólusú komponensei ionizált atomokban;** (előadások kivonatai i.Budapest, OMIKK, p. 104); Magyarok Szerepe a Világ Természettudományos és Műszaki Haladásában, Tudományos Találkozó 1989. aug. 21-27

Berényi D.; **Legújabb eredmények az ATOMKI-ban (Debrecen) az ion-atom ütközések területén;** *ibid.*

Kövér L., Cserny I., *Fiser, M., *Brabec, V., *Dragoun, O.,
*Novák J.; **Combined application of ICES and XPS methods for
quantitative electron spectroscopy of Tc compounds;**
ECASIA'89, European Conference on Applications of Surface and
Interface Analysis, Antibes-Juan-les-Pins, France,
23-27. Oct, 1989

*Dragoun, O., *Brabec, V., *Kovalik, A., *Fiser, M.,
*Novák J., *Rysavy, M., Kövér L., Cserny I.,
*Zashkvara, V. V., *Ashimbaeva, B. U.; **High-resolution
spectroscopy of low-energy electrons emitted in nuclear
transformation;** VIIIth Intern. Conf. of Hyperfine Interactions,
Prague, Czechoslovakia, 14-19 Aug, 1989

MATERIALS SCIENCE AND ANALYSIS

Szelecsényi F., Ditrói F., Mahunka I., Andó L., Fenyvesi A,
Takács S., Tárkányi F., *Molnár T; **Primenenie tsiklotrona MGC-
20 dlya prikladnyh tselej vtoroe mezhdunarodnoe soveshchanie
po tsiklotronam i ih primeneniyu,** Bechine Csehszlov@kia,
1989. máj. 29-jun. 3.

Ditrói F., Takács S., Mahunka I., *Gémesi Z.; **Trace element
study of glass samples by using activation methods;**
(abstr.:p.84.); 1st European Conference on Accelerators in
Applied Research and Technology, Frankfurt am Main, FRG, 5-9
Sept., 1989

Borbély-Kiss I., Koltay E., Szabó Gy., *Pintye E., *Groska E.,
Kiss A.; **The effect of radiotherapeutic irradiation on the
elemental concentration of iron in human erythrocytes and
blood plasma;** (Programme and Abstracts Vrije Universiteit,
Amsterdam, p.15); The 5th International Conference on Particle
Induced X-ray Emission and Analytical Application, Amsterdam,
the Netherlands, 21-25 Aug., 1989

Borbély-Kiss I., Koltay E., Szabó Gy., *Bozó L., *Mészáros E.,
*Molnár A.; **An evaluation of elemental concentrations in
atmospheric aerosols over Hungary: regional signatures and
long-range transport modelling;** (ibid. p.14)

Vad K., Mészáros S., Halász G., *Balanyi Sz.; **Temperature and
magnetic field dependence of transport critical current
density in $\text{YBa}_2\text{Cu}_3\text{O}_{7-x}$ ceramics;** Critical Currents in High T_c
Superconductors, Karlsruhe, FRG, 24-25 Oct., 1989

Kalinka G.; **új részecske és foton detektálási elvek és
módszerek;** Röntgenfluoreszcenciás Anket, Veszprém, 1989. nov.
27-29.

Kalinka G.; **Izotópperjesztésű szekunder-targetes forrás tervezése félvezető detektoros röntgenspektrométerekhez;** ibid.

Kormány Z., Mahunka I., Valek A.; **Applications and developments at the MGC cyclotron;** 26th European Cyclotron Progress Meeting, Louvain-la-Neuve, Belgium, 23-25 Nov., 1989

Bohátka S.; **Monitoring of fermentation processes with mass spectrometer;** (Abstr.: Bratislava, Dom Techniky Cstvts, 1989., pp.1-4); v. Biotechnologické dni Bratislava '89, Bratislava, Czechoslovakia, 5-6 Dec., 1989

*Kispéter J., *Beczner J., Borbély-Kiss I., *Horváth L., *Novák A.; **Investigation of milk protein concentrate powder with respect to protein concentration and the gamma dose absorbed;** (ESNA XXth Ann. Meeting, Final Progr. and Book of Abstr.); XXth Annual Meeting of ESNA (European Society of Nuclear Methods in Agriculture) Lunteren/Wageningen, The Netherlands, 16-20 Oct., 1989

EARTH AND COSMIC SCIENCES, ENVIRONMENTAL RESEARCH

Hunyadi I.; **Radonészlelések a természetben nyomdetektorokkal, földrengés előrejelzés lehetősége;** (abstr.: ELFT, Sugárvédelmi Szakcsoport, Budapest., 1989. ki-e-9); XIV. Sugárvédelmi Továbbképző Tanfolyam, Balatonkenese, Hungary, 1989. ápr. 16-18.

*Germán E., *Bolyos A., *Daróczy S., *Pázsit A., *Nagy J., *Dezső Z., Hunyadi I., Tóth-Szilágyi M., *Stur D., *Koblingerné-Bokor E.; **Kievi talaj-, fű- és moha-minták radioaktivitása (1987);** ibid. (abstr: nk. p-4)

Csige I., Hakl J., *Géczy G., *Lénárt L.; **Study of underground radon transport;** Workshop on Radon Monitoring in Radioprotection, Environmental Radioactivity and Earth Science, Trieste, Italy, 2-14 April 1989.

*Várhegyi A., *Gerzson I., *Baranyi I., *Palyi, A., Hakl J.; **Application of methods based on microbubble radon transport theory for different geological tasks;** 34th Int. Geophys. Symp., Budapest, 4-8 Sep 1989.

Borbély-Kiss I., Koltay E., Szabó Gy., *Bozó L., *Mészáros E., *Molnár A.; **An evaluation of elemental concentrations in atmospheric aerosols over Hungary: regional signatures and long-range transport modelling;** (Programme and Abstracts, Vrije Universiteit, Amsterdam, p. 14); 5th Int. Conf. on PIXE and Analytical Application, Amsterdam, the Netherlands, 21-25 Aug 1989.

Borbély-Kiss I., *Bozó L., Koltay E., *Mészáros E., *Molnár A., Szabó Gy.; **Elemental composition of aerosol particles under background conditions in Hungary;** Aerosols and Background Pollution, Galway, Ireland, 13-15 June 1989.

Kovács A.; **Izotóp geokronológiai és földtani kutatás;** Magyarok Szerepe a Világ Természettudományos és Műszaki Haladásában II., Tudományos Találkozó, Budapest, 1989. aug. 21-27.

*Géczy G., Csige I., Somogyi Gy.; **Air circulation in caves traced by natural radon;** 10th Int. Congress of Speleology, Budapest, 13-20 Aug 1989.

Hakl J., *Lénárt L., Somogyi Gy.; **Time integrated radon measurements performed in a karstic well water;** *ibid.*

*Lénárt L., Somogyi Gy., Hakl J., Hunyadi I.; **Radon mapping in caves of Eastern Bükk region;** *ibid.*

Somogyi Gy., Hunyadi I., Hakl J.; **Historical review of one decade radon measurements in caves in Hungary, performed by solid state nuclear track detection technique;** *ibid.*

Arva-Sós E., *Ravasz-Baranyai L.; **Kalij-argonovaya izotopnaya geohronologiya mezozojskikh magmaticeskikh porod nekotorykh pajonov vengrii;** Carpatho-Balkan Geological Association 14th Congress, Sofia, Bulgaria, 20-23 Sep 1989.

Balogh K., *Ravasz-Baranyai L., *Nagy-Melles M., *Vass, D.; **Interpretation of K/Ar ages of young basalts: methods for eliminating unreliable ages;** *ibid.*

*Székyné-Fux V., Pécskay Z.; **New radiometric data to the chronology of covered neogene volcanic rocks from boreholes in the Great Hungarian Plain;** *ibid.*

Borbély-Kiss I., Koltay E., *Mészáros E., *Molnár A., Szabó Gy.; **Légtéri aeroszolok PIXE analizisének környezetkutatási lehetőségei;** (abstr. p. 25); I. Magyar Aeroszol Konferencia, Veszprém, Hungary, 1989. okt. 5-6.

Hertelendi E.; **Sources of random errors in Debrecen ¹⁴C laboratory;** Int. Workshop on Inter-Comparison of ¹⁴C Laboratories, East Kibbride, Glasgow, UK, 12-15 Sep 1989.

*Uchrin G., *Ormai P., Hertelendi E.; **Local and global impact of tritium and carbon-14 released from paks nuclear power plant;** 30th Anniversary Symposium of Radiation Protection in the Boris Kidric Institute of Nuclear Sciences, Dubrovnik, Yugoslavia, 2-6 Oct 1989.

Hertelendi E.; **Isotopically light aquatic kerogen in the hungarian oligocene;** (abstr); 5th Working Meeting Isotopes in Nature, Leipzig, GDR, 25-29 Sep 1989.

Csige I., Hunyadi I., *Marennny, A. M., *Hertzen, G. P.;
**A kozmikus nehézion-sugárzás dozimetriai vizsgálata
nyomdetektorokkal bioszputnyikokon; A Magyar Élettani Társaság
LIV. Vándorgyűlése, Debrecen, 1989. aug. 27-30.**

*Kozák M., Andó J., Pécskay Z., *Székyné-Fux V.; **Analisi de
edad radiogena K/Ar en la region de Holguin; I. Kubai
Nemzetközi Földtani Kongr., Havanna, Kuba, 1989. ápr. 28-30.**

Tóth J., Kövér L., *Vajasdi-Perczel I., Mikecz P.,
*Tarnóczy T.; **An XPS study of the surface composition of urban
aerosols fractionized by their sizes by the help of cascade
impactors; (abstr.); ECASIA'89 European Conference on
Applications of Surface and Interface Analysis, Antibes-Juan-
les-Pins, France, 23-27. Oct 1989.**

BIOLOGICAL AND MEDICAL RESEARCH

Bacsó J., Uzonyi I., *Bakulin, A. V., *Rahmanov, A. S.,
*Oganov, V. A.; **A patkányszőr és patkánycsont ásványianyag-
tartalmának, és mechanikai paramétereinek összefüggése;
A magyar élettani társaság LIV. Vándorgyűlése, Debrecen,
1989. aug. 27-30.**

Csige I., Hunyadi I., *Marennny, A. M., *Hertzen, G. P.;
**A kozmikus nehézion-sugárzás dozimetriai vizsgálata
nyomdetektorokkal bioszputnyikokon; ibid.**

Borbély-Kiss I., Koltay E., Szabó Gy., *Pintye É., *Groska E.,
Kiss A. Z.; **The effect of radiotherapeutic irradiation on the
elemental concentration of iron in human erythrocytes and
blood plasma; (Programme and Abstracts Vrije Universiteit,
Amsterdam, p.15); 5th Int. Conf. on PIXE and Analytical
Application, Amsterdam, the Netherlands, 21-25 Aug 1989.**

Takács S., Ditrói F., *Pankotai M., *Fodor P.; **Microelemental
measurement of tomato plants by using PIXE and ICP methods;
ibid. p. 14.**

*Sági F., Langer G., *Mozsik L., Csatlós M.; **Role of internal
gas components of the wheat stalk: physical or metabolic?; 4th
Int. Conf. Physical Properties of Agricult. Materials,
Rostock, GDR, 4-8 Sep 1989.**

*Csejtei A., Fenyvesi A., *Molnár T., *Marian T., *Balkai L.,
*Pásti G., *Pintye É., *Groska E., *Miltényi L.;
**Sugárbiológiai vizsgálatok az ATOMKI ciklotronjánál
Debrecenben; Magyar Onkológiai Társaság XVIII. Kongr.,
Budapest, 1989. nov. 9.**

Szűcs Z., *Norseev, Yu. V., *Cuong, D. D., *Vasáros L.; **^{211}Ru izotóp előállítása ^{211}At -generátor számára;** Korszerű radio-izotópos eljárások és eszközök, különös tekintettel a nyomjelzéstechnikára, Hajdúszoboszló, Hungary, 1989. okt. 25-27.

*Palotás B., *Kovács I., Kovács Z., *Sik T.; **A p-OH-V-penicillin bioszintézis útjának vizsgálata triciált prekursorral;** ibid.

DEVELOPMENT OF INSTRUMENTS AND METHODS

Medveczky L., Dajkó G., Uray I.; **Szilárdtest nyomdetektoros és termolumineszcens doziméterek együttes alkalmazásának lehetősége ciklotronnál;** (abst.:ELFT Sugárvédelmi Szakcsoport, Budapest, 1989. MSV-E-15); XIV. Sugárvédelmi továbbképző tanfolyam, Balatonkenese, Hungary, 1989. ápr. 16-18.

Medveczky L., Hakl J., Fenyvesi A., *Molnár T.; **Neutron dózisteljesítmény térbeli eloszlása víz fantomban a debreceni ciklotronnál;** ibid.SVM-P-19.

Tóth-Szilágyi M., Hunyadi I., Hakl J.; **PVC padlóburkolók radon áteresztő képességének vizsgálata ma-nd/alfa nyomdetektorral;** ibid. NKV-P-6.

Medveczky L., Uray I., Dajkó G.; **Response of TL and SSNT dosimeters: a comparison;** (abstr.:III/7 p. 8); 21st International Symposium Radiation Protection Physics, Bad Schandau-Ostrau, GDR, 3-7 Apr 1989.

Bartha L., Kiss A. Z., Koltay E., Szabó Gy.; **Light-heavy ions and molecular beams from a radio-frequency ion source;** 5th International Conference on Electronic Accelerators and Associated Boosters, Strasbourg-Heidelberg, 24-30 May 1989.

Fenyvesi A.; **Az MGC-20 ciklotronhoz fejlesztett neutron-orrások;** XIII. DOTE-ATOMKI együttes tudományos ülés; A neutronterápia helye és szerepe az onkológiai ellátásban, Debrecen, 1989. április 29.

Mahunka I.; **Use of cyclotron in applied research and isotope production in Debrecen;** Symposium on "use of cyclotron", Department of Physics, University of Jyväskylä, Jyväskylä, Finland, 25-26 May 1989.

Gál I., Takács S., Tárkányi F., Andó L.; **Beam splitting for parallel isotope production;** (abstr.:ed.: S. J. Heselius, Turku, 1989. printed by Gillot Oy. pp.31-32); 5th Symposium on the Medical Application of Cyclotrons, Turku, Finland May 31-June 3 1989.

Tárkányi F., Szelecsényi F., Takács S.; **Measurement of excitation functions via stacked foil technique;** ibid. pp. 29-30.

Kormány Z., Lakatos T., Valek A.; **A microcomputer-based versatile profile monitoring system;** (abstr.: Hahn-Meitner-Institut Berlin GmbH, 1989, p.98); 12th International Conference on Cyclotrons and Their Applications, West-Berlin, 8-12 May 1989.

Valek A., Kormány Z.; **Opyty trekhletnej ekspluatatsii tsiklotrona MGTS-20E v IYai(ATOMKI) VAN;** Btoroe Mezhdunarodnoe Soveshchanie po Tsiklotronam k ikh Primeneniyu, Bekhine, CHSSR, 29 maya-3 iyunya, 1989.

Berényi D., Bibók Gy., Berecz I.; **Spektroskopicheskie izmeritelnye pribory, razrabotannye v IYai(ATOMKI) VAN;** Nauchpribor'89 - Scientific Instrumentation'89, Berlin, 11-16 Sep 1989.

Valek A.; **Az MGC-20E ciklotron mint a műszerközpont nagyberendezése;** Az OTKA debreceni műszerközpontja - helyzetkép és perspektívák, Debrecen, 1989. okt. 5.

Török I.; **High resolution PIXE with a crystal spectrometer;** 8. Celostátní Seminar Jaderné Metody v Hornictví, Geologii, Geofyzice a Geochemii, Strbské Pleso, Czechoslovakia, 9-13. oct. 1989.

Langer G., Berecz I., Bohátka S., Futó I., Gál I., Simon M.; **Application of different stages of an oil diffusion pump for pumping different gas inlets;** (abstr.: Final Program p.282); 11th Int. Vacuum Congress, Köln, FRG, 25-29 Sep 1989.

Uzonyi I.; **Energia-diszperzív röntgenemissziós analitika (REA) alkalmazása biológiai és geológiai minták elemösszetétel meghatározására;** Röntgenfluoreszcenciás Ankét, Veszprém, Hungary, 1989. nov. 27-29.

Bacsó J.; **Total-reflexiós XRFA;** ibid.

Kis-Varga M.; **Röntgensőves gerjesztés ED röntgenspektrométerekben-eredmények és lehetőségek;** ibid.

Kalinka G.; **új részecske és foton detektálási elvek és módszerek;** ibid.

Kalinka G.; **Izotópperjesztésű szekunder-targetes forrás tervezése félvezető detektoros röntgenspektrométerekhez;** ibid.

Máthé Gy.; **Gázexpanziós hűtésű Si(Li) röntgendetektor;** ibid.

Bohátka S.; **Monitoring of fermentation processes with mass spectrometer**; (abstr.: Bratislava, Dom Techniky CSVTS, 1989, pp.1-4); v. Biotechnologické dni Bratislava '89, Bratislava, Czechoslovakia, 5-6 Dec 1989.

Bohátka S.; **Vacuum physics and biotechnology - MS analysis in gases, liquids and tissues**; (abstr.:p.23); Int. Symp. on Devices of Vacuum Sci. and Tech., Debrecen, 9-11 Oct 1989.

Máthé Gy.; **Miniature refrigerator**; ibid.

Molnár J., Biri S., *Samoylov, V. N.; **16 single-ended channels IBM PC-XT/AT interface for signal analysis**; 8th Summer School on Computing Techniques in Physics, Skolsky Dvor, Czechoslovakia, Sep 1989.

Dajkó G.; **Nukleáris membránok fejlesztése és előállítása**; II. Országos Membrántechnikai Konferencia, Nyergesújfalu, Hungary, 1989. okt. 18.

Dajkó G., Uray I.; **Solid state detectors in cyclotron radiation field**; (abstr.: p3. 31); 9th Int. Conf. on Solid State Dosimetry, Wien, Austria, 6-10 Nov 1989.

Dajkó G.; **Fast neutron spectrometry using CR-39 track detectors**; (abstr.:p 4.6); ibid.

Lakatos T.; **Extra gyors röntgenfluoreszcencia analízis új típusú spektrométerrel**; XXXII. Magyar Szinképelemző Vándorgyűlés, V. Magyar Molekulaspektroszkópiai Konferencia, Sárospatak, Hungary, 1989. jún. 19-22.

Paál A., Berecz I., Murányi-Szeleczy A., Langer G.; **Szerves mikroszennyezők azonosítása és mennyiségi meghatározása kvadrupól tömegspektrométer alkalmazásával**; Kémikusok a Környezetvédelem kérdéseiről, Debrecen, 1989. ápr. 13.

Mikecz P.; **Opyty i vozmozhnosti proizvodstva radioizotopov na MGC-20 ciklotrona**; Seminar of Methods of Production of Radionuclides for Medical Purposes, Rez, Czechoslovakia, 20-24 Nov 1989.

Kertész L., *Környei J., *Kemenes M., Mikecz P., *Nagy K.; **The adherence of radioindium-labelled mononuclear cells on mucous membranes**; 5th Int. Symposium on Radioactive Labelled Blood Cell Elements, Wien, Austria, 11-15 Sep 1989.

Mikecz P., Tóth Gy., Ditrói F., Takács S., Mahunka I.; **Nagy tisztaságú gallium térfogati oxigén tartalmának meghatározása**; Korszerű radioizotópos eljárások és eszközök, különös tekintettel a nyomjelzéstechnikára, Hajdúszoboszló, Hungary, 1989. okt. 25-27.

Tóth Gy., Mikecz P., Szelecsényi F.; **¹¹¹In elválasztása kadmium célananyagból**; ibid.

THESIS COMPLETED

Doctor of the Physical Science

J. Pálinkás, Alignment in ion-atom collisions

Candidate of the Physical Science

A. Krasznahorkay, A new effect in the conversion and the structure of nuclei ^{108}In and ^{110}In

PhD in Physics

L. Gulyás, Electron capture into the continuum states and electron loss of light ion projectiles, Supervisor: D. Berényi

Diploma works

G. Géczy, Air flow in caves traced by natural radon, Supervisor: I. Csige

A. Agoston, Study of K satellite lines for a few elements by X-ray crystal spectrometer, Supervisor: I. Török

I. Szabó, Control of quadrupole mass spectrometer and evaluation of mass spectra by IBM PC, Supervisor: I. Juhász

K. Sebők, Studies of oil diffusion pumps, Supervisor: I. Berecz

J. Bálint, Interfacing of Q-300 MS to IBM PC, Supervisor: A. Paál

N. Hegman, Study of magnetic properties of high T_c superconductors, Supervisor: S. Mészáros

A. Csótó, Study of the resonance function by complex scaling Supervisor: A. Kruppa

SEMINARS IN THE ATOMKI

January 12

Models for the description of high-spin states

K. F. Pál

January 19

Instrumental requirements of mass spectrometric analysis of organic microcontaminations

Z. Dinya, A. Paál, G. Langer

January 26

Collective states in the region of $A \sim 130$ nuclei

B. M. Nyakó

February 2

Processor theory

E. Gesztelyi, Dept. of Math., Univ. of Kossuth Lajos, Debrecen (KLTE)

February 9

Computer physics in the 90-s

L. Zolnai

February 16

Long term plans in the field of earth sciences and the research of cosmic radiation

K. Balogh, J. Hakl, E. Hertelendi

February 23

New possibilities of fusion-energy generation

A. Kovács

March 1 *

Topological and dynamical properties of the components of cellular membranes

L. Trón, Dept. of Biophysics, Univ. of Med. School, Debrecen, (DOTE)

March 9 **

Theoretical aspects of electron-molecule scattering

W. Domcke, Inst. für Physikalische und Theor. Chem. der TU München, FRG

March 16

A new effect in the internal conversion and the structure of nuclei ^{108}In and ^{110}In

A. Krasznahorkay

March 23

Heavy ion sources for MGC cyclotrons

S. Biri

March 30

Long term plans in the field of materials testing and materials sciences

F. Ditrói, L. Kövér, S. Mészáros

April 12 *

Do we need fusion power-station?

L. Pócs, Central Research Institute of Physics of the Hung. Acad. of Sci., Budapest, Hungary

April 12 **

Production of stable isotopes in the Kurchatov Institute for radionuclide production

A. N. Chelcov, I. A. Suvorov, Kurchatov Atomic Energy Institute, Moscow, USSR

April 18 **

Use of Gamow resonances in response functions

P. Curutchet, Manne Siegbahn Inst. of Phys., Stockholm, Sweden

April 19 *

Slowpoke nuclear reactor (with emphasis on communal heating)

J. Lynch, AECL, Chalk River, Canada

April 20

The application of isotope-hydrogeological methods with the aim of estimating the environmental effects of water basins along the river Danube

D. Rank, BVFA Arsenal Geotechnisches Inst., Wien, Austria and

Hydrological aspects of some environmental problems along the river Danube, in Austria

F. Boroviczeny, Geologische Bundesanstalt, Wien, Austria

April 26 **

Isoscalar E2 strength and cluster structure in light nuclei

Kiyoshi Kato, Sapporo, Japan

April 27

Research in the field of medicine, biology, agriculture and environment protection: present conditions and long-term plans in the ATOMKI

G. Langer, I. Borbély-Kiss, F. Tárkányi

May 3 *

Unity of the nature and the society

I. Gyarmati, Technical University (BME), Budapest, Hungary

May 5 **

(e,e'p) reactions and distribution of the single-particle strength in nuclei

J. B. J. M. Lanen, Fysisch Lab. Rijksuniversiteit Utrecht, the Netherlands

May 10

Effect of electron screening on low-energy fusion cross sections

E. Somorjai

May 18

The future of nuclear physics in the ATOMKI

A. Z. Kiss, A. Krasznahorkay, R. G. Lovas

May 25

Directions of the future atomic physics research

D. Berényi, J. Pálinskás, L. Sarkadi

June 1

Nuclear cluster study in Japan

Kiyoshi Kato, Sapporo, Japan

June 8

Analysis with ion beams

A. Z. Kiss

June 12 **

Recent developments in cuspology

D. H. Jakubassa-Amundsen, Sect. Phys., Univ. München, FRG

June 15

Development of accelerators

A. Valek

June 19 **

Application of accelerated beam for trace elements analysis at Nagoya University

T. Katoh, Nagoya University, Nagoya, Japan

June 20 **

Semi-microscopic three alpha and four alpha cluster models for ^{12}C and ^{16}O

Kiyoshi Kato, Sapporo, Japan

June 22

Physical problems of ball lightnings

Gy. Egely, Central Research Institute of Physics (KFKI), Budapest, Hungary

June 29

Long-term plans for instrumental development in the ATOMKI

J. Gaál, Z. Kormány, Gy. Szabó, L. Zolnai

July 31 **

Dynamic target-screening two active electron Classical Trajectory Monte Carlo calculations for $\text{H}^+ + \text{He}$ collisions

V. J. Montemayor, HMI, Berlin

September 7

The limits of the independent electron approximation in ion-atom collisions

L. Vègh

September 14

The infrastructure of information in Hungary

L. Csaba, Research Institute of the Computational Sciences of the Hung. Acad. of Sci. (SZTAKI), Budapest, Hungary

September 21

The many-body problem at the University of Georgia

M. G. Menendez, Univ. of Georgia, USA

September 28

Angle resolved electron spectroscopy of the projectile-centered forward peak in fast, heavy ion-atom collisions

S. Elston, Oak Ridge Nat. Phys. Lab., Oak Ridge, USA

During September, four lectures at KLTE **

Fast ion-atom collisions and three-body Coulomb problem;

M. G. Menendez, Dept. of Phys. and Astronomy, Univ. of Georgia, USA; (see the printed material on these lectures in the ATOMKI Report 1989/5-R))

October 11 **

Production of short lived radioisotopes and radiopharmaceuticals at a Babycyclotron in Jülich

B. Nebeling, KFA, Jülich, BRD

October 12

Direct thermic exploitation of solar energy

S. Keresztes, Research Institute of Electric Industry (VEIKI), Budapest, Hungary

October 13 **

Study of the molecular gas dynamics and its application for molecular pump

Pang Shijin, Beijing Laboratory of Vacuum Physics, Chinese Acad. of Sci., China

October 19

The measurement of electron-electron scattering in the p-He capture processes

J. Pálinskás

October 26

An atomic interferometer

H. C. Bryant, Dept. of Phys. and Astr., Univ. of New Mexico, Albuquerque, USA

November 1 *

Heavy ion physics

W. Greiner, Dept. of Theor. Phys., Univ. of J. W. Goethe, Frankfurt/m, FRG

November 9

The greenhouse effect

A. Kovács

November 16

The structure of nucleus ^{106}In

J. Gulyás

November 23

Determination of the wave function by complex scaling

A. Csótó

November 30

The effect of the rotation on the structure of nuclear states

K. F. Pál

November 30

Intercomparison of data of multielemental analysis of human organs obtained by different analytical methods and from different countries

Junko Matsubara, Department of Epidemiology, School of Medicine, University of Tokyo, Tokyo, Japan

December 6

Studying the chemical reactions going on in the solid-liquid interfaces by the help of radioactive isotopes

J. Kónya, Institute of Isotopes, Univ. of Kossuth Lajos (KLTE), Debrecen

December 12

Review of long-term plans of the ATOMKI: further tasks

D. Berényi, E. Koltay

December 18

Research project for trace element analysis in Nagoya

S. Amemiya, Nagoya University, Nagoya, Japan

December 20

Instrumental developments for the study of prompt nuclear reactions induced by fast neutrons

T. Sztaricskai, Dept. of Exper. Phys., Univ. of Kossuth Lajos (KLTE), Debrecen

Comments:

1. unmarked: hebdomadal seminars
2. * denotes: seminars at the Szalay Physical Centre of Debrecen (which consists of Kossuth Univ., Medical School, ATOMKI)
3. ** denotes: seminars at the divisions and sections in the ATOMKI

AUTHOR INDEX

(* denotes author from other establishment)

Andó L. 78, 96, 100

*Arnould M. 1

Arva-Sós E. 64

Bartha L. 87

Bacsó J. 74

Balogh K. 64

Berényi D. 29, 31, 35, 37

*Béres Cs. 66

*Björnberg M. 13

Borbély-Kiss I. 84

*Burgdörfer J. 43

*Champagne A. E. 1

*Chelcov A. N. 78

*Cuong D. D. 104

Cseh J. 20, 22, 24

*Csejtei A. 80

*Cser M. A. 74

Cserny I. 106

Csige I. 72

*Csótó A. 27

Ditrói F. 60

Dombrádi Zs. 5

*Dominguez J. 13

*Elston S. B. 35

*Endt P. M. 1

Fényes T. 5, 7, 9

Fenyvesi A. 66, 80, 94

Fülöp Zs. 4, 13

Gácsi Z. 7, 9

Gál I. 89, 96

*Géczy G. 72

Gulyás J. 5

Gulyás L. 35, 37, 41

Gyarmati B. 27

Hakl J. 68, 70

Halász G. 51, 53, 55

*Hegman N. 53

Hertelendi E. 63

Hock G. 49

*Horváth F. 7, 9

Hunyadi I. 68, 70

*Iliadis Ch. 1

*Jakucs P. 66

Józsa M. 12

*Julin R. 5

Kalinka G. 102

*Kato K. 24

Kádár I. 29, 31

*Kikstra S. W. 1

Kiss A. Z. 4, 13, 87

Kis-Varga M. 62

Koltay E. 84, 87

*Kopeczky P. 2

Kormány Z. 86

*Kovács I. 82

Kovács Z. 66, 76, 82

*Költő L. 62

Kövér A. 33, 35, 37, 43, 91

Kövér L. 73

Kruppa A. T. 17, 27

*Kumpulainen J. 5

*Lanen J. B. J. M. 17

*Lénárt L. 70

Lévai G. 20, 22, 24

Lovas R. G. 15, 17

Mahunka I. 60, 66, 78, 85, 94

Máté Z. 12

Mészáros S. 51, 53, 55

Mikecz P. 59, 66, 73, 78

*Molnár T. 66, 94

*Mukoyama T. 39, 40

Nagy A. 87

*Norseev Yu. V. 104

*Palotás B. 82

Papp T. 45

*Passoja A. 5

*Paulus G. 1

*Páli A. 59

Pálinkás J. 33

Pécskay Z. 64

*Rauhala E. 13

*Räisänen J. 13

Ricz S. 29, 31

*Rolfs C. 1

*Rysavy M. 93

Sarkadi L. 33, 35, 39, 40, 47

*Schange Th. 1

*Schröder U. 1

Somorjai E. 1, 4

Sulik B. 29, 31, 47

*Suvorov I. A. 78

Szabó Gy. 37, 41, 43, 84, 87

Szelecsényi F. 2, 76, 98

Szücs Z. 104

Takács S. 60, 96, 98

*Tarnóczy T. 73

Tárkányi F. 2, 76, 94, 96, 98, 100

Timár J. 5

Tóth B. 100

Tóth Gy. 59, 76

Tóth J. 57, 73, 78

*Tóth Z. 57

Török I. 14, 45, 47

Tökési K. 49, 91, 93

*Trautvetter H. P. 1

*Trón L. 80

Uzonyi I. 74

Vad K. 51, 53, 55

*Vajasdy-Perczel I. 73

*Vajnai T. 33, 35, 37

Valek A. 86

Varga D. 29, 31, 91

Varga K. 15

*Vasáros L. 104

Vertse T. 12

*Vető I. 63

Végh J. 29, 31, 33, 47, 98, 106

Vitéz J. 59

*Wolke K. 1

Zolnai L. 12

Kiadja a
Magyar Tudományos Akadémia Atommag Kutató Intézete
A kiadásért és a szerkesztésért felelős
Dr. Berényi Dénes, az Intézet igazgatója
Készült a Piremon Kisvállalat Nyomdájában
Törzsszám: 65782
Debrecen, 1990. március

